




EX LIBRIS
UNIVERSITATIS
ALBERTENSIS

The Bruce Peel
Special Collections
Library



Digitized by the Internet Archive
in 2025 with funding from
University of Alberta Library

<https://archive.org/details/0162014938144>

University of Alberta

FACULTY OF GRADUATE STUDIES AND RESEARCH

Library Release Form

Name of Author: Min Ding
Title of Thesis: Flow Injection Electrospray
Mass Spectrometry
Degree: Master of Science
Year this Degree Granted: 2001

Permission is hereby granted to the University of Alberta Library to reproduce single copies of this thesis and to lend or sell such copies for private, scholarly or scientific research purposes only.

The author reserves all other publication and other rights in association with the copyright in the thesis, and except as herein before provided, neither the thesis nor any substantial portion thereof may be printed or otherwise reproduced in any material form whatever without the author's prior written permission.

UNIVERSITY OF ALBERTA
FACULTY OF GRADUATE STUDIES AND RESEARCH

The undersigned certify that they have read, and recommend to the Faculty of Graduate Studies and Research for acceptance, a thesis entitled “**Flow Injection Electrospray Mass Spectrometry**” submitted by Min Ding in partial fulfillment of the requirements for the degree of Master of Science.

University of Alberta

Flow Injection Electrospray Mass Spectrometry

by

Min Ding



A thesis submitted to the Faculty of Graduate Studies and Research in partial fulfillment
of the requirements for the degree of **Master of Science**.

Department of Chemistry

Edmonton, Alberta, Canada

Fall, 2001

Abstract

A modified chromatographic injector can be used as the sample introduction device for an electrospray mass spectrometer. The modification which was made by inserting a 2 mm thick flat ring between the stator and rotor of the injector was necessary to obtaining reliable electrospray signals.

Parametric characterization of flow injection electrospray mass spectrometry is presented. The carrier solution was made up of K^+ dissolved in methanol. Among the important parameters which characterize the features of flow injection were the flow rate and concentration of the carrier solution. These parameters affected the peak shape and analyte signal intensities contrarily. Higher flow rate and carrier ion concentration of the carrier solution would bring about less tailed analyte peaks but lower intensities of analyte signals.

The flow injection electrospray mass spectra of some inorganic solution ions, ranging from singly and multiply charged monoatomic ions to oxoanions, are demonstrated. In order to catch the mass spectrum of a sample solution which passed through the electrospray tip quickly, the largest available sample volume of 0.5 μL was used. The flow rate of carrier solution was 1.0 $\mu\text{L}/\text{min}$. The carrier solution concentration was 0.5 mM. The mass spectra captured provides information similar to those revealed in continuous electrospray mass spectra.

The quantitative performance of the flow injection electrospray mass spectrometer was investigated. Linear calibration curve over three orders of magnitude for simple metal ions can be achieved with employment of an internal standard.

Acknowledgments

There are many people to whom I wish to express my appreciation.

First and foremost, my deepest thanks go to Dr. Gary Horlick. Regardless of how little I knew about research, he kindly took me in his group and guided me throughout the completion of this thesis. For all his encouragement, consideration, and advice I am truly grateful.

I wish to thank my research group colleagues: Youbin Shao, Russel Handy, Shi Liu, and Jianqi Wang. They not only helped me with techniques and computer skills, but also supported me with friendship. My gratitude also goes to the members of the electronics and machine shops, especially Henry Stolk for his help in the development of the instrument used in this thesis.

The financial support that was provided by the Department of Chemistry at the University of Alberta and the National Science and Engineering Research Council (NSERC) is gratefully acknowledged.

Finally, thanks to my husband and son for their help and support.

Table of Contents

Chapter		Page
1	Introduction	
1.1	Objective	2
1.2	Electrospray	3
1.2.1	Mechanistic Aspects of Electrospray Ionization	4
1.2.2	Electrolytic Aspects of Electrospray	6
1.2.3	Nebulization in Electrospray Ionization	9
1.3	Electrospray Mass Spectrometry	10
1.3.1	Electrospray Interface	11
1.3.2	Collision Induced Dissociation	13
1.4	Flow Injection Electrospray Mass Spectrometry	16
1.4.1	Flow Injection Analysis	16
1.4.2	Flow Injection Electrospray Mass Spectrometry	18
1.5	References	19
2	Instrumentation	24
2.1	Introduction	25
2.2	Flow Injection Electrospray Source	28
2.3	Interface	33
2.3.1	Design of Electrospray Interface	33
2.3.2	Curtain Gas	37
2.4	Mass Spectrometer	37
2.5	Spectrum and Data Acquisition	40
2.6	References	42
3	Parametric Characterization of FI-ES-MS	43

3.1	Introduction	44
3.2	Experimental	44
3.2.1	Reagents	45
3.2.2	Carrier Solution	45
3.3	Influence of Flow Injection on the Steady-State Electrospray	45
3.4	Dependence of Analyte Ion Signals on Operating Parameters	47
3.4.1	Effect of Flow Rate of Carrier Solution	47
3.4.2	Effect of Concentration of Carrier Ion	51
3.4.3	Effect of the Electrospray Tip Length	60
3.5	Conclusions	61
3.6	References	64
4	Flow Injection Electrospray Mass Spectra of Inorganic Solution Ions	
4.1	Introduction	66
4.2	Experimental	67
4.2.1	Some Important Features	67
4.2.2	Reagents	68
4.3	Results and Discussion	68
4.4	Conclusions	85
4.5	References	89
5	Quantitative Performance of FI-ES-MS	91
5.1	Introduction	92
5.2	Experimental	93
5.2.1	Reagents	93
5.3	Results and Discussion	93
5.4	Conclusions	97
5.5	References	99

6	Conclusions	100
6.1	Summary	101
6.2	Future Work	103

List of Tables

Table		Page
2.1	Operation parameters of flow injection electrospray mass spectrometry on the modified ELAN 250 ICP-MS with the modified Cheminert internal injector for both positive and negative ions.	38

List of Figures

Figure	Page
1.1 A schematic diagram of the ESI events in air at the atmospheric pressure.	7
1.2 Schematics of the sampler-skimmer interface.	12
1.3 Schematic of a FIA method.	17
2.1 Schematic diagram of continuous sample delivery electrospray source.	26
2.2 The syringe to fused silica capillary connection.	27
2.3 Flow injection electrospray ion source.	29
2.4 A detailed view of the modified injector.	31
2.5 An expanded view of the original two position 4 port internal injector, supplied by Cheminert.	32
2.6 An expanded view of the stator and an example of the flat sample plate.	34
2.7 A general representation of the two position function of the injector.	35
2.8 Schematic diagram of the modified SCIEX/Perkin Elmer Elan Model 250 ICP-MS.	39
3.1 Selective ion monitoring mass spectrum of a 0.1 mM methanolic solution of KCl acquired at conditions: valve voltage 4.0 kV, tip voltage 3.3 kV, carrier solution flow rate 1.0 $\mu\text{L}/\text{min}$. The injector was initially in 'inject' position, then switched to 'load' position and turned back to 'inject' again after a while. The injected solution and carrier solution were the same.	46
3.2 Selective ion monitoring mass spectra of 1 mM CsCl methanolic solution at various flow rates of carrier solution, 0.1 mM KCl, (a) 1.5 $\mu\text{L}/\text{min}$, (b) 2.5 $\mu\text{L}/\text{min}$, (c) 4.0 $\mu\text{L}/\text{min}$, (d) 6.0 $\mu\text{L}/\text{min}$, acquired under conditions: valve voltage 6.1 kV, tip voltage 3.2 kV.	48

3.3	Effect of flow rate of carrier solution: (a) 1 mM KCl in MeOH, (b) 0.5 mM KCl in MeOH, on signal intensities of Cs ⁺ (area of Cs ⁺ peak).	49
3.4	Connection between capillary and injector port.	50
3.5	Selective ion monitoring mass spectra of 1.0 mM CsCl methanolic solution with varying concentrations of carrier ion K ⁺ , (a) 0.1 mM, (b) 0.5 mM, (c) 1.0 mM, acquired under spray conditions: valve voltage 6.1 kV, tip voltage 3.2 kV, flow rate 2.0 µL/min.	53
3.6	Selective ion monitoring mass spectra of 0.1 mM RbCl and CsCl methanolic solutions obtained with 0.5 mM KCl as carrier ion, 1.0 µL/min flow rate, 7.8 kV valve voltage, 3.2 kV tip voltage, 70/5 V sampling plate/skimmer voltage, and 0.2 µL sample volume.	54
3.7	Liquid-solid adsorption isotherm --- convex curve.	55
3.8	Selective ion monitoring mass spectra of 0.1 mM RbCl and LiCl methanolic solution with varying concentrations of carrier ion Na ⁺ : (a) 0.01 mM, (b) 0.03 mM, (c) 0.1 mM, (d) 0.3 mM, (e) 1.0 mM, acquired under conditions: 2.0 µL/min flow rate, 8.5 kV valve voltage, 3.3 kV tip voltage, 70 V sampling plate, 5 V skimmer voltage.	57
3.9	Effect of concentration of carrier ion, (a) NaCl, (b) KBr, on signal intensity (area of analyte peaks) of analytes: RbCl and LiCl.	58
3.10	Selective ion monitoring mass spectra of 0.5 mM methanolic solution of SrCl ₂ , BaCl ₂ , CaCl ₂ , with 0.5 mM KCl as carrier ion, at varying length of ES tip, (a) 1 mm, (b) 4 mm, acquired under conditions: 2.0 µL/min flow rate, 7.1 kV valve voltage, 3.3 kV tip voltage, 180 V sampling plate, 5 V skimmer voltage.	62
4.1	Mass spectra of 0.5 mM alkali metals in methanol, (a) SIM spectrum, (a) flow injection ESMS spectrum, (c) continuous ESMS spectrum.	69
4.2	FI-ESMS spectra of 0.5 mM Mg ²⁺ in methanol at ΔV settings of (a) 25.7 (SIM) (b) 25.7 (c) 35 volts.	71
4.3	FI-ESMS spectra of 0.5 mM Ca ²⁺ in methanol, ΔV= 65 volts.	73
4.4	FI-ESMS spectra of 0.5 mM Sr ²⁺ in methanol, ΔV= 65 volts.	74

4.5	FI-ESMS spectra of 0.5 mM Sr^{2+} in methanol, $\Delta V = 175$ volts.	75
4.6	FI-ESMS spectra of an equimolar mixture of Mg^{2+} , Ca^{2+} , Sr^{2+} , Ba^{2+} , $\Delta V = 180$ volts.	76
4.7	FI-ESMS spectra of 0.5 mM Co^{2+} in methanol at ΔV settings of (a) 25 (b) 25 (c) 75 (d) 75 volts.	78
4.8	FI-ESMS spectra of 0.5 mM $\text{Ni}(\text{NO}_3)_2$ methanolic solution at ΔV settings of (a) 30 (b) 30 (c) 50 (d) 50 volts.	79
4.9	FI-ESMS spectra of 0.5 mM copper bromide methanolic solution at ΔV settings of (a) 75 (b) 75 (c) 55 (d) 55 (e) 35 volts.	81
4.10	FI-ESMS spectra of 0.5 mM zinc nitrate in methanol at ΔV settings of (a) 95 (b) 95 (c) 55 (d) 55 (e) 45 volts.	82
4.11	Flow injection electrospray mass spectra of (a), (b) a 0.5 mM methanolic solution of fluoride, chloride, bromide and iodide at ΔV of -65 volts and (c), (d) a 0.5 mM methanolic solution of chloride, chlorate and perchlorate at ΔV of -95 volts.	84
4.12	Flow injection electrospray mass spectra of a 0.5 mM HNO_3 methanolic solution acquired with varying ΔV settings: (a) -35 V, (b) -55 V, (c) -75 V.	86
4.13	Flow injection electrospray mass spectra of a 0.5 mM Na_2SO_4 methanolic solution acquired with varying ΔV settings: (a) -25 V, (b) -55 V, (c) -75 V.	87
5.1	Analytical curves for (a) Rb and (b) Cs, employing 0.1 mM Cs and Rb, respectively, as an electrospray stabilizer and internal standard.	95
5.2	Analytical curves for (a) Na and (b) Ca, employing 0.1 mM Rb and Sr, respectively, as an electrospray stabilizer and internal standard.	96
5.3	Analytical curves for (a) Sr and (b) Ba, employing 0.1 mM Ba and Sr, respectively, as an electrospray stabilizer and internal standard.	98

Chapter 1

Introduction

1.1 Objective

Electrospray mass spectrometry (ESMS) has gained prominence as an analytical tool since it was first introduced by Yamashita and Fenn [1, 2], and Gall' et al. [3] in 1984. It has been investigated extensively in the aspects of both fundamental properties and applications. Numerous publications related to ESMS show that it is valuable for obtaining structural information and identification of various chemical species ranging from elemental and inorganic species, organic and organometallic compounds, to biological molecules. Currently, electrospray mass spectrometers are present in virtually all pharmaceutical and biotechnology laboratories [4].

The majority of research effort on the instrumentation and method development of ESMS has been focused on improving its capability and diversity in terms of high sensitivity, wide applications, less matrix effects, accurate quantitation and accurate identification. The sample introduction device as a component of an electrospray source plays a minor role in the process of ESMS, but is of significance in the practical sense. Where ESMS is coupled with on-line separation techniques, such as liquid chromatography, capillary electrophoresis, the separation device also acts as the sample introduction device to the electrospray source. However, most stand-alone ESMS system employ a continuous sample delivery device, which often involves manual handling of washing, connecting and syringe operation in order to change samples. When a number of samples are analyzed, these manual tasks are time consuming. Thus, it is desirable to reduce manual operations associated with sample introduction in ESMS.

The desire for the automation of serial assays in clinical chemistry laboratories in which a large number of tests are run every day originally promoted the development of flow injection analysis (FIA) [5]. FIA is based on the injection of a liquid sample into a moving, continuous carrier stream of a suitable liquid. The injected sample forms a zone, which is then transported toward a detector that continuously records the absorbance, electrode potential, or other physical parameter as it continuously changes due to the passage of the sample material through a flow cell. In this discrete analyzer, each sample

in a container is delivered sequentially, which makes the automation quite easy and eliminates most of manual tasks.

The objective of this study was to adapt the method of flow injection delivery of discrete samples to ESMS. As one of the characteristic features of the electrospray process, stable electrospray operation is liquid composition dependent, therefore, electrospray behavior of a stream with composition changing due to sample injection was observed to recognize the compatibility of these two processes. The quantitative performance of flow injection electrospray mass spectrometry (FI-ESME) was investigated using some typical elements. Efforts were also given to obtain transient signals with minimized peak tailing. The adaption of flow injection technique to ESMS provides such advantages as simple operation, faster sampling rate and ease of automation.

1.2 Electrospray

When the interface between a gas and a conducting liquid flowing out of a capillary is charged to a sufficiently high voltage, it can take a stable conical shape frequently referred to as a 'Taylor cone', whose apex emits a microscopic liquid filament that disperses as a fine charged aerosol. Such a remarkable phenomenon, now called 'electrospray', was first reported and studied systematically by Zeleny [6, 7, 8] in 1914 - 1917. Different shapes of the liquid meniscus at various spray voltages were documented by high speed photography. Several fundamental studies [9-28] of the ES phenomenon have ensued from his preliminary work and led to a wide variety of applications. The unique ability of electrospray to generate a fine, consistent aerosol has been exploited in the analytical chemistry field as a sample deposition technique for laser desorption experiments [29] and as an aerosol sample introduction device for atomic spectrometry [30-32]. Among the more notable industrial applications of electrospray are paint and crop spraying, electrostatic printing and fuel atomization.

Dole and co-workers [33] were the first who used electrospray to produce gas phase ions of macromolecules and characterize them by ion mobility spectrometry in 1968.

However, interest in electrospray did not really take off until Yamashita and Fenn [1, 2], and Gall' et al. [3] employed electrospray as a ion source for mass spectrometry in 1984. The use of this approach for mass spectrometry quickly became widespread. A very large amount of work has gone into understanding the fundamentals of the electrospray ionization (ESI) process, optimization of analytical methods utilizing ESI, and the design and development of instrumentation.

1.2.1 Mechanistic aspects of electrospray ionization

Electrospray ionization differs from classical ionization processes, such as EI, CI, in that it does not truly create ions, rather it facilitates the transfer of pre-existing solution ions to the gas phase. There are two major steps in ESI: the dispersion of a liquid into charged droplets through a controlled electrostatic spraying process and the generation of gas-phase ions from very small charged droplets. A generic description of the ESI process is given below.

A sample solution is fed through an open ended capillary tube which is held at a high potential relative to a counter electrode (e.g. the mass spectrometer sampling orifice). When a potential is applied to the capillary, an electric field exists between the capillary tip and counter electrode. The magnitude of the electric field (E) at the tip of the electrospray capillary can be calculated [34] using the following equation:

$$E = 2 V_c / r_c \ln(4d / r_c) \quad 1.1$$

where V_c is the voltage difference between the spray capillary and its counter electrode, r_c is the outer radius of the spray capillary and d is the capillary to counter electrode separation. Because the capillary spray tip is very narrow (r_c is very small), the electric field at the tip is very high ($E \approx 10^6$ V/m). The imposed field will also partially penetrate the liquid at the capillary tip. Under the influence of the electric field, (let's take the case of a positive field,) positive ions in the liquid at the tip migrate towards the surface, whereas negative ions migrate away from the surface. Such electrophoretic migration of solution ions results in a partial separation of charge at the liquid surface and the surface

acquiring an overall positive charge [35]. When the electric field is sufficiently high, the excess positive charges at the liquid surface are drawn out downfield, destabilizing the liquid surface such that the liquid surface adopts a conical shape referred to as a ‘Taylor cone’ [17] and positively charged liquid is emitted from the apex of the cone as a liquid filament. One point should be addressed here is that the conductivity of the liquid plays an important role in both the charge separation and the formation of Taylor cone by affecting the field strength imposed on the liquid. The electric field required for the onset of liquid filament emission (i.e. the onset of ES) is designated V_{on} and can be approximated by equation 1.2 [34]

$$V_{on} \approx 2 \times 10^5 (\gamma r_c)^{1/2} \ln (4d/r_c) \quad 1.2$$

Where γ is the surface tension of the solvent, r_c is the outer radius of capillary, and d is the distance between capillary tip and counter electrode. Two forces are responsible for this process. There are the repulsive force due to the excess surface charge and the holding force due to the cohesive interaction between solvent molecules. A stable Taylor cone represents a balance between the repulsive force and the holding force referred to as surface tension of a liquid. When the repulsive force exceeds the surface tension, the liquid filament forms. For this reason and the additional requirement of conductivity, polar solvents of low surface tension such as methanol, acetonitrile or isopropyl alcohol are preferred for electrospray, rather than water. Binary or ternary mixtures of these solvents and water are also commonly used.

At some distance downstream, the charged jet stream breaks apart into charged droplets (initial droplets) of roughly 1 μm in diameter. These droplets then undergo solvent evaporation. As the initial droplet shrinks, the level of excess non-volatile ions on the droplet surface remain the same. So the surface charge density increases, eventually leading to droplet instability and subsequent expulsion of a number of smaller droplets (offspring droplets) carrying a portion of the excess charge. This process is called droplet fission or Rayleigh fission. The offspring droplet emitted by this asymmetric fission carries out about 2% of the mass of the parent droplet and about 15% of the parent's

charge [34]. Both the residual parent droplets and their offspring droplets undergo the same sequence of solvent evaporation and fission continuously, generating families of smaller and smaller droplets, which forms a voluminous spray due to space-charge effects. The aerosol generated becomes finer and finer with time and distance.

It is from these very small droplets that gas phase ions are generated. The precise mechanism responsible for the generation of gas phase ions still remains unclear. Iribarne and Thomson [28,36] proposed ‘ion evaporation theory’ (IET) which suggests direct desorption of a solvated ion from the surface of a very small droplet of some critical size and charge density. An alternative explanation first proposed by Dole and co-workers [33], and later developed and renamed by Kebarle and Tang [34] is called ‘single ion in droplet theory’ (SIDT). This theory suggests that successive evaporation / fission events eventually lead to offspring droplets containing only one ion with accompanying solvation, $M(\text{solvent})_m^{n+}$ or $X(\text{solvent})_m^n$. It is these gas phase ion-solvent clusters that are sampled and detected by a mass spectrometer. The degree of solvation of the ion-solvent cluster may be controlled by mass spectrometric interface parameters that will be discussed in detail in subsequent chapters. To-date no overall consensus has been achieved on which ion generation mechanism is correct [35, 37, 38]. The observation of involatile ‘residues’ such as NaCl_2^- and Na_2Cl^+ provides evidence in support of the SIDT, meanwhile the IET may provide good explanation to the differences in analyte sensitivities which means the preferential liberation of volatile or surface active compounds. A schematic of the ESI events in air at atmospheric pressure is shown in Fig. 1.1.

1.2.2 Electrolytic Aspects of Electrospray

Considering that charge balance is required in the ES device, Kebarle and co-workers [40] initiated an investigation of the electrolytic nature of the electrospray process. For positive electrospray, a continuous mist of positive charge departs from the capillary tip (e.g. the working electrode) to the mass spectrometer sampling orifice (e.g. the counter electrode). This results in an ES current, i_{ES} , ions or coulombs per unit time, and a charge

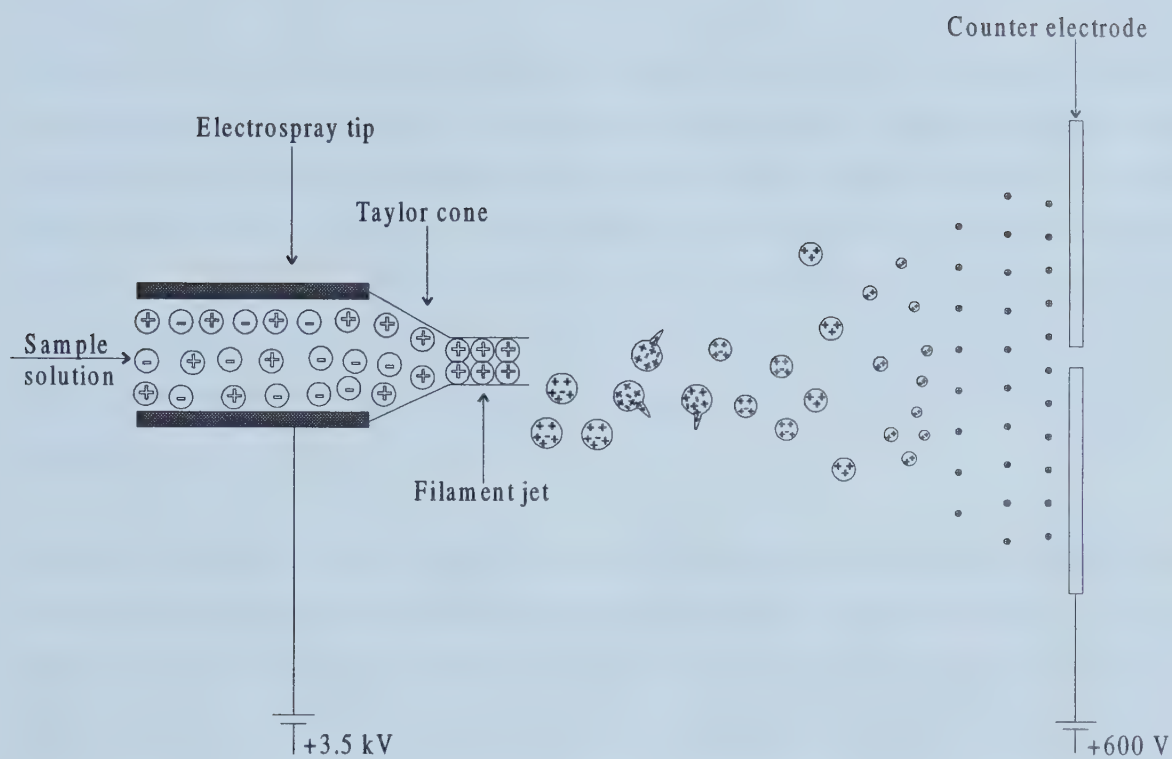


Figure 1.1 A schematic diagram of the ESI events in air at the atmospheric pressure

imbalance at both electrodes. At the counter electrode there exists an excess of positive ions whereas at the working electrode there exists an excess of negative ions. So an electrolytic processes must occur to maintain the charge balance in the ES device and charge neutrality in the analyte bulk solution, via oxidation/reduction of the excess ions or via creation of ions of the appropriate polarity, or both.

Electrons flow onto the counter electrode and result in reduction reactions which may be a conventional wet reaction as a consequence of deposition of charged droplets on the electrode surface, or an unconventional discharge upon the arrival of gas-phase ions. To balance the supply of electrons required at the counter electrode and the accumulated negative ions at the working electrode, oxidation reactions must occur within the capillary, which may be one of three sorts: a oxidation of an anion, dissolution of the working electrode (oxidation of iron from the stainless steel capillary), or ionization of a neutral species.

Electrons produced at the working electrode flow into the connecting metal wire supplying the electric potential to the electrode, resulting in a faradaic current, i_f , which should be equal in magnitude to the ES current because of charge balance considerations [41]. That is $i_{ES} = i_f$. Typical values of the ES current range from 0.05-0.1 μA for 10^{-5} - 10^{-3} M dissolved electrolyte in methanolic solution. The magnitude of i_{ES} can be related to the experimental parameters that affect i_{ES} , as shown in Equation 1.3 [34], which is originally proposed by Hendricks [42].

$$i_{ES} = A_H V_f^\nu E^\epsilon (\lambda_m^\circ C)^n \quad 1.3$$

where A_H is a constant, the value of which depends on the dielectric constant and surface tension of the solvent, V_f is the volume flow rate of the solution through the ES capillary, E is the imposed electric field at the capillary tip, λ_m° is the equivalent molar conductivity of the electrolyte, and C is the concentration of the electrolyte in solution. The product of λ_m° and C expresses the conductivity of the solution.

The reactions occurring at the working electrode are of greater interest than those at the counter electrode since they lead to a change of composition of the ions in the sprayed solution. This change could be enhanced such that the reactions at the working electrode can be used to oxidize (positive ion mode) or reduce (negative ion mode) certain types of neutral analytes for subsequent analysis. Van Berkel and co-workers [41, 43, 44] have demonstrated that an ES ion source functioning as a controlled-current electrolytic cell, when operated under appropriate conditions, generates ions of neutral, nonpolar compounds, such as aliphatic hydrocarbons and polycyclic aromatic hydrocarbons (PAH's), which are not normally amenable to ESMS since they can not be ionized by conventional acid/base solution chemistry. In addition to expanding the universality of ES as an ion source, the utility of the electrolytic processes inherent to ES has also promoted the study of electrochemistry on-line with mass spectrometry[41, 44-50].

1.2.3 Nebulization In Electrospray Ionization

As discussed in Section 1.2.1, true electrospray is the dispersion of a liquid into charged droplets through the application of an electric field. It is the electric field alone that is responsible for both nebulization and charging, which does not present a problem if the liquid's flow rate, surface tension and conductivity are low. An increase in one or more of these variables makes it more difficult for the electric field to nebulize the liquid into the desired charged aerosol. When one or more of these variables are very high, the liquid would jet out from the spray tip in a continuous stream without forming a charged spray [51]. The electric field strength can be increased to try and overcome the adverse effect of these variables, but too high an electric field will give rise to an electric discharge (i. e. a corona discharge) and subsequent ionization of ambient gaseous molecules including atmospheric gases and solvent vapors. An electric discharge is particularly troublesome in the formation of negatively charged droplets since the spray capillary is biased to a high negative potential and is thus electron rich. Reduction of the tendency towards electric discharge generally involves using a smooth, uniform capillary tip, volatile solvents and capture of electrons by means of adding electron-scavenging gases, such as O_2 , CO_2 , and SF_6 to the region surrounding the spray capillary[52-54]. The inability of

pure electrospray to be used with sample solutions which have high conductivity, high surface tension and volumetric flow rate exceeding approximately 8 $\mu\text{L}/\text{min}$ has placed severe limits on the range of its application including the coupling of electrospray with liquid chromatography.

Modifications to conventional unassisted electrospray have been developed to increase the tolerance towards liquid flow rate and matrix variation. Coaxial addition of a sheath flow of organic solvents to the aqueous sample solution was used to reduce surface tension[55]. In this technique, it is still the electric field alone that is used to disperse and charge the liquid in one operation. From experience with pneumatic nebulizers, Bruins et al. [56] proposed a pneumatically assisted electrospray system, called ionspray, wherein a nebulizing gas blowing coaxially around the spray capillary assists the aerosol formation while the electric field charges the droplets. This combination of pneumatic nebulization and an electric field is more tolerant of higher liquid flow rate and is less susceptible to various compositions of the sprayed solution, therefore, overcoming the non-robust nature of electrospray to some degree. As a result, ionspray has gained widespread application for aqueous sample analysis and coupling capillary electrophoresis and liquid chromatography. However, ionpray presents several drawbacks. Since the formation and direction of the spray are mostly controlled by the high velocity gas flow, the ionspray source must be positioned off-axis to the mass spectrometer to avoid penetration of droplets and liquid solvent into the vacuum system, which leads to analyte signal attenuation. Mass spectra acquired with an ionspray source tend to be very dependent on the relative position of the source [57] and suffer from high levels of ion adducts.

Banks et al. suggested that the aerosol could also be produced by some mechanical means, i. e., ultrasonic vibration, and developed an ultrasonically assisted electrospray system[51, 58]. It offers advantages similar to ionspray, but is a more complex and more expensive combination of mechanical and electronic devices.

1.3 Electrospray Mass Spectrometry

Since the pioneering work by Yamashita and Fenn[1, 2], and Gall' et al. [3] in 1984 on the coupling of electrospray with mass spectrometry, the use of ESMS has quickly become a valuable analytical tool of extraordinary utility. A electrospray ion source offers a relatively simple means to transfer non-volatile solution phase ions and polar molecules to the gas phase. It has allowed observation of mass spectra for very large molecules such as proteins [59] since these species are subject to multiple protonation. The mildness of the electrospray ionization process ensures little sample fragmentation, therefore molecular ions of fragile molecules and thermally-sensitive compounds can be observed. Important solution information such as intact chemical forms and oxidation states of target ions tend to be preserved as well. Combining the sensitive and direct detection of mass spectrometry, ESMS has gained application with enormous scope embracing analytical inorganic, organic, organometallic, synthetic polymer and biological chemistry.

1.3.1 Electrospray interface

The function of the electrospray interface is to sample gas phase ions from the atmosphere into the vacuum of the mass spectrometer. With the appropriate atmospheric pressure interface, virtually any mass spectrometer may be used to mass analyze electrospray generated ions. Most electrospray interfaces involve a two-stage pumping system in order to handle the gas load. The interface usually consists of a sampling plate with a small diameter orifice through which gas at atmospheric pressure expands into a low-pressure region (~ 1 torr), referred to as expansion region that is immediately behind the sampling plate. The expanding gas, consisting of ion-solvent clusters and neutrals (predominantly N_2 curtain gas) is then further sampled by a skimmer from which ions are guided with the appropriate ion optics into the mass analyzer. A schematic of the sampler-skimmer interface is shown in Fig. 1.2. The specifics of the interface are presented in the next chapter.

The expansion region located between the sampling plate and the skimmer plays an important role in the analytical performance of ESMS. In addition to completing analyte

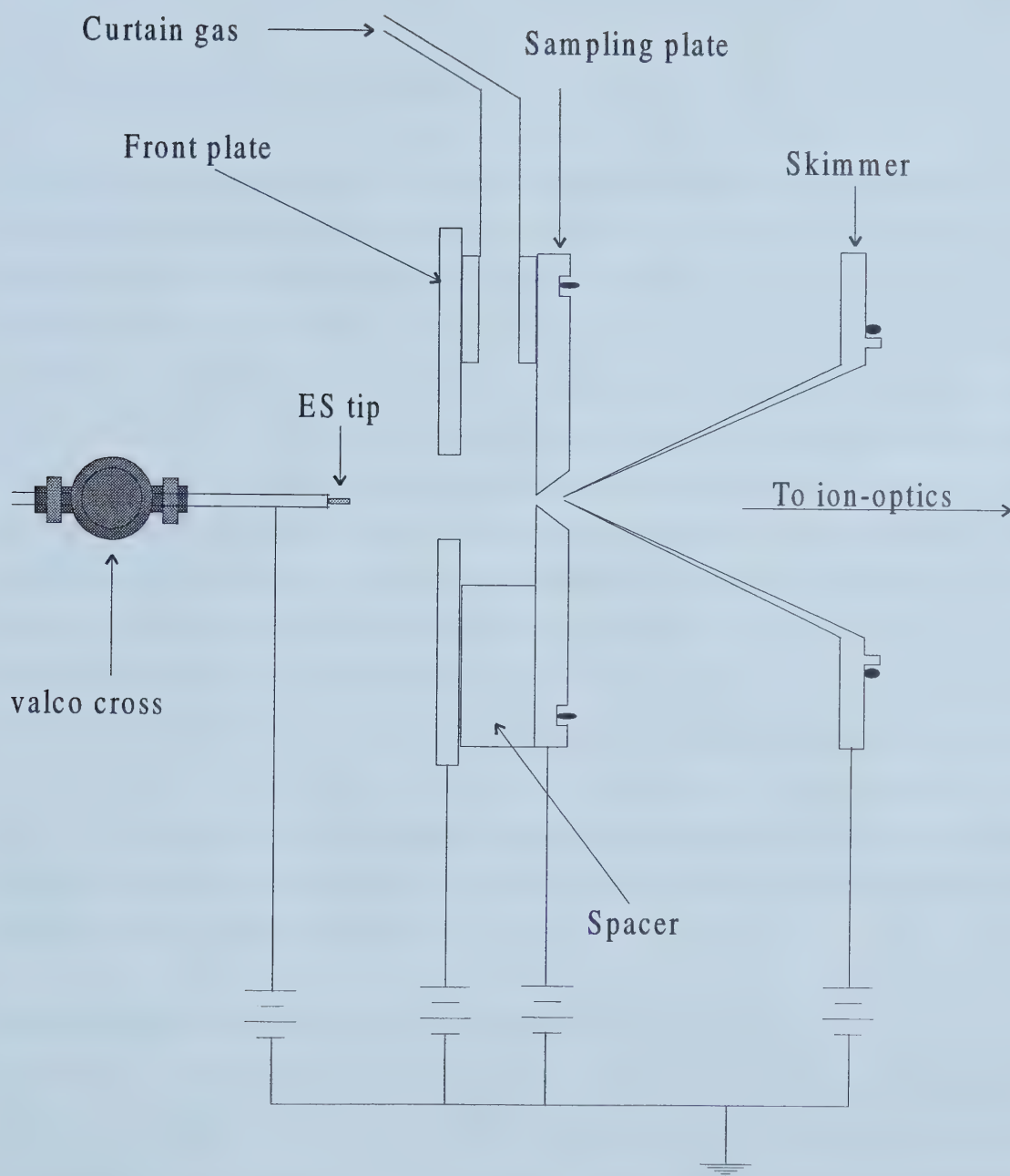


Figure 1.2 Schematics of the sampler-skimmer interface

desolvation as a fundamental part of the technique, it can also be used as a collision cell for generation of fragment ions. Such collision induced dissociation (CID) in the interface region is commonly referred to as 'high pressure' or 'up front' (1 torr) CID.

1.3.2 Collision Induced Dissociation

The collisions in the expansion region happen between ions and neutrals. In most electrospray environments, the ambient atmosphere is rich in solvent molecules due to the evaporation of charged droplets. So most electrospray interfaces employ the counter electrode in the form of a plate, called a front plate, with a relatively large orifice that precedes the sampling orifice. In addition, nitrogen gas referred to as the curtain gas is introduced between the front plate and the sampling plate to remove solvent vapor and to help the drying of droplets and solvated ions. Analyte ion-solvent clusters or 'nano-droplets' along with other species (predominantly nitrogen gas) pass through the sampling orifice as a result of the pressure differential across the sampling plate. Both neutral species and ions will be accelerated into the free jet expansion. However, when a potential difference is applied between the sampling plate and the skimmer, charged species are accelerated with respect to neutral species, resulting in energetic neutral/ion collisions. The energy and frequency of collisions are dependent on the magnitude of the applied potential difference and gas density in the region. If the relative amount of background gas including curtain gas is considered constant, then the extent of CID is controlled by the potential difference.

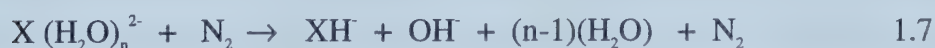
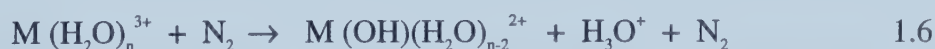
Collision induced dissociation has important analytical implications because it can significantly modify the form of ions recorded at the mass spectrometer. It can result in processes as simple as the loss of solvent resulting in bare ions, or as severe as the fragmentation of a molecular ion. Ion pairs and adducts may also be generated. Concerning the application of ESMS to inorganic and elemental species, Horlick and colleagues have given some interpretation of the decomposition pathways of metal ion-solvent clusters in the expansion region [60-64].

As previously discussed, it is gas phase ion-solvent clusters and ‘nano-droplets’ that are sampled by the ES interface. Removal of the solvent sphere is facilitated somewhat through the flow of curtain gas, but mainly through high pressure CID. The magnitude of the potential difference required for desolvation varies with different analytes. Ions of high charge density or low polarizability will require a higher declustering voltage difference. For monovalent inorganic ions, the desolvation process is simple and summarized by the following equations[65]:



Where M^+ and X^- are singly charged metal cations (e. g. alkali metals) and simple anions (e. g. halides), respectively. The mass spectra observed are simple even at mild desolvating conditions. Confirmation of identity can be accomplished by going from relatively gentle CID conditions which show the solvated distribution of an ion to harsh conditions whereby solvating ligands are removed sequentially leaving only a ‘bare’ metal ion.

For multiply charged ions, the desolvation process becomes more complicated. When the diminished solvation sphere is no longer able to stabilize the multiple charge on the metal ion center, the overall charge of the cluster ion is reduced through the ionization of one of the solvent ligands. A general reaction scheme for this process, referred to as charge separation or charge reduction, is presented below:



The form of the above reaction is similar to that of metal ion hydrolysis reactions in solution. The product formed therefore contains a new coordinate covalent bond (e. g. the metal-ligand bond]. Continual desolvation might result in further charge reduction:



Jayaweera et al. [66], Blades et al. [67-69] and Stewart [39] have described the charge reduction process for multiply charged metal ion clusters in some detail. Among the important factors that influence the extent of charge separation or charge reduction are the relative ionization potentials or electron affinities of analyte and solvent, and the dissociation energy of the metal-ligand bond as well. Large values of ionization potential of metallic analyte, small values of ionization potential of solvent, and large values of the dissociation energy of the metal-ligand bond will contribute favorably to charge reduction. As a rule of thumb, charge reduced species form when $IE(M^{n+}) > IE(L)$ (where L refers to solvent ligand), and the tendency to form charge reduced species declines when $IE(M^{n+}) < IE(L)$.

Under harsh CID conditions, which means the potential differences between the sampling plate and skimmer is in excess of 80 volts in most cases, not only the solvent sheath of an analyte is removed completely, but also fragmentation of the molecular form of the analyte occurs, such as:



where MO_n^- is a generic oxo-anion. High pressure CID, although efficient, is generally difficult to control and is not selective since there is no means to isolate for a particular parent ion, which can result in a very complex spectrum for multi-component solutions. However, skilled manipulation of the interface voltages does enable electrospray to be operated as a multiple mode ion source which can generate both atomic and molecular spectra from the same sample components [70]. Chromatographic separation

methodology may also be used to simplify spectra by reducing the number of analyte species in the CID region at a particular time.

1.4 Flow Injection Electrospray Mass Spectrometry

1.4.1 Flow Injection Analysis (FIA)

Since Ruzicka and Hansen proposed the concept of flow injection analysis in 1975 [71], FIA has been intensively developed and widely applied in many areas. It was originally designed to automate serial assays, and quickly emerged as a general solution handling and information gathering technique, applicable to a variety of tasks such as titration, pH and conductivity measurements, enzymatic assays etc[72-78].

In FIA, a small sample is injected into a flowing liquid stream which may act as both a carrier and reagent. The sample zone may undergo controlled dispersion and reaction, forming species which are sensed by a suitable detector. The transient signal recorded during the passage of the dispersed sample zone has the form of a peak, the height, width, or area of which contains the analytical information. Most FIA systems are constructed with pumps, injection ports, reaction coils, detectors and readout devices. The system resembles that of liquid chromatography in which the column has been replaced by the reaction coil. As a result of this replacement, a FIA system is operated at a low back pressure. A schematic of a FIA method is shown in Fig.1.3.

Outstanding features of FIA are shorter analysis time than in conventional, manual procedures, reduced human participation in time-consuming operations, and versatility. In its simplest form, FIA provides a means of transporting samples to a detector quickly and reproducibly. An example of this is the combination of FIA with atomic spectrometry (flame absorption and emission spectrometry and inductively-coupled plasma emission and mass spectrometry) [79]. A great deal of the interest is in the possible benefits offered by FIA in on-line sample pretreatment and matrix removal

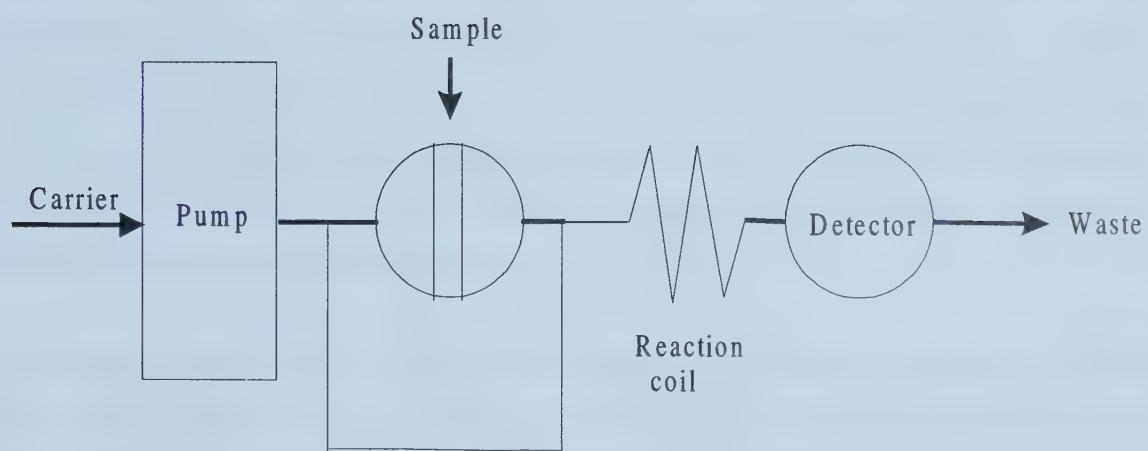


Figure 1.3 Schematic of a FIA method

in addition to high sampling rate, minimum sample consumption and automation. Other commonly used detectors in FIA are electrochemical detectors and optical detectors[80].

1.4.2 Flow Injection Electrospray Mass Spectrometry

A very large amount of work on the instrumentation development of ESMS has gone into the elements of ES ion source design. A literature search gave very few results on the development of sample introduction methods. The sample introduction tools commonly employed in stand-alone ESMS fall into the category of continuous sample delivery leading to steady-state analyte signals. Changing sample involves manual handling of washing, connecting, and syringe operation, which takes considerable time when a number of samples are to be analyzed.

Although no results were obtained in the search for publications containing the words flow injection and electrospray mass spectrometry in the title, the combination of these two techniques should be worthwhile. The adaption of flow injection techniques to electrospray mass spectrometry provides the benefits of reduced manual operation, minimum sample consumption, fast sampling rate, and ease of automation. In addition, it presents the encouraging promise of ESMS as a versatile detector for FIA, therefore, exhibiting the extraordinary potential of FI-ESMS as a generic routine analysis tool.

1.5 References

1. Yamashita, M.; Fenn, J. B., *J. Phys. Chem.*, **1984**, 88, 4451-4459.
2. Yamashita, M.; Fenn, J. B., *J. Phys. Chem.*, **1984**, 88, 4671-4675.
3. Gall, L. N.; Krasnov, N. V.; Yu, S.; Kusner, V. I.; Nikolaev, V. G.; Siminova, G. V., *Sov. Phys. Tech. Phys.* **1984**, 29, 911-918.
4. Hop, C. E. C. A.; Bakhtiar, R., *J. Chem. Ed.*, **1996**, 73, A162-A169.
5. Ruzicka, J.; Hansen, E. H., *Flow Injection Analysis*, 2nd edn., Wiley, New York, 1988.
6. Zeleny, J., *Phys. Rev.*, **1914**, 3, 69-91.
7. Zeleny, J., *Proc. Cambridge Philos. Soc.*, **1915**, 18, 71-83.
8. Zeleny, J., *Phys. Rev.*, **1917**, 10, 1-6.
9. Cloupeau, M.; Prunet-Foch, B., *J. Electrostatics*, **1989**, 22, 135-139.
10. Cloupeau, M.; Prunet-Foch, B., *J. Electrostatics*, **1990**, 25, 165-184.
11. Cloupeau, M., *J. Aerosol Sci.*, **1994**, 25, 1143-1157.
12. Cloupeau, M.; Prunet-Foch, B., *J. Aerosol Sci.*, **1994**, 25, 1021-1036.
13. Ganan-Calvo, A. M.; Lasheras, J. C.; Davila, J.; Barrero, A., *J. Aerosol Sci.*, **1994**, 25, 1121-1142.
14. Kelly, A. J., *J. Aerosol Sci.*, **1994**, 25, 1159-1177.
15. Grace, J. M.; Marijnissen, J. C. M., *J. Aerosol Sci.*, **1994**, 25, 1005-1019.
16. Mora, J. F. D. L.; Loscertales, I. G., *J. Fluid Mech.*, **1994**, 260, 155-184.
17. Taylor, G. I., *Proc. Roy. Soc. Lond. A.*, **1964**, 280, 383-397.
18. Taylor, G. I., *Proc. Roy. Soc. Lond. A.*, **1969**, 313, 453.
19. Hamdam, M.; Curcuruto, O., *Int. J. Mass. Spectrom. Ion. Proc.* **1991**, 108, 93-113.
20. Bruins, A. P., *J. Chim. Phys.*, **1993**, 90, 1335-1344.

- 21 Gomez, A.; Tang, K., *Phys. Fluids*, **1994**, 6, 404-414.
- 22 Chen, D. R.; Pui, D. Y. H.; Kaufman, S. L., *J. Aerosol Sci.*, **1995**, 26, 963-977.
- 23 Hayati, I.; Bailey, A.; Tadros, T. F., *J. Coll. Int. Sci.*, **1986**, 117, 222-230.
- 24 Hayati, I.; Bailey, A.; Tadros, T. F., *J. Coll. Int. Sci.*, **1986**, 117, 205-221.
- 25 Hayati, I.; Bailey, A.; Tadros, T. F., *Nature*, **1986**, 319, 41-43.
- 26 Grigor'ev, A. I.; Shir'aeva, S. O., *J. Phys. D: Appl. Phys.*, **1990**, 23, 1361-1370.
- 27 Wilm, M. S.; Mann, M., *Int. J. Mass. Spectrom. Ion. Proc.* **1994**, 136, 167-180.
- 28 Thomson, B. A.; Iribarne, J. V., *J. Chem. Phys.*, **1979**, 71, 4451-4463.
- 29 McCreery, D. A.; Gross, M. L., *Anal. Chim. Acta*, **1985**, 178, 105-116.
- 30 Gotz, R.; Elgersma, J.W.; Kraak, J. C.; Poppe, H., *Spectrochim.Acta B*, **1994**, 49, 761-768.
- 31 Elgersma, J.W.; Kraak, J. C.; Poppe, H., *J. Anal. Atom. Spectrom.*, **1997**, 12, 1065-1068.
- 32 Raynor, M. W.; Dawson, G. D.; Balcerzak, M.; Pretorius, W. G.; Ebdon, L., *J. Anal. Atom. Spectrom.*, **1997**, 12, 1057-1064.
- 33 Dole, M.; Mack, L. L.; Hines, R. L.; Mobley, R. C.; Ferguson, L. D.; Alice, M. B. *J. Chem. Phys.*, **1968**, 49, 2240-2249.
- 34 Kebarle, P.; Tang, L., *Anal. Chem.*, **1993**, 65, 972A-986A.
- 35 Kebarle, P.; Ho, Y., In *Electrospray ionization mass spectrometry*; Cole, R. B., Ed.; John Wiley & Sons: New York, 1997, pp 3-63.
- 36 Iribarne, J. V.; Thomson, B. A., *J. Chem. Phys.*, **1976**, 64, 2287-2294.
- 37 Ashton, D. S.; Beddell, C. R.; Cooper, D. J.; Green, B. N.; Oliver, R. W. A., *Org. Mass Spectrom.*, **1993**, 28, 721-728.
- 38 Siu, K. W. M.; Geuvremont, R.; LeBlanc, J. C. Y.; O'Brien, R. T.; Berman, S. S., *Org. Mass Spectrom.*, **1993**, 28, 579-584.
- 39 Stewart, I. I., *Spectrochim.Acta B*, **1999**, 54, 1649-1695.
- 40 Blades, A. T.; Ikonomou, M. G.; Kebarle, P., *Anal. Chem.*, **1991**, 63, 2109-2114.

- 41 Van Berkel, G. J.; Zhou, F., *Anal. Chem.*, **1995**, 67, 3958-3964.
- 42 Pfeifer, R. J.; Hendricks, C. D., *AIAA J.*, **1968**, 6, 496.
- 43 Van Berkel, G. J.; McLckey, S. A.; Glish, G. L., *Anal. Chem.*, **1992**, 64, 1586-1593.
- 44 Van Berkel, G. J.; Zhou, F., *Anal. Chem.*, **1995**, 67, 2916-2923.
- 45 Van Berkel, G. J.; Zhou, F., *Anal. Chem.*, **1994**, 66, 3408-3415.
- 46 Zhou, F.; Van Berkel, G. J., *Anal. Chem.*, **1995**, 67, 3643-3649
- 47 Van Berkel, G. J.; Zhou, F.; Aronson, J. T., *Int. J. Mass Spectrom., Ion Processes*, **1997**, 162, 55-57.
- 48 Van Berkel, G. J., *J. Anal. Atom. Spectrom.*, **1998**, 13, 603-607.
- 49 Bond, A. M.; Colton, R.; D'Agostino, A.; Downard, A. J.; Traeger, J. C., *Anal. Chem.*, **1995**, 67, 1691-1695.
- 50 Pretty, J. R.; Van Berkel, G. J., *Rapid Commun. Mass Spectrom.*, **1998**, 12, 1644-1652.
- 51 Banks, J. F., Jr.; Quinn, J. P.; Whitehouse, C. M., *Anal. Chem.*, **1994**, 66, 3688-3695.
- 52 Chowdhury, S. K.; Chait, B. T., *Anal. Chem.*, **1991**, 63, 1660-1664.
- 53 Wampler, F. M.; Blades, A. T.; Kebarle, P., *J. Am. Soc. Mass Spectrom.*, **1993**, 4, 289-295.
- 54 Ikonomou, M. G.; Blades, A. T.; Kebarle, P., *J. Am. Soc. Mass Spectrom.*, **1991**, 2, 497-505.
- 55 Bruins, A. P., *J. Chrom. A*, **1998**, 794, 345-357.
- 56 Bruins, A. P.; Covey, T. R.; Henion, J. D., *Anal. Chem.*, **1987**, 59, 2642-2646.
- 57 Olesik, J. W.; Thaxton, K. K.; Olesik, S. V., *J. Anal. At. Spectrom.*, **1997**, 12, 507-516.
- 58 Banks, J. F., Jr.; Shen, S.; Whitehouse, C. M.; Fenn, J. B., *Anal. Chem.*, **1994**, 66, 406-414.

- 59 Colton, R.; D'Agostino, A.; Downard, A. J.; Traeger, J. C., *Mass Spectrom. Rev.*, **1995**, 14, 79-106.
- 60 Agnes, G. R.; Horlick, G., *Appl. Spectrosc.*, **1994**, 48, 655-661.
- 61 Agnes, G. R.; Horlick, G., *Appl. Spectrosc.*, **1995**, 49, 324-334.
- 62 Agnes, G. R.; Stewart, I. I.; Horlick, G., *Appl. Spectrosc.*, **1994**, 48, 1347-1359.
- 63 Stewart, I. I.; Horlick, G., *J. Anal. At. Spectrom.*, **1996**, 11, 1203-1214.
- 64 Stewart, I. I.; Barnett, D. A.; Horlick, G., *J. Anal. At. Spectrom.*, **1996**, 11, 877-886.
- 65 Barnett, D. A., Ph. D. Thesis, University of Alberta, Edmonton, Alberta. 1999.
- 66 Jayaweera, P.; Blades, A. T.; Ikonomou, M. G.; Kebarle, P., *J. Am. Chem. Soc.* **1990**, 112, 2452-2454.
- 67 Blades, A. T.; Jayaweera, P.; Ikonomou, M. G.; Kebarle, P., *J. Chem. Phys.* **1990**, 92, 5900-5906.
- 68 Blades, A. T.; Jayaweera, P.; Ikonomou, M. G.; Kebarle, P., *Int. J. Mass Spectrom., Ion Processes*, **1990**, 101, 325-336.
- 69 Blades, A. T.; Jayaweera, P.; Ikonomou, M. G.; Kebarle, P., *Int. J. Mass Spectrom., Ion Processes*, **1990**, 102, 251-267.
- 70 Agnes, G. R., Ph. D. Thesis, University of Alberta, Edmonton, Alberta. 1994.
- 71 Ruzicka, J.; Hansen, E. H., *Anal. Chim. Acta*, **1975**, 78, 145.
- 72 Ruzicka, J.; Hansen, E. H.; Mosbæk, H., *Anal. Chim. Acta*, **1977**, 92, 235.
- 73 Bergamin F, H.; Medeiros, J. X.; Reis, B. F.; Zagatto, E. A. G., *Anal. Chim. Acta*, **1978**, 101, 9.
- 74 Ramsing, A. U.; Janata, J.; Ruzicka, J.; Levy, M., *Anal. Chim. Acta*, **1980**, 118, 45
- 75 Kelly, T. A.; Christian, G. D., *Talanta*, **1982**, 29, 1109.
- 76 Olsson, B.; Ogren, L.; Johansson, G., *Anal. Chim. Acta*, **1983**, 145, 101-108.
- 77 Abdullahi, G. L.; Miller, J. N.; Sturley, H. N.; Bridges, J. W., *Anal. Chim. Acta*, **1983**, 145, 109-116.

- 78 Worsfold, P. J., *Anal. Chim. Acta*, **1983**, 145, 117.
- 79 Tyson, J. F., *Anal. Chim. Acta*, **1988**, 214, 57-75.
- 80 Ruzicka, J.; Hansen, E. H., *Flow Injection Analysis*, 2nd edn., Wiley, New York, 1988.

Chapter 2

Instrumentation

2.1 Introduction

This chapter is devoted to a discussion of the instrumentation used for the work in this thesis, with emphasis on the design of an electrospray ion source employing a flow injection sample introduction device. In considering stand-alone electrospray ion sources, the most widely used sample introduction method is continuous delivery of samples by a pump. An example of a continuous sample delivery electrospray source which was developed by Barnett [1], is shown in Fig. 2.1. A length of fused silica capillary (FSC) coated with a 17 μm thick layer of polyimide, was used as both the sample transfer line and the spraying capillary. A tee union was used to hold the capillary in a fixed position inside a stainless steel support tubing. The right port of the tee was used to hold the steel tubing. The left port of the tee was lined with a flexible Teflon insert that when tightened held the FSC firmly in place and formed an airtight seal. The bottom port was used for introduction of a low flow of dry helium, not to pneumatically nebulize the sprayed solution, but to dry the outer wall of the capillary after rinsing the system with sample. The gas flow was stopped prior to collection of spectra due to its flow being detrimental to both signal stability and sensitivity. The length of FSC that protrudes from the end of the steel support tubing is between 1.5 to 2.5 mm. The sample solution was pumped through the FSC to the spray tip at flow rates ranging from 0.5 to about 10 $\mu\text{L}/\text{min}$ by a syringe pump. Electrical contact with the solution was accomplished by connecting a high voltage lead to the stainless steel luer adapter of the syringe. A high voltage was also applied to the steel support tubing resulting in the formation of a 'sheath' electric field.

The connection between the sample syringe and the FSC is depicted in Fig. 2.2. Teflon sleeves were mounted inside both 1/16" nuts of a internal union. The capillary passed through the union uninterrupted, held in place by the Teflon insert on the right side of the union. After loading the sample syringe, the FSC was inserted into the steel needle of the luer adapter, the steel needle was then inserted through the 1 mm Teflon insert on the left side of the union and sealed by tightening the nut.

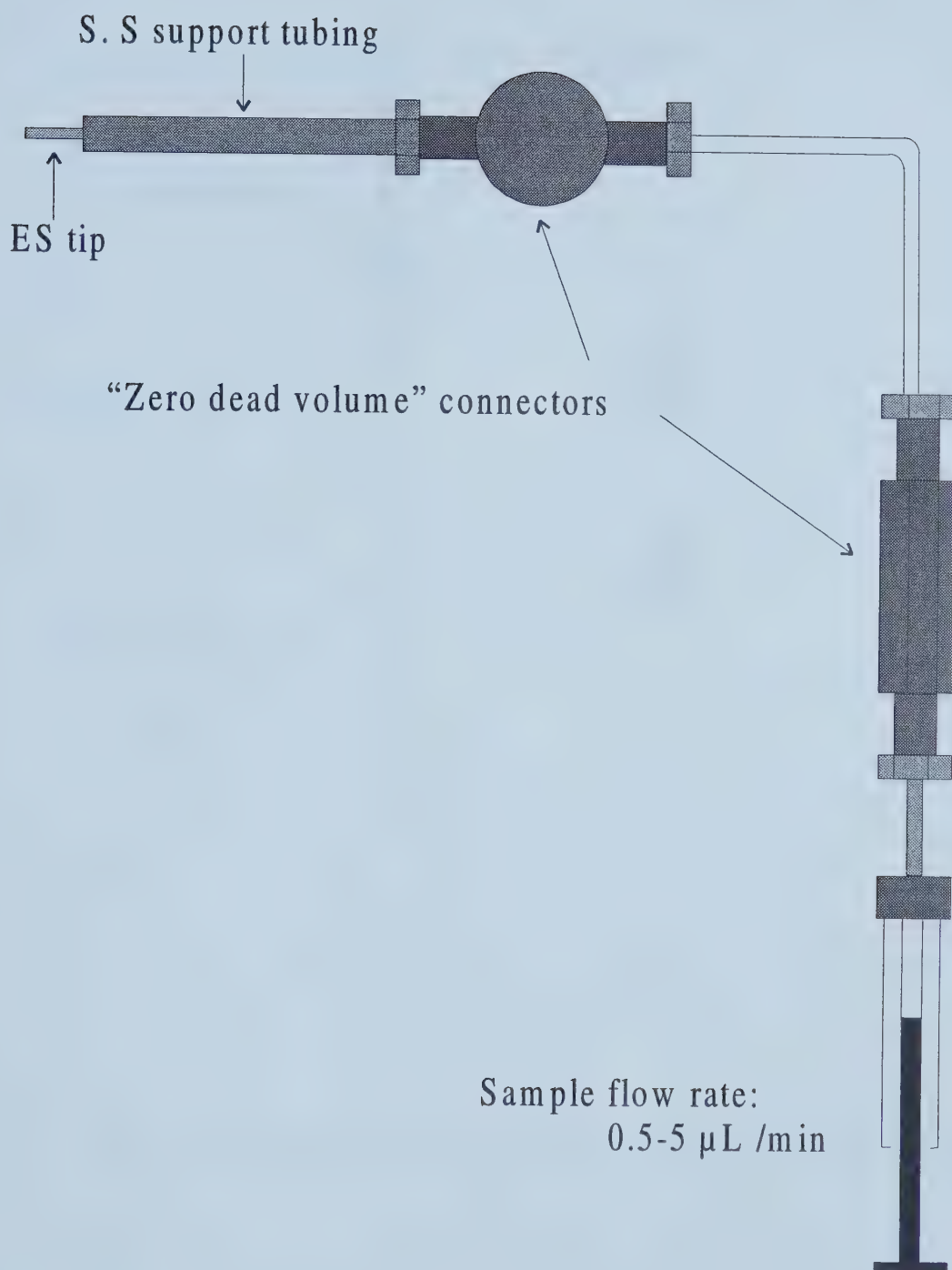


Figure 2.1 Schematic diagram of continuous sample delivery electrospray source

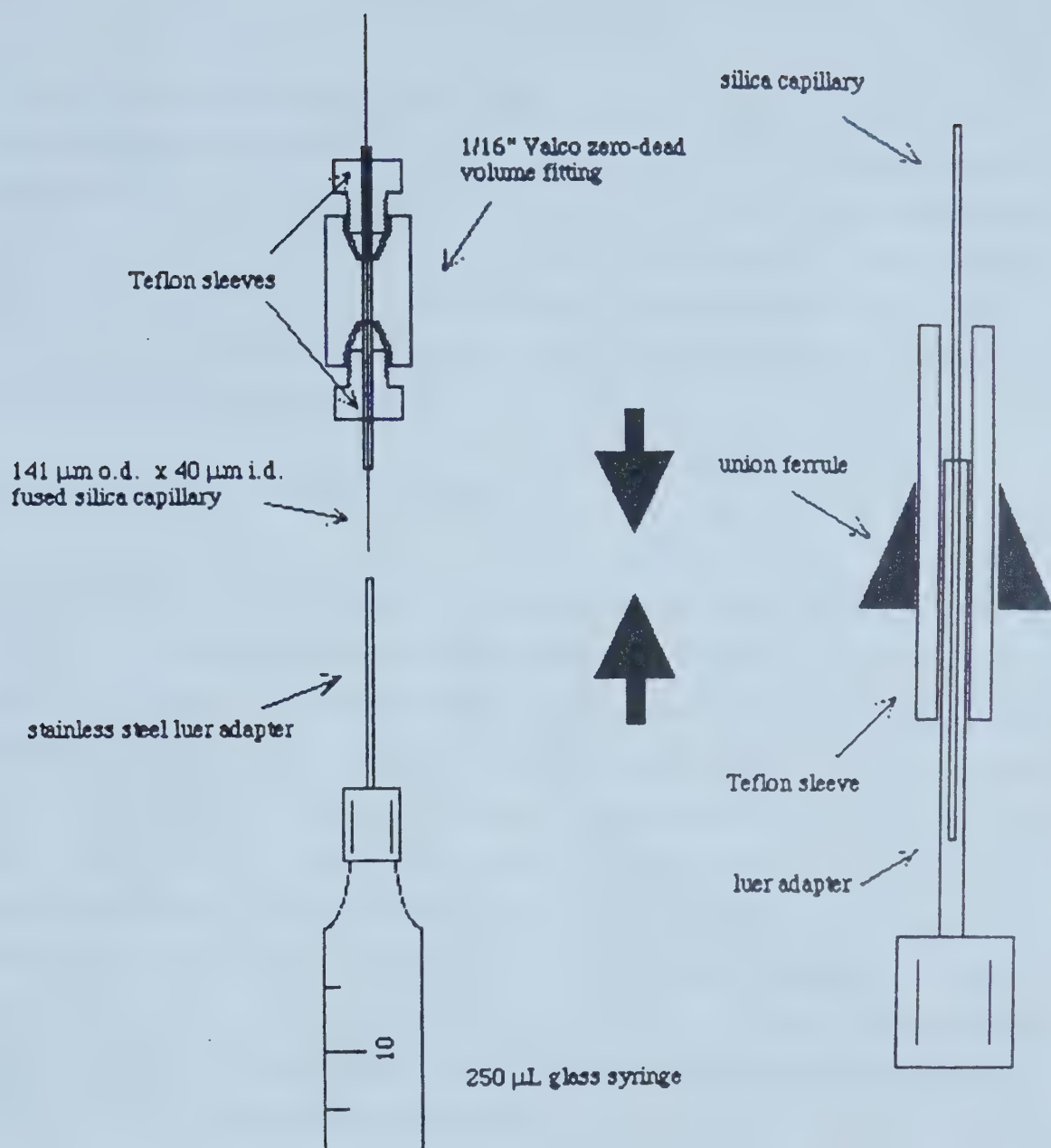


Fig. 2.2: The syringe to fused silica capillary connection.

There is a major disadvantage to this design. For one change of sample solution, disassembling and assembling the sample syringe and FSC must be performed twice for loading the wash liquid and sample solution in turn. Adding the washing of the sample transfer line and handling of the syringe, it takes about 5 minutes to change samples. This low sampling rate and manual operation is a serious shortcoming when a number of samples are to be analyzed as in routine analysis. It is therefore desirable to develop new methods for sample introduction.

2.2 Flow Injection Electrospray Source

The configuration of a flow injection electrospray system is shown in Fig. 2.3. A tiny portion of an approximately 20 cm length of FSC coated with a 17 μm thick layer of polyimide, referred to as the electrospray capillary, served as the electrospray tip. The dimensions of electrospray capillary are important features which were 150 μm outer diameter and 30 μm inner diameter. A two port cross supplied by Valco (Houston, TX) was utilized to hold the electrospray capillary in a fixed position inside a wide bore stainless steel tubing (1/16" o.d. \times 250 μm i.d. \times 10 cm) used for structure support and electric contact. The length of the ES tip that protrudes from the end of the steel support tubing was between 1.0 to 4 mm. The right port of the cross was used to hold the steel support tubing. The left port of the cross was lined with a flexible Teflon insert that when tightened held the spray capillary firmly in place.

A modified two position 4-port internal chromatographic injector (Cheminert C4-1004.02 A) was employed to perform flow injection. Its sample inlet port, labeled S, was connected to a peristaltic pump through a 20 cm length of Teflon tubing (1/16" o.d. \times 250 μm i.d.). The inlet tubing of the peristaltic pump was inserted into a vial containing a sample solution. A carrier liquid was delivered into the inlet port labeled P through a 30 cm length of FSC with dimensions of 151 μm o.d. and 41 μm i.d. by a syringe pump (Harvard Apparatus, model 22) at flow rates range from 0.5 to 8 $\mu\text{L}/\text{min}$. The outlet port labeled C was joined with the electrospray capillary through which both carrier and sample solutions were transferred toward the spray tip. Another 20 cm long Teflon tubing

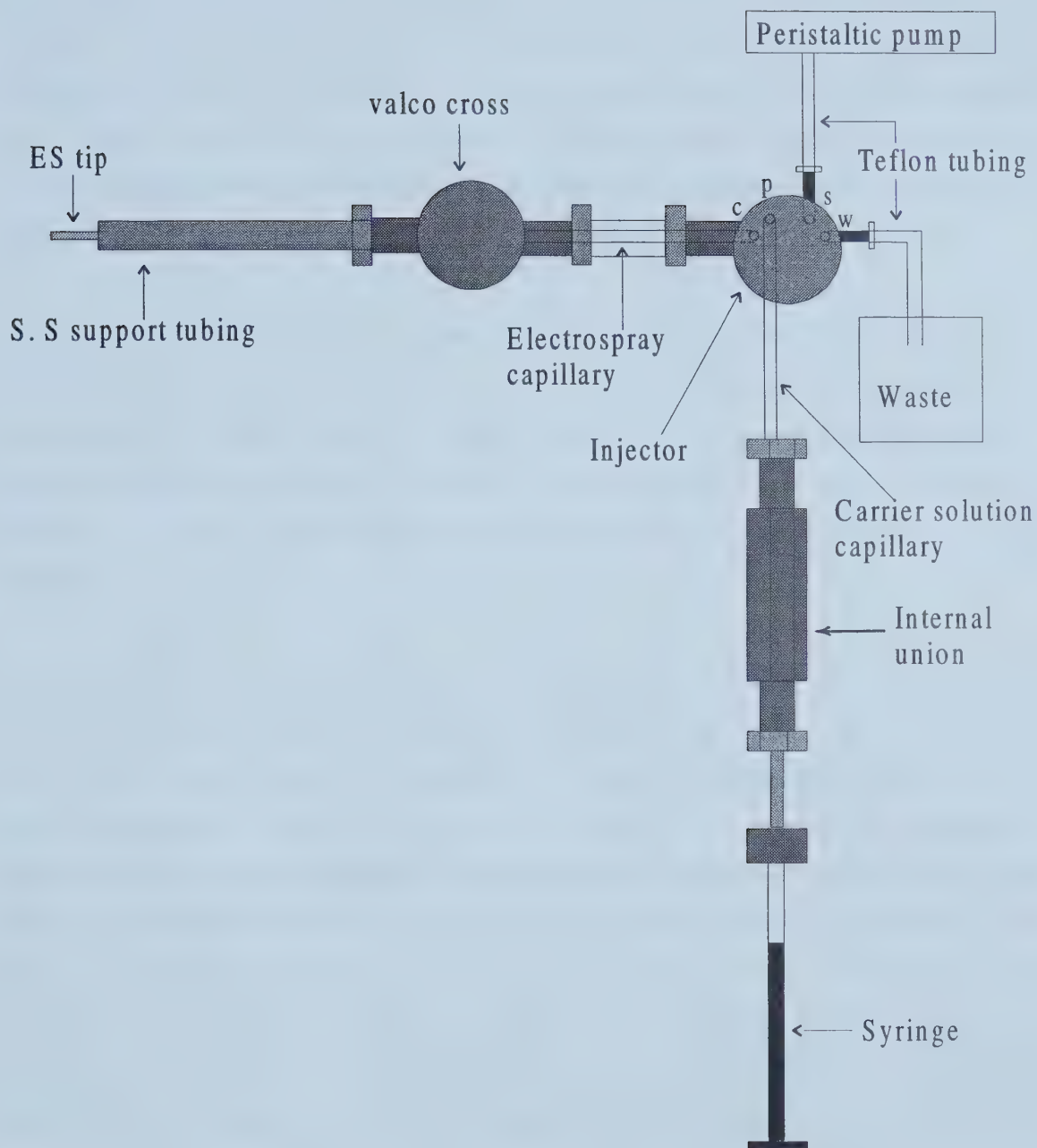


Figure 2.3 Flow injection electrospray ion source

(1/16" o.d. \times 250 μ m i.d.) was connected to the outlet port labeled W as the waste line.

The connection between the carrier capillary and the stainless steel luer adapter of the syringe is similar to that in continuous sample introduction, shown in Fig. 2.2. A potential of 3.0-4.0 kV was applied to the steel support tubing resulting in the formation of a 'sheath' electric field. A potential of 5.0-9.0 kV was applied to the liquid by connecting a high voltage lead to the injector. Those bias voltages were provided by EH-series (0-10 kV) Glassman high-voltage power supplies.

The wide bore stainless steel support tubing was mounted on a three-dimensional translation stage and positioned on axis with the sampling orifice of the mass spectrometer. The spray tip and its support tubing were electrically isolated from the translation stage by a cylindrical (10 cm \times 2.5 cm diameter) Teflon mount. The injector was set in a plastic case for electrical isolation and pneumatically actuated by using N₂ (58 psi).

A detailed view of the modified injector is shown in Fig. 2.4. The original two position 4 port internal injector supplied by Cheminert, shown in Fig. 2.5, consists of a stator, a rotor, and a sample plate. It is designed for a liquid chromatography system operated under high pressure from 5000 psi up to 7000 psi. With the original chromatographic injector, the electrospray behavior of the system was unreliable. The transient signal appeared significantly different from injection to injection with the same solution injected under exactly the same conditions. The reason may be related to the low back pressure in the flow injection electrospray system using an open end capillary without any packing. The high pressure designed chromatographic injector may have features that interfere with the FI-ES system of low pressure design[2]. This incompatibility was substantially overcome by inserting a 2 mm thick flat ring, made of brass, between the stator and rotor of the injector.

There are 4 holes, labeled S, P, C, W, on the stator which is held at a constant, pre-set force against the rotor. The positions of the holes were held fixed during the operation. The rotor holds the sample plate and can be put into two positions: load and inject, which

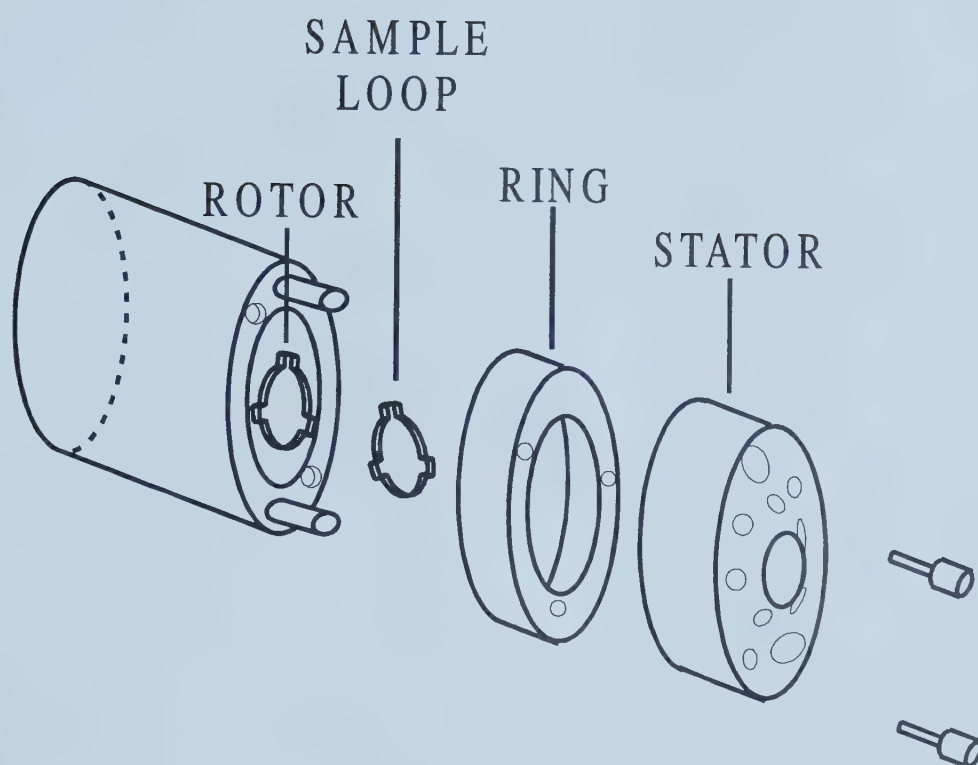


Figure 2.4 A detailed view of the modified injector

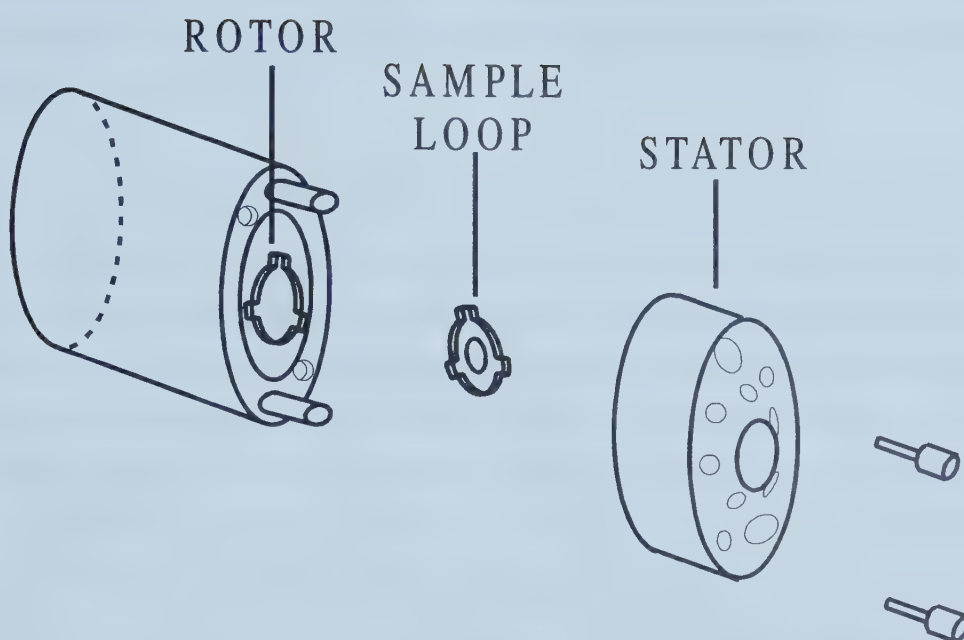


Figure 2.5 An expanded view of the original two position 4 port internal injector, supplied by Cheminert

is controlled by a switch. The flat sample plate which can be rotated along with the rotor was engraved with slots. These slots are in line with the holes on the stator when the rotor and stator are joined together by two screws. An expanded view of the stator and an example of the flat sample plates are shown in Fig. 2.6. There are three slots engraved on a sample plate. The middle slot is the sample 'loop' which connects two ports on the stator and is sized to contain an exact, specified amount of sample volume. With different depth and shape of the sample slot, 5 types of sample sizes are available, which are 0.02, 0.05, 0.1, 0.2, 0.5 μL .

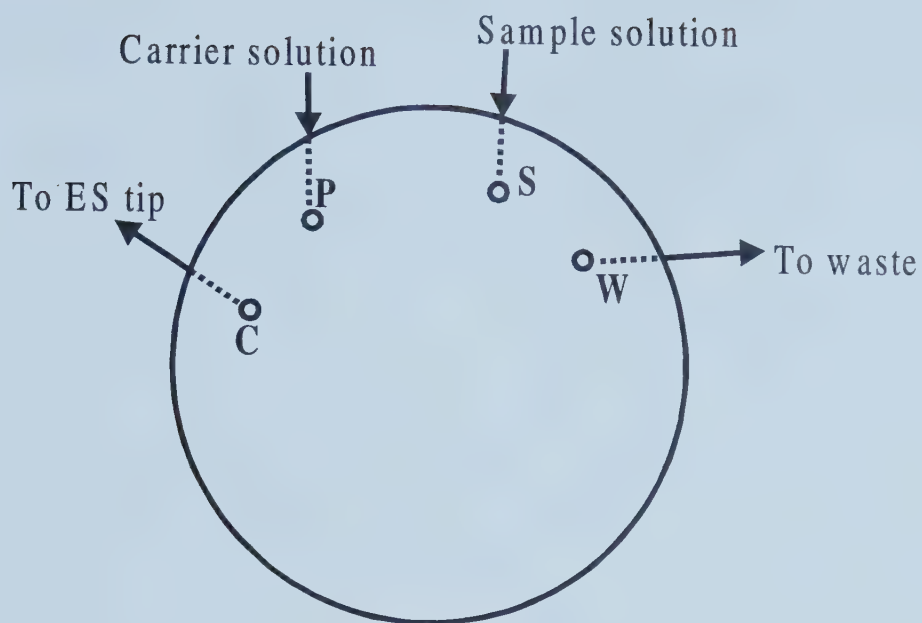
Fig. 2.7 shows the two position function of the injector. When the injector is in 'load' position, the sample slot is aligned with sample inlet port S and waste outlet port W. As a result, the sample solution fills the sample slot and excessive sample solution flows into the waste line, meanwhile the carrier solution flows through the right short passage directly into the ES capillary. The left short passage is not in use. When the injector is switched from 'load' to 'inject' position, the rotor and the flat plate as well turn 90° to the left, as a result, the sample slot is aligned up with carrier inlet port P and to-ES-capillary outlet port C. The carrier solution flows through the sample slot and sweeps the sample solution out of sample slot into the ES capillary. The left short passage which is not in use in load position now is lined with the sample inlet port and the waste outlet port, allowing the sample solution to continue flowing without interruption. The right short passage is not in use in this case.

2.3 Interface

2.3.1 Design of Electrospray Interface

A diagram of the electrospray interface used to transfer ion-solvent clusters into the mass spectrometer (SCIEX/Perkin-Elmer ELAN Model 250) was shown in Fig. 1.2 (page 12). The interface consists of four major components: a front plate, spacer, sampling plate and skimmer cone. The ES tip was positioned along the central axis of the orifice in the front plate, at a separation distance of 5 mm. The front plate is a brass disk with a 3 mm

Stator

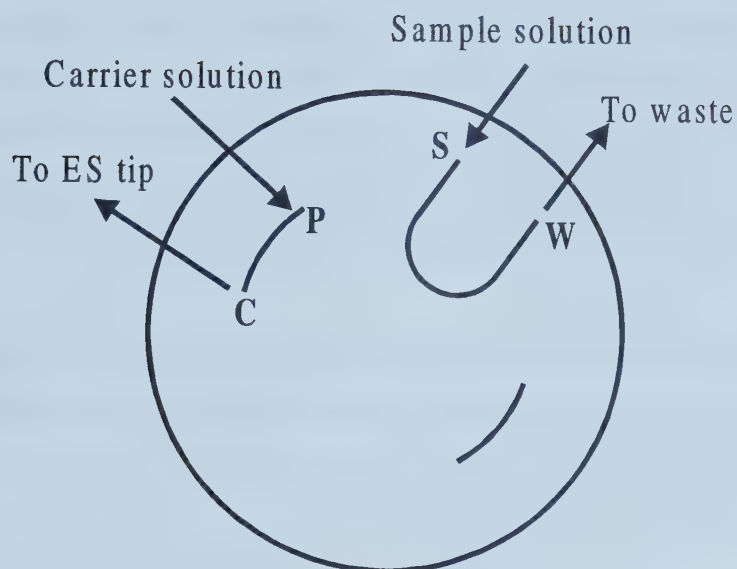


Sample plate



Figure 2.6 An expanded view of the stator and an example of the flat sample plate.

Load



Inject

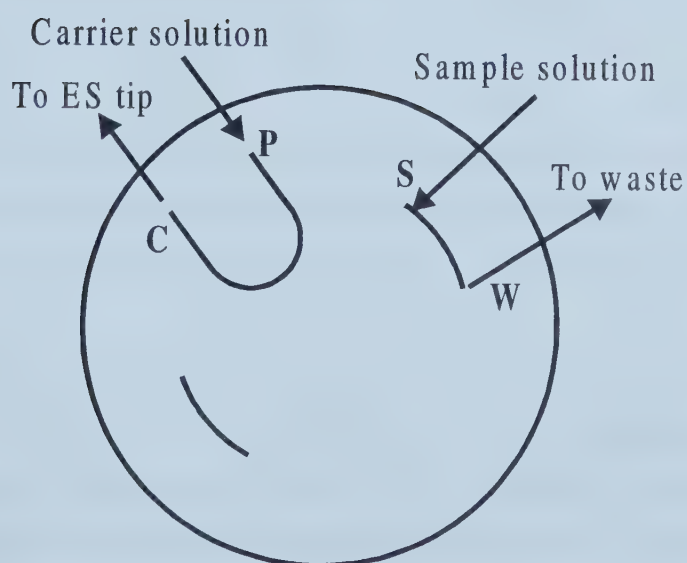


Figure 2.7 A general representation of the two position function of the injector.

diameter orifice at its center, mounted to a 4 mm thick brass spacer. A thin Teflon insulating plate separates the front plate from the spacer so that the two components can be differentially biased. The region immediately behind the front plate is used for introduction of dry nitrogen gas. The gas inlet is located at the top of the spacer such that nitrogen enters perpendicular to the ES tip position and flows through the front plate orifice countercurrent to the ES tip. The functions of the curtain gas and criteria for its selection are discussed in detail in the next sections.

At the rear of the curtain gas region is a flat copper sampling plate. The sampling plate has an orifice or 'nozzle' with a diameter of 100 μm which replaces the sampling cone (0.75 to 1 mm orifice) originally used for ICP-MS measurements. The back of this plate is cut out in the shape of a cone with a half angle of 37° . The pressure to the right of the sampling plate is approximately 400 mTorr. This region is evacuated by an Edwards E2M18 double stage roughing pump at a pump speed of approximately 7 L/sec. Sample and atmospheric gases that pass through the sampling plate nozzle experience a jet expansion due to the drop in pressure across the plate. Details of the mechanics of free jet expansion are well documented in the literature [3, 4] and will not be repeated here. The final component of the source is the skimmer cone which is 1.9 cm high and has an orifice diameter of 1.2 mm. The skimmer is positioned to sample the jet expansion exiting the sampling plate. To the right of the skimmer is the main vacuum chamber of the mass spectrometer. The pressure in this region is maintained in the low μTorr range, typically 5×10^{-6} Torr, by a Cryo-Torr 8 cryopump using helium as a refrigerant.

During regular operation in the negative ion mode the electrospray tip and front plate are biased at -2.7 kvolts and -600 volts, respectively. This establishes a potential difference of -2.1 kV, which is the potential responsible for electrostatic nebulization of sample. Potentials are also applied to the sampling plate and skimmer. Variation of the potential difference, ΔV , between these components is used to effect collisional processes on analyte species, as discussed in Section 1.3.2 of the previous chapter (page 13). The absolute potential applied to the skimmer is used to optimize analyte ion kinetic energies to give optimal ion currents reaching the quadrupole analyzer rods and detector. A list of

the various operation parameters used throughout this work for both negative and positive ion studies is given in Table 2.1.

2.3.2 Curtain Gas

Addition of the nitrogen curtain or ‘bath’ gas into the interface region serves several functions. The flow of dry nitrogen gas countercurrent to the electrospray tip not only aids in droplet desolvation, but also serves to prevent buildup of solvent vapor in the interface. Its function is particularly important since solvent evaporation results in adiabatic cooling of a droplet which dramatically decreases droplet evaporation rates. The degree of droplet cooling may be approximated by equation 2.1 [3].

$$T = T_o + \Delta H_v / C_p \ln X \quad 2.1$$

Where T is the temperature of the droplet when fraction 1-X has evaporated, T_o is the initial droplet temperature, ΔH_v is the enthalpy of vaporization of the solvent, and C_p is the heat capacity of the solvent. Collisions with nitrogen at atmospheric pressure are effective in compensating for this adiabatic cooling. Nitrogen may also be entrained through the sampling plate nozzle into the free jet expansion of the differentially pumped mass spectrometer, where it can be used as an effective collision gas for collision induced dissociation. Use of curtain gases other than nitrogen have been documented in the literature including carbon dioxide, oxygen and argon. Nitrogen is the most widely used owing to its high dielectric constant, reasonably large collisional cross-section, low cost and lack of a dipole moment.

2.4 Mass Spectrometer

A modified, first generation inductively coupled plasma quadrupole mass spectrometer, Perkin Elmer SCIEX Elan Model 250 ICP-MS, was used for all the experiments presented in this thesis. A schematic of the mass spectrometer is given in Fig. 2.8. Several modifications were made to the mass spectrometer by Agnes and Horlick [5] in

Table 2.1 Operation parameters of flow injection electrospray mass spectrometry on the modified ELAN 250 ICP-MS with the modified Cheminert internal injector for both positive and negative ions.

Parameter	Positive-Ion Mode	Negative-Ion Mode
Voltage		
Injector	5.8 to 8.0 kV	-6.0 to -6.5 kV
ES tip	2.9 to 3.5 kV	-3.2 kV
Front Plate	600 V	-600V
Sampling Plate	25 to 180 V	-20 to -120 V
Skimmer Cone	4 to 6 V	-4 to -5 V
Flow Rate		
Carrier Solution	1.0 to 6.0 μ L/min	
Curtain Gas (N ₂)	1.7 L/min	
Capillary		
ES Capillary	150 μ m (o.d.) x 30 μ m (i.d.), 25 cm long	
Carrier Line Capillary	151 μ m (o.d.) x 41 μ m (i.d.), 33 cm long	
Material	Fused silica	
Separation Distance	5 mm (on MS axis)	
Tip Extension	1.0 to 4.0 mm	
Teflon Tubing		
Sample Line	1/16" (o.d.) x 0.01" (i.d.)	
Waste Line	1.6 mm (o.d.) x 250 μ m (i.d.)	
Delivery Syringe		
Volume	250 μ L or 1 mL	
Inner Diameter	2.30mm or 4.78mm	
Timing		
Loading Before Injection	20 seconds	
Sample Line Washing	2 minutes	

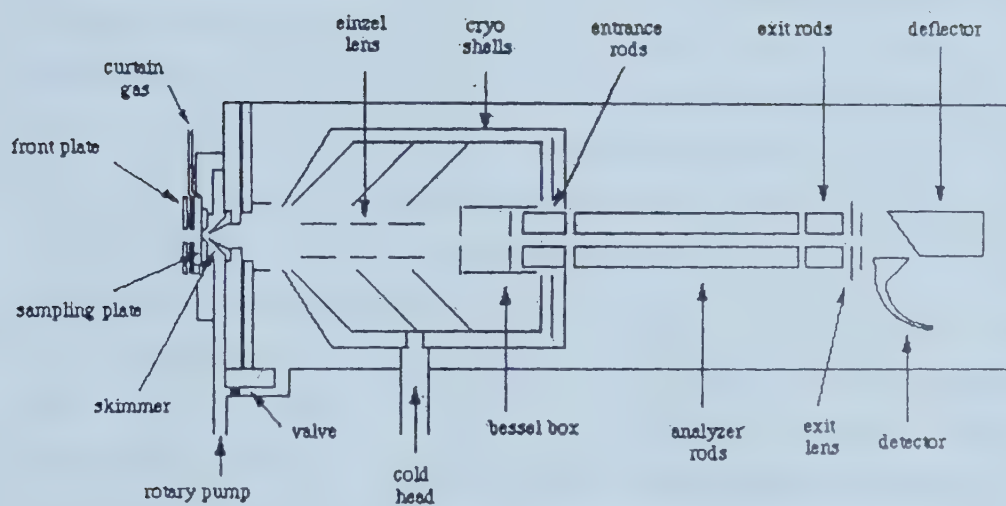


Fig. 2.8: Schematic diagram of the modified SCIEX/Perkin Elmer Elan Model 250 ICP-MS

order to accommodate an electrospray source. Modifications to the mass spectrometer include removal of the ICP source, adaptation of the atmospheric pressure sampling interface and removal of both photon stops that were originally intended to block intense argon emission and neutrals from reaching the detector. Removal of the photon stops improved ion transmission by at least two orders of magnitude. Changes to the interface were described in Section 2.3.1.

A set of three einzel lenses: E1, E2 and E3, are used to focus and guide the electrospray ion beam from the skimmer cone to a Bessel box. The majority of new mass spectrometers designed for atmospheric pressure sampling employ radio-frequency beam guides (quadrupoles, hexapoles and octapoles), rather than the simple electrostatic ion optics described here. The Bessel box consists of two plate electrodes at either end of a cylindrical ring electrode. The original function of the Bessel box was to manipulate ions around a photon stop. However, for ES applications its value is mostly nostalgic. This does not imply that its presence may be taken for granted since minimum threshold voltages must be applied to both the ring and plate electrodes, below which ion transmission at all values of m/z decays rapidly. Above these thresholds, ion transmission is essentially independent of voltage. However, if the plate voltage is set too high, defocusing collisions may be generated in the entrance optic region[1]. The rest of the mass spectrometer was unchanged from its original factory specifications.

2.5 Spectrum and Data Acquisition

Mass spectra were collected by scanning with an integration time of either 10 or 100 ms per point (10 points per amu), while data used for quantitation were acquired in the peak-hopping mode with dwell times of 10 ms and total measurement times of 100 ms per point (1 point per amu). Average signal intensities were calculated for 10 measurements, resulting in typical relative standard deviations of 2-5%. In order to detect the presence of a corona discharge, which has negative effects on analyte intensities, background levels at m/z -32 (O_2^-) and 33 ($CH_3OH_2^+$) for negative and positive ion mode electrospray, respectively, were always monitored to alert the investigator to the presence of a

discharge. The original ELAN software (version 11.0) was used to control data acquisition and routine instrument maintenance. Mass spectra may be viewed either on the screen or relayed through a printer port to a remote terminal where data are captured with a commercial data acquisition program, Red Ryder (version 10.3). Data files generated by Red Ryder were filtered using an executable program written in Pascal, designed to remove extraneous text. The resultant files are then processed using Igor Pro 2.0.1.(Wavemetrics, Lake Oswego, OR, USA).

2.6 References

1. Barnett, D. A., Ph. D. Thesis, University of Alberta, Edmonton, Alberta. 1999.
2. Ruzicka, J.; Hansen, E. H., Flow Injection Analysis, 2nd edn., Wiley, New York, 1988.
3. Hamdam, M.; Curcuruto, O., *Int. J. Mass. Spectrom. Ion. Proc.* **1991**, 108, 93-113.
4. Campargue, R., *J. Phys. Chem.* **1984**, 88, 4466-74.
5. Agnes, G. R. Ph. D. Thesis, University of Alberta, Edmonton, Alberta, 1994.

Chapter 3

Parametric Characterization of FI-ESMS

3.1 Introduction

The instrument setup described in the previous chapter was used for the work described in this chapter. A carrier solution containing an electrolyte was continuously pumped through an internal injector to a capillary held at a high voltage. The sample solution, entrapped in the geometrically well-defined volumetric cavity in the injector was injected into the carrier stream, forming a sample zone thus creating transient signals of analyte ions. Another potential, referred to as the valve voltage, was applied to the carrier stream and sample solution by connecting a high voltage lead to the injector. This was necessary to obtain electrospray signals. The charged droplets drifted toward the front plate and some of them passed into the curtain gas zone which was kept dry with respect to solvent vapor by adjustment of the flow rate of curtain gas. The ion-solvent clusters passed through the sampling plate nozzle and underwent a jet expansion and CID, then were sampled by a skimmer from which ions are guided with ion optics into the quadrupole mass analyzer. Mass spectra were collected and processed using Igor Pro.

The nature of mass spectra observed in ESMS is critically dependent on the source and interface parameters. In elemental electrospray mass spectrometry using continuous sample introduction, the effect of important variables, such as electrospray voltages, interface voltages, flow rate of curtain gas and flow rate of sample solution on analyte signals have been investigated extensively [1-7]. With a new sample introduction method it is similarly important to recognize and understand the behavior of experimental variables affecting the analytical performance characteristics of the technique. Through such studies FI-ESMS could be refined, and the analytical utility of the technique could be improved.

3.2 Experimental

All the experiments were carried out in the positive ion mode because selective ion monitoring (SIM) was not available in negative ion mode on the modified Perkin-Elmer SCIEX ELAN Model 250 ICP-MS. Variations of ES tip voltage, valve voltage and flow

rate of carrier solution were used to optimize the flow injection electrospray performance. All other parameters were essentially constant at the settings shown in Table 2.1, because they were found to have little influence on the FI-ES behavior once optimized.

3.2.1 Reagents

Stock solutions of metal ions were prepared by dissolving the ACS-grade salt (halogen salts) in distilled, deionized water to a concentration of 0.01 M or 0.1 M. The stock solution was then diluted to a volume with reagent-grade methanol, unless otherwise stated. This approach results in most solutions being essentially methanol-based with a small amount of water present (< 5%).

3.2.2 Carrier Solution

In order to minimize the potential interference and accommodate the conductivity requirement, the carrier solution was made up of one metal ion dissolved in methanol. The choice of the metal ion was made based on several considerations. Singly charged ions with simple isotope patterns are preferred. The background needs to be taken into consideration as well. For essentially all solutions, K^+ and Na^+ already existed as background ions. In this study, K^+ was chosen as the carrier ion for most of the work.

3.3 Influence of Flow Injection on the Steady-State Electrospray

For all FI-ESMS experiments, steady-state electrospray was initially established by continuous flow of the carrier solution. It is desired that switching between ‘load’ and ‘inject’ exhibits little influence on the established stable state of electrospray. To be sure of this, experiments wherein the carrier solution was run as the injected sample solution were implemented. An example of the results is shown in Fig. 3.1. The ion signal presented a ‘transient’ in response to each switching event, which indicates that rapid switching builds up no appreciable back pressure and perturbation on the continuousness

of the liquid flow and electrospray. The recovery period of the steady-state spray is short enough to allow the sample portion of the stream to reach the ES tip under stable spray conditions and yield stable ES signals. This feature is important for coupling the flow injection method with ESMS. If the recovery of steady-state spray took a long time, then the sample portion of the stream would pass before any meaningful ES signals of analytes could be captured.

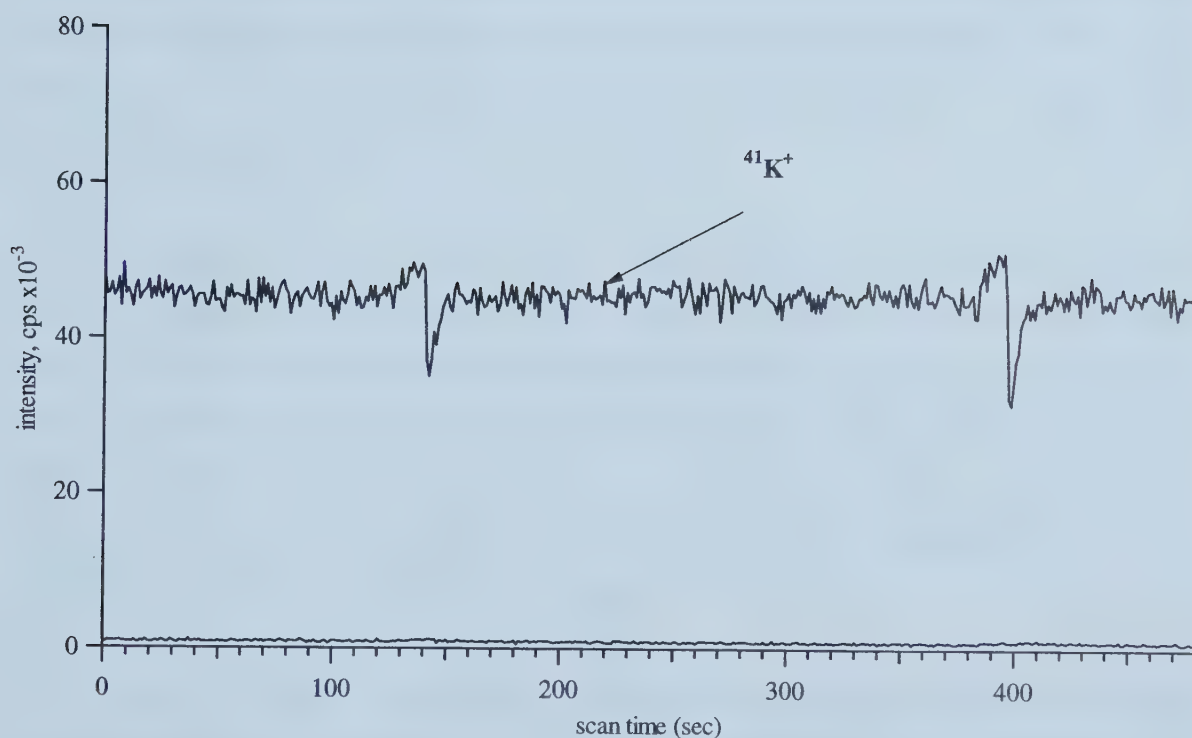


Figure 3.1 Selective ion monitoring mass spectrum of a 0.1 mM methanolic solution of KCl acquired at conditions: valve voltage 4.0 kV, tip voltage 3.3 kV, carrier solution flow rate 1.0 $\mu\text{L}/\text{min}$. The injector was initially in 'inject' position, then switched to 'load' position and turned back to 'inject' again after a while. The injected solution and carrier solution were the same.

3.4 Dependence of Analyte Ion Signals on Operating Parameters

3.4.1 Effect of Flow Rate of Carrier Solution

The effect of varying the flow rate of the carrier solution was evaluated by spraying 1 mM CsCl methanolic solution and holding all other parameters constant (see Fig. 3.2). The sampling plate and skimmer voltages were set to 70 V and 5 V at which the alkali metal ions are observed as bare metal ions (see page 77 Fig. 4.1). In fact, cesium was chosen as the analyte for most parametric studies based on the relative ease with which this ion can be declustered. Alkali metals and many other ions responded similarly to the change in flow rate, but only the cesium signal is presented as an example. The sample volume was 0.2 μ L. The injector was first set in 'load' position for 1 minute, then switched to 'inject' position.

The data presented in Fig. 3.2 show that the greater the flow rate of the carrier solution, the analyte signal exhibited less peak tailing and had a smaller peakwidth. Another aspect of the effect of flow rate is that with an increase in flow rate, the signal intensities decrease, which can be observed more clearly in Fig. 3.3. In Fig. 3.3 the area of the Cs⁺ peak is plotted as a function of flow rate of carrier solution. It is noticed that the signal response dropped very fast in the low flow rate region with increased flow rate and gradually leveled off in the high flow rate region.

Peak tailing is an inherent and persistent problem of the flow injection method utilizing the setup described in Section 2.2. The connection between the ES capillary and outlet port C on the injector is depicted in detail in Fig. 3.4. The port is of 250 μ m diameter and 1/16" (1.6 mm) fitting size. A Teflon sleeve (1/16" o.d. \times 250 μ m i.d. \times 2 cm) was mounted inside a 1/16" stainless steel nut. The ES capillary (150 μ m o.d. \times 30 μ m i.d. \times 20 cm) was held in place inside the Teflon sleeve when tightened and end-paralleled with the square end of Teflon sleeve. Even though the square end of the Teflon sleeve and the outlet bore in the injector make a zero dead volume connection, there would be considerable mixing occurring around the corners of the bore due to the much smaller

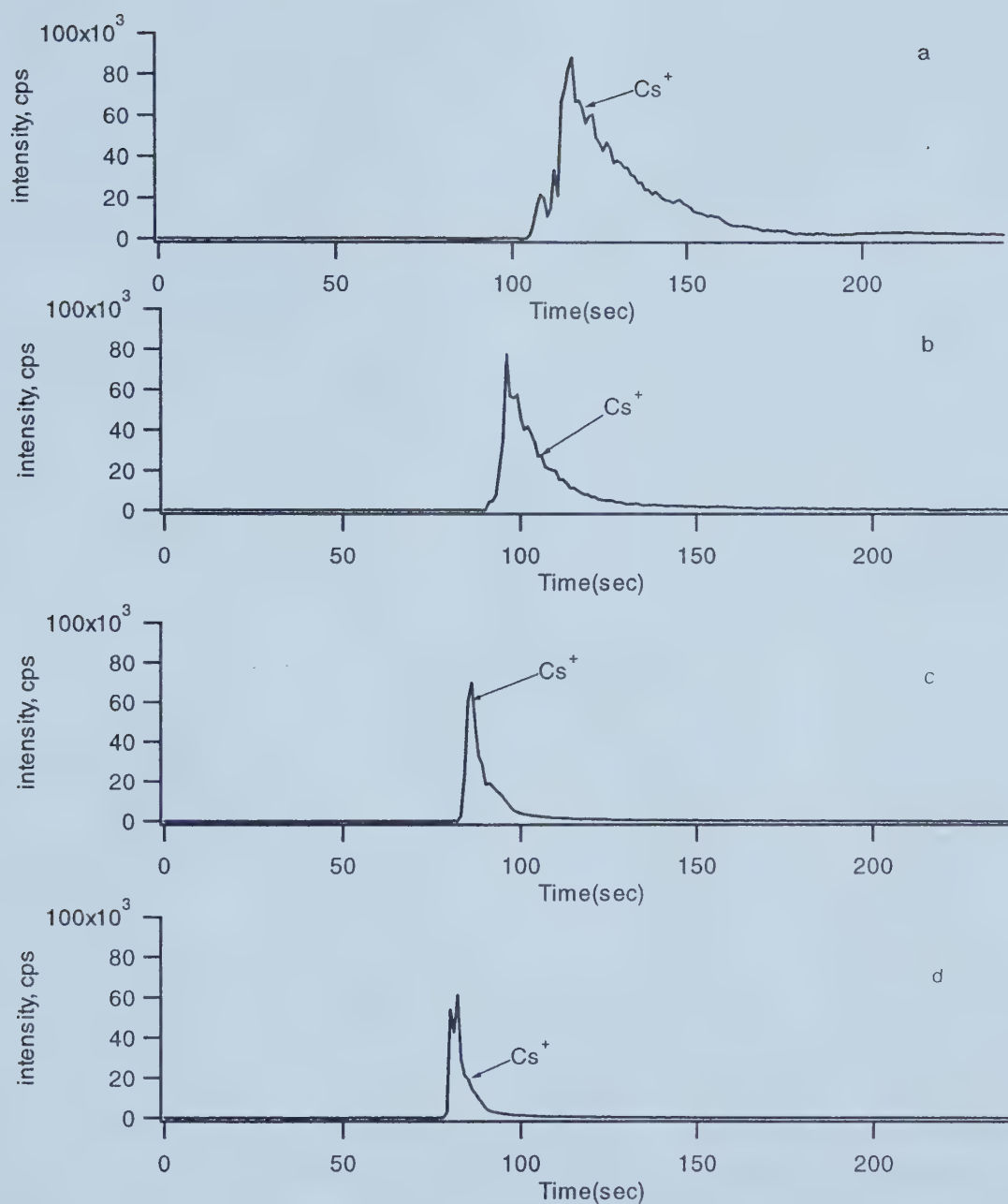


Fig. 3.2 Selective ion monitoring mass spectra of 1 mM CsCl methanolic solution at various flow rates of carrier solution, 0.1 mM KCl, (a) 1.5 $\mu\text{L}/\text{min}$, (b) 2.5 $\mu\text{L}/\text{min}$, (c) 4.0 $\mu\text{L}/\text{min}$, (d) 6.0 $\mu\text{L}/\text{min}$, acquired under conditions: valve voltage 6.1 kV, tip voltage 3.2 kV.

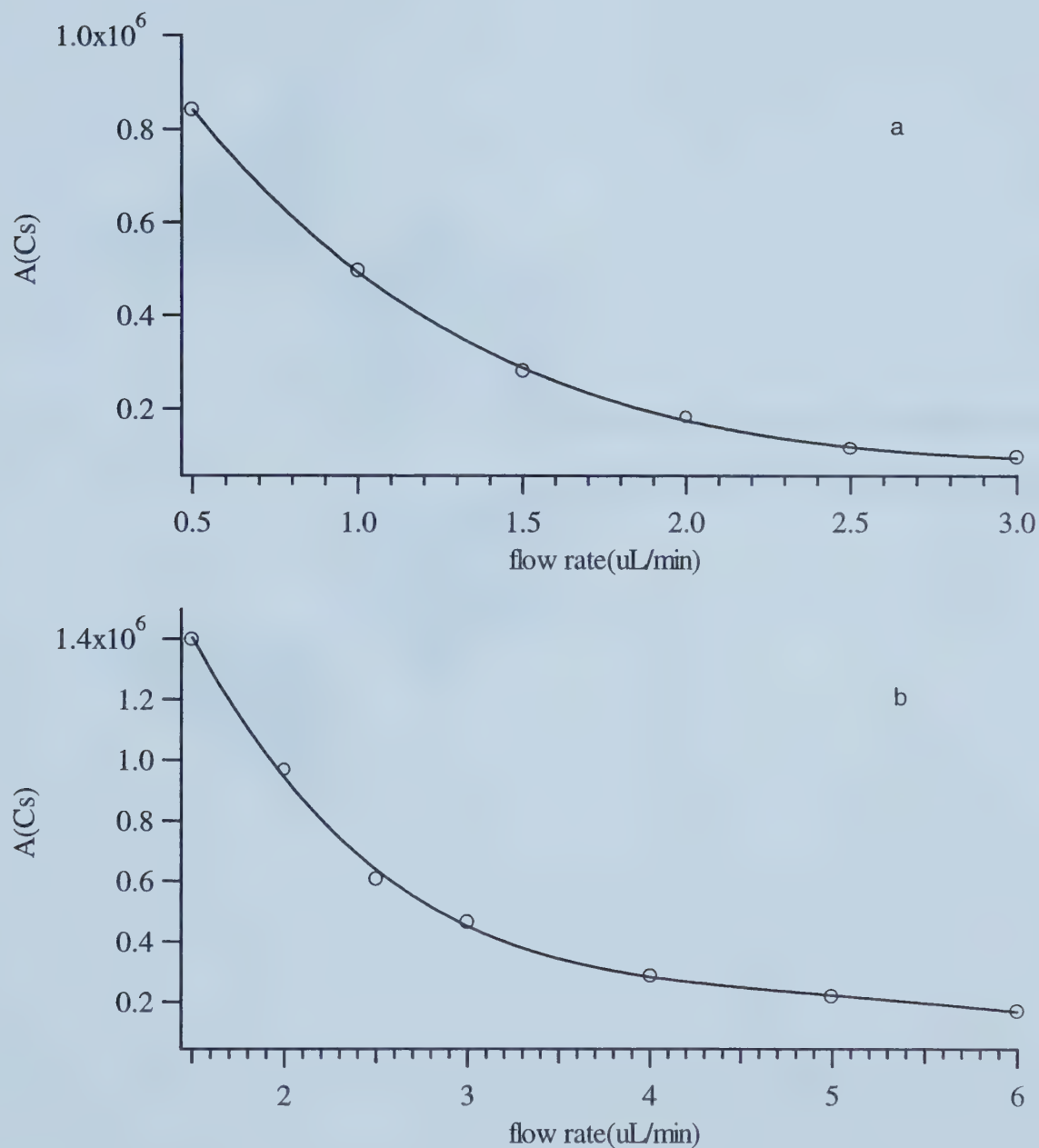


Fig. 3.3 Effect of flow rate of carrier solution: (a) 1 mM KCl in MeOH, (b) 0.5 mM KCl in MeOH, on signal intensities of Cs^+ (area of Cs^+ peak).

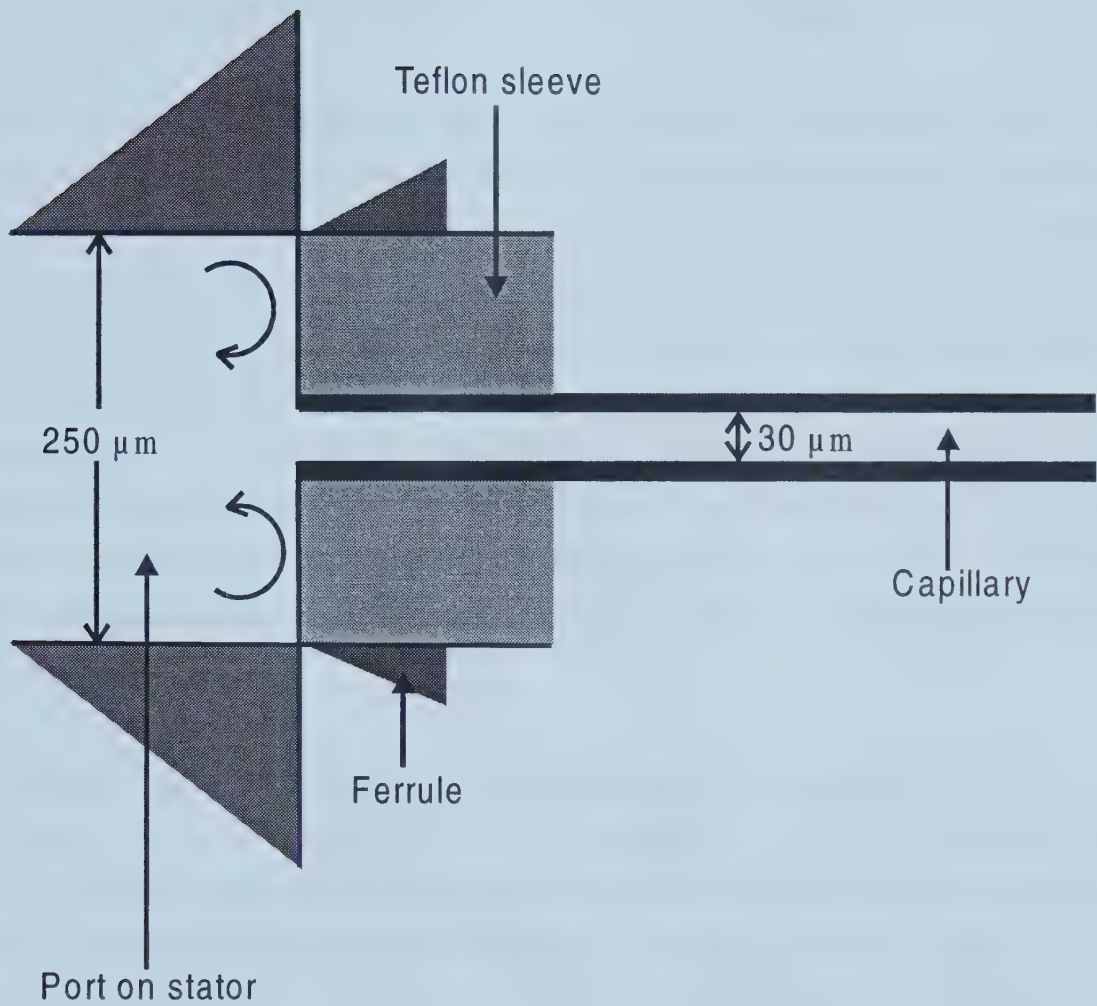


Fig. 3.4: Connection between capillary and injector port.

inner diameter of the ES capillary. The 0.2 μL sample plug when motionless is 0.41 cm long in the out-let port (250 μm i.d.) of the injector and 28.31 cm long in the ES capillary (30 μm i.d.). As a result, the transference of the sample zone is subject to a severe mixing chamber effect, and excessive peak tailing is expected.

Constructional elimination of this origin of peak asymmetry is out of the scope of this thesis. Efforts have been put into reducing peak tailing through parametric adjustment. One of the most effective parameters was found to be the flow rate of carrier solution. With higher flow rate, there is less time available for the development of mixing and diffusion, resulting in less peak tailing. This approach did show promising improvement of peak shape as depicted in the above example. However, this approach is also accompanied by the decrease in signal intensities. With higher flow rate of the sprayed liquid, the initial charged droplets produced by electrospray would be larger. The transfer efficiency of ions to the gas phase will decline due to the greater charge-to-liquid mass ratio. Consequently, the signal intensity and ultimate sensitivity obtainable by FI-ESMS decreases [8-9].

The effects of flow rate on both peak tailing and sensitivity are profound in the low flow rate region. The data presented in Fig. 3.3 also show that the range within which flow rate of carrier solution exhibits great effects is related to the concentration of the carrier ion. With 1 mM KCl in MeOH as the carrier solution, the effective flow rate range was about 0.5-2.0 $\mu\text{L}/\text{min}$. With 0.5 mM KCl in MeOH as the carrier solution, the effective flow rate range was about 0.5-4.0 $\mu\text{L}/\text{min}$. In fact, when flow rate goes above 6 $\mu\text{L}/\text{min}$, the peak shape does not exhibit appreciable improvement upon further increase in flow rate, but the signal intensity drops a great deal to a relatively low value. Therefore, the flow rate that is practically useful should be below 6 $\mu\text{L}/\text{min}$.

3.4.2 Effect of Concentration of Carrier Ion

Another important parameter in the process of FI-ESMS is the concentration of carrier solution. The peak tailing inherently associated with the system used for this study was

illustrated and discussed in the last section. Analyte profiles were also found to be related to the ionic concentration of carrier solution. Selective ion monitoring mass spectra shown in Fig. 3.5 were collected under increasing concentration of carrier solution and other parameters unchanged. Severe peak tailing was observed with 0.1 mM K^+ as the carrier ion. When K^+ concentration was increased to 0.5 mM, the analyte peak shape was much improved. Further increase of the carrier ion concentration to 1.0 mM resulted in little improvement on the profile of the signal, but did result in considerable decrease of signal intensity and peak area. Carrier ion concentration has such an important influence on peak shape that for some analyte ions proper choice of carrier ion concentration could provide a good peak shape even with a relatively low flow rate. An example of this is shown in Fig. 3.6.

In Fig. 3.6 analyte peaks still reveal some degree of asymmetry. A closer look at Figs. 3.2, 3.5, and 3.6 should give a sense that the peak tailing caused by the system set-up is not the dominant component affecting the overall analyte peak shape. There is clearly another cause which gives rise to peak distortion which is related to carrier ion concentration.

A tentative explanation of the observations described above is provided as follows. The inside surface of the ES fused silica capillary acquires negative charges due to ionization of silanol groups. As a result, adsorption of cations onto the inside wall of the capillary can be expected. In general, the adsorption isotherm for a sample species i between a solid and liquid phase is nonlinear, a convex curve, shown in Fig. 3.8. According to the theory about the effect of a distribution isotherm on peak shape, a linear distribution isotherm produces a Gaussian elution peak; a convex isotherm produces a tailing peak; and a concave isotherm produces a fronting peak. When the actual isotherm deviates from linearity further, the tailing of the sample peak will be more severe.

In FI-ESMS operation, stable electrospray is initially formed by running carrier solution. So the active sites on the capillary wall are first occupied by carrier ions. The coverage would be incomplete if carrier ion concentration is small. When the sample band passes

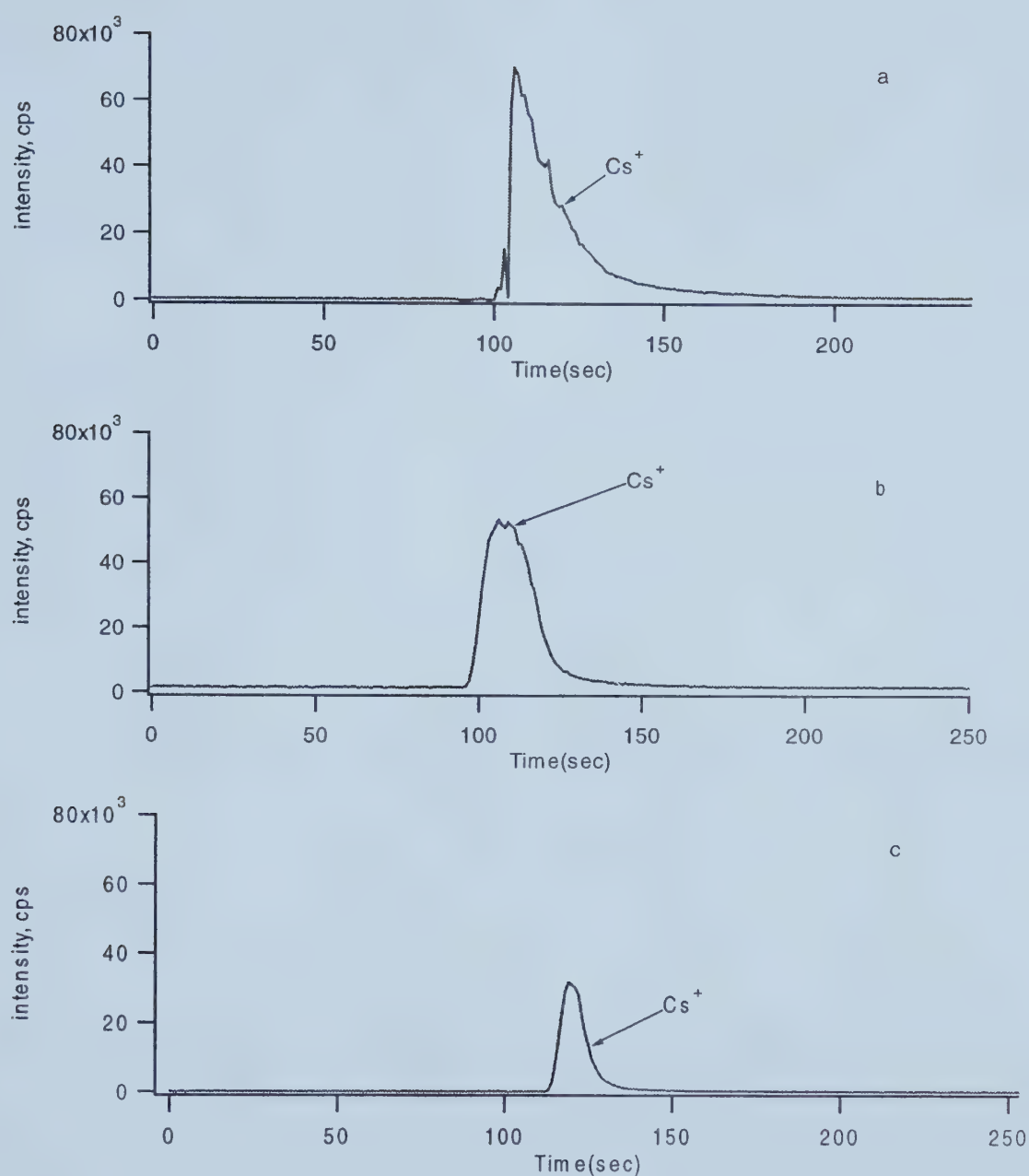


Fig. 3.5 Selective ion monitoring mass spectra of 1.0 mM CsCl methanolic solution with varying concentrations of carrier ion K^+ , (a) 0.1 mM, (b) 0.5 mM, (c) 1.0 mM, acquired under spray conditions: valve voltage 6.1 kV, tip voltage 3.2 kV, flow rate $2.0 \mu\text{L}/\text{min}$.

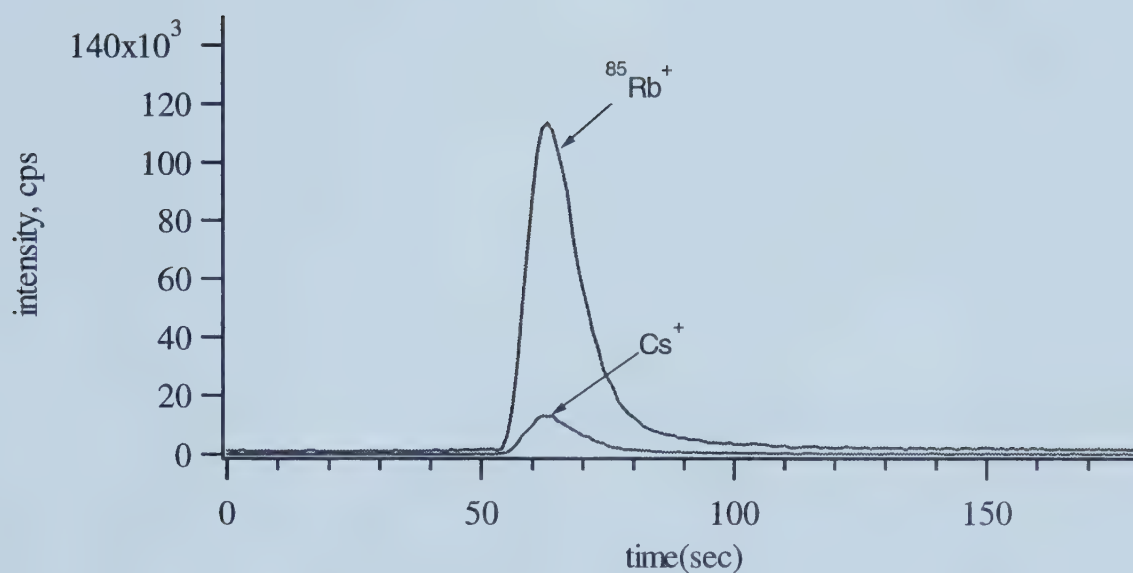


Fig. 3.6 Selective ion monitoring mass spectra of 0.1 mM RbCl and CsCl methanolic solutions obtained with 0.5 mM KCl as carrier ion, 1.0 $\mu\text{L}/\text{min}$ flow rate, 7.8 kV valve voltage, 3.2 kV tip voltage, 70/5 V sampling plate/skimmer voltage, and 0.2 μL sample volume.

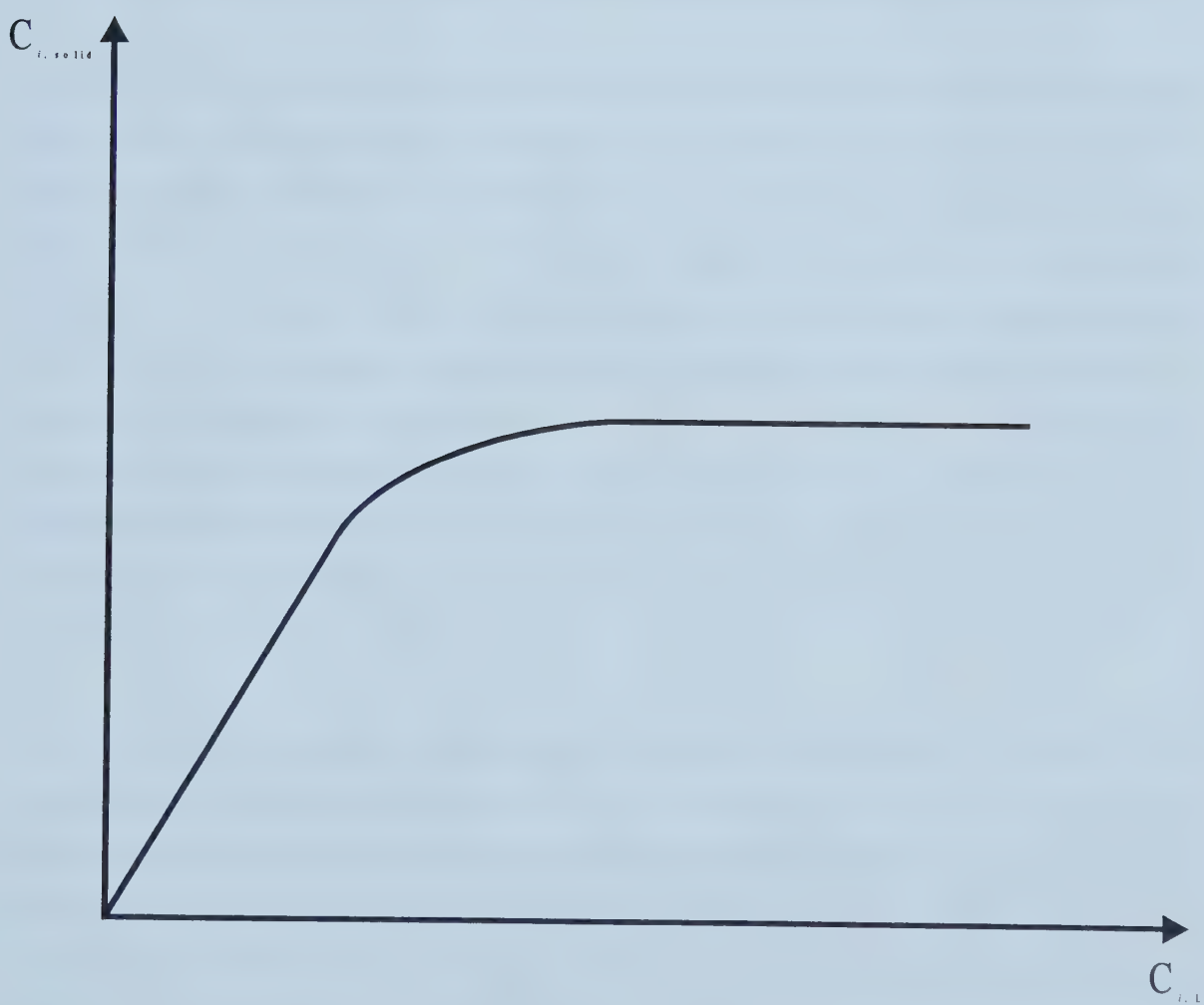


Figure 3.7: Liquid-solid adsorption isotherm --- convex curve

through the ES capillary, some analyte ions will be adsorbed on to the open sites on the wall, resulting in a tailed peak. If carrier ion concentration is large (> 0.5 mM), the sites on the capillary wall may be entirely occupied with carrier ions. Replacement of attached carrier ions by sample ions can only occur to a slight degree because of the limited time available (for 2.0 $\mu\text{L}/\text{min}$ flow rate, the linear velocity was about 5 cm/sec). Because few analyte ions are adsorbed, the contribution of analyte adsorption to peak tailing will be small. Hence less tailing is associated with high carrier ion concentration as observed.

The effect of the adsorption process of sample ions is also illustrated by the observations shown in Fig. 3.8 (c), (d) and (e). The data in Fig. 3.8 were acquired using Na^+ as the carrier ion under conditions: 2.0 $\mu\text{L}/\text{min}$ flow rate, 8.5 kV valve voltage, 3.3 kV tip voltage, 70 V sampling plate, 5 V skimmer voltage. All analytes had the same concentration of 0.1 mM. In Fig. 3.8 (a) and (b), the carrier ion concentrations were 0.01 mM and 0.03 mM respectively. Considering the conductivity requirement of electrospray process, we can expect that carrier solution of such low concentrations would not be able to establish stable electrospray. Consequently, sample solutions reached the spray tip under unstable electrospray. Analyte peaks demonstrated fluctuating distortion. In Fig. 3.8 (c), (d), and (e) the carrier ion concentrations were increased to 0.1 mM, 0.3 mM and 1.0 mM, analyte peaks became smooth and had less tailing.

There is another important phenomenon associated with effect of carrier ion concentration. By examining the peaks in Fig. 3.6 and Fig. 3.8 once more, it can be seen that the area of the analyte peaks decreased with an increase in carrier ion concentration. This can be seen more clearly by plotting the area as a function of the carrier ion concentration, which is shown in Fig. 3.9. The carrier ion was Na^+ in (a), and K^+ in (b). Carrier ion concentrations were started from 0.1 mM because severe distortion of analyte peaks occurs with carrier ion concentration smaller than 0.1 mM. The rate at which analyte intensities decrease differs with different analyte ions.

The decrease of analyte signals with carrier ion concentration should not be surprising as ion signal suppression in electrospray ionization process is well known. For analytical

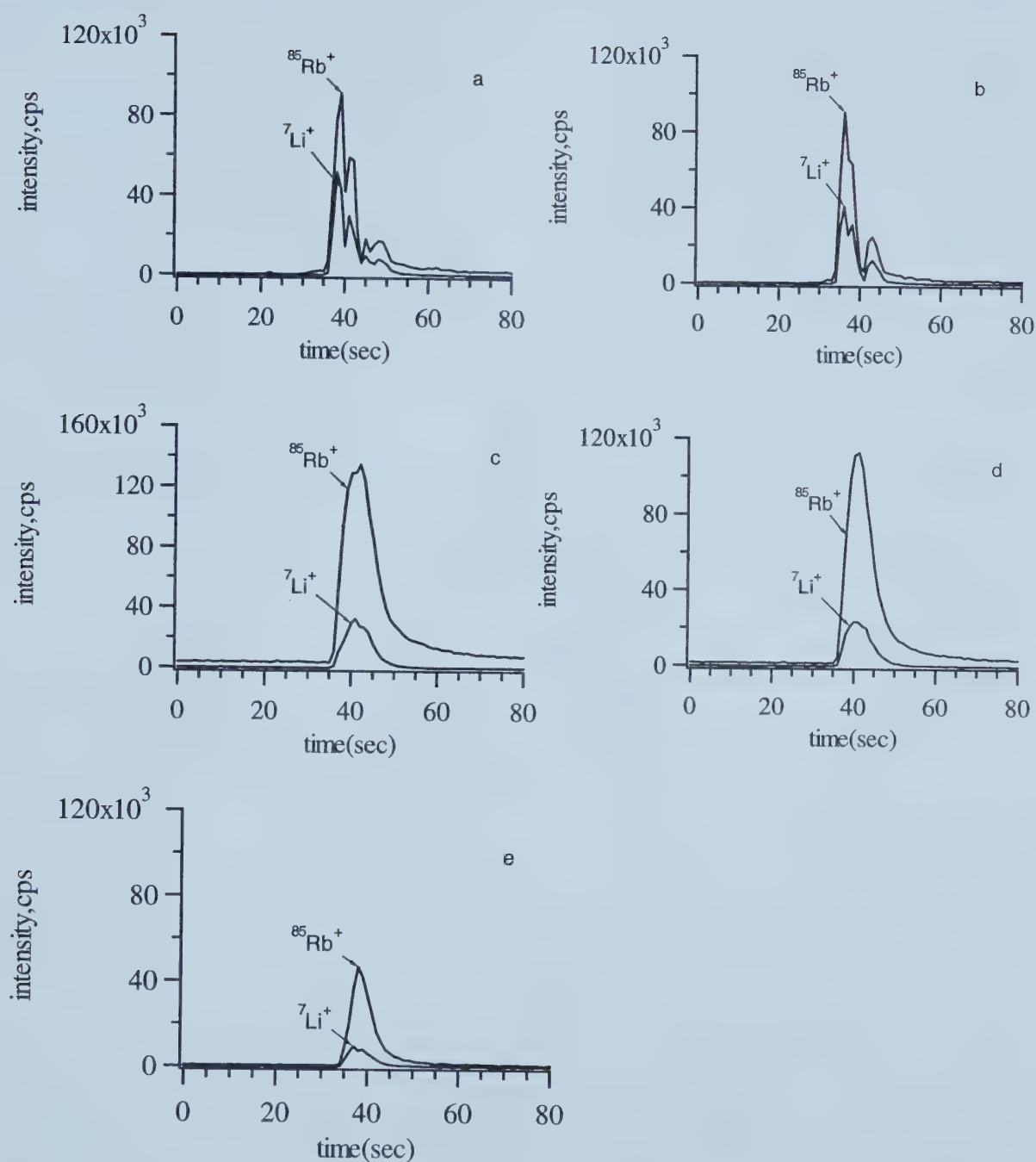


Fig. 3.8 Selective ion monitoring mass spectra of 0.1 mM RbCl and LiCl methanolic solution with varying concentrations of carrier ion Na^+ : (a) 0.01 mM, (b) 0.03 mM, (c) 0.1 mM, (d) 0.3 mM, (e) 1.0 mM, acquired under conditions: 2.0 $\mu\text{L}/\text{min}$ flow rate, 8.5 kV valve voltage, 3.3 kV tip voltage, 70 V sampling plate, 5 V skimmer voltage.

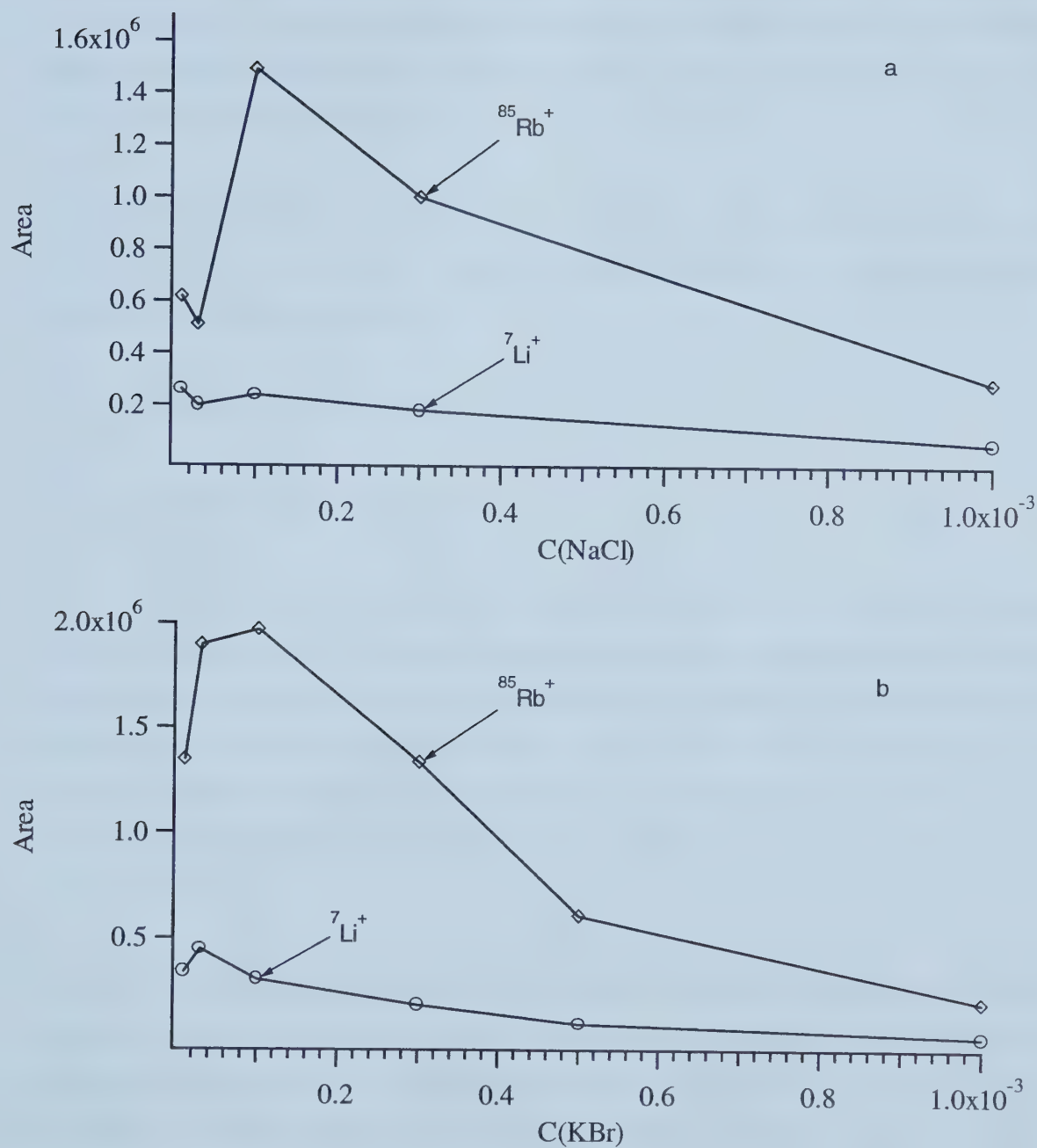


Fig. 3.9 Effect of concentration of carrier ion, (a) NaCl, (b) KBr, on signal intensity (area of analyte peaks) of analytes: RbCl and LiCl.

applications, the relationship between sample ion abundance observed and the corresponding concentration of sample ions in solution is of decisive importance. The question is whether an ESI mass spectrum is a true and quantitative representation of the concentration of sample components in solution. Since ESI is based on the transfer of sample ions from liquid droplets to the gas phase, it does not necessarily give a true picture of bulk solution chemistry.

Tang and Kebarle [9] proposed equations 3.1, 3.2, for a two-electrolyte system, that describe how the presence of an electrolyte A in the solution will suppress the signal intensity of the other electrolyte B.

$$I_A = I f p \{ k_A[A^+] / (k_A[A^+] + k_B[B^+]) \} \quad 3.1$$

$$I_B = I f p \{ k_B[B^+] / (k_A[A^+] + k_B[B^+]) \} \quad 3.2$$

Where I_A and I_B are mass spectrometrically detected ion intensities of A^+ and B^+ , I is the total electrospray current, f is a proportionality factor representing the fraction of droplet charges that get converted into gas phase ions, p is also a proportionality factor representing the fraction of gas phase ions that get transported into the mass analyzer, k_A or k_B are defined as sensitivity coefficient that expresses the transfer rate of the ion, A^+ or B^+ , from the droplets to the gas phase, $[A^+]$ and $[B^+]$ are the concentrations of the electrolyte ions.

The above equations explicitly show the importance of solution conductivity in ESMS applications in terms of total spray current I . In addition, I_A would be reduced if $k_B[B^+]$ in the denominator increases. So at higher concentrations of carrier ion, the signal intensity and peak area of the analyte ion are reduced. The suppression effect of various electrolytes will be different due to differences in their sensitivity coefficients k_i which is dependent on the nature of ions. Volatile and surface active ionic components in droplets would have high k values and are preferentially transferred into gas phase resulting in high sensitivity and signal intensity in the ESMS spectra.

3.4.3 Effect of the Electrospray Tip Length

The electrospray tip length is the extent of the ES capillary that protrudes from the end of the stainless steel support tubing. Although there is no direct electric contact made at the electrospray tip, a high voltage lead is connected to the stainless steel support tubing. The electric field necessary for electrophoretic migration of solution ions, charging of the liquid surface, and dispersion of the liquid, is a combination of the 'sheath' electric field (voltage applied to stainless steel support tubing) and the potential applied to the solution through the high voltage lead connected to the injector. The 'sheath' electric field is an indispensable component in this dual-voltage system. When it is removed, no signal is detected. For the same reason, the ES tip length protruding from the capillary can't be very long. The optimal range of the extent of the ES tip was 1.0~4.0 mm. When the ES tip was longer than 4.0 mm, liquid would accumulate on the tip and form large droplets which were released periodically. When the ES tip was shorter than 1.0 mm, the liquid emerging from the tip partially migrated backwards along the outer wall of the ES capillary and accumulated at the stainless steel support tubing. It is unfortunate that there is no means to figure out the potential value of the liquid at the tip due to the complexity of the dual voltage setup. The voltage applied to the injector was normally higher than the one at the steel tubing. Although the potential experienced by the liquid at the spray tip was enhanced by the penetration of the 'sheath' field, it is possible that the tip liquid potential became smaller than the potential applied at the steel tubing due to the IR drop over the body of the injector and air actuator and the length of the ES capillary. With this assumption, the positive ions in the liquid will be drawn out down field to the MS interface which is held at much lower voltage than the liquid potential at the tip, meanwhile, the negative ions in solution will be drawn up field to the stainless steel tubing, resulting in backward migration of the liquid.

It was found that the change in the ES tip length within a certain range (1.0 to 4.0 mm) did not have a significant impact on the observed analyte signals as long as the ES tip length was kept within the optimal range. This is illustrated in Fig. 3.10. The experiments were actually done with a gradual increase of the ES tip length. Only results from tip

length of 1.0 mm and 4.0 mm are presented here. The longer length of tip protrusion does provide a more stable base line, but peak area precision were similar for the two cases.

3.5 Conclusions

Flow injection sample introduction can be coupled with electrospray mass spectrometry because the operation of switching the injector and resulting change in the composition of the fluid bring about little perturbation on the continuance of the steady state of established electrospray. Operational parameters which determine the stable spray conditions and signal intensities can be studied more conveniently by using continuous sample introduction. Only parameters which characterize the features of flow injection were investigated as part of the objective of this thesis.

Peak tailing has been a major concern for the system constructed for this study. The adsorption of analyte ions onto the inside wall of the ES capillary may be one of the origins of the tailed peaks. Tailing can be reduced by increasing the carrier ion concentration. On the other hand, the increase of carrier ion concentration has the unwanted effect of suppressing the intensities of analyte signals. As a compromise, the optimal carrier solution concentration used for most work in this thesis is 0.5 mM. It is important to note that the carrier solution has many functions in the FI-ESMS system. Basically it carries sample solutions to the ES tip. With respect to the electrospray process, carrier ions are the major contributor to the required conductivity of the sprayed liquid, and may also function as an electrospray stabilizer. The ES signal of carrier ion can be monitored continuously as an indicator of the status of the on-going electrospray. Furthermore, carrier ions can block the active sites of the capillary wall and attenuate the degree of peak tailing due to the adsorption of analyte ions.

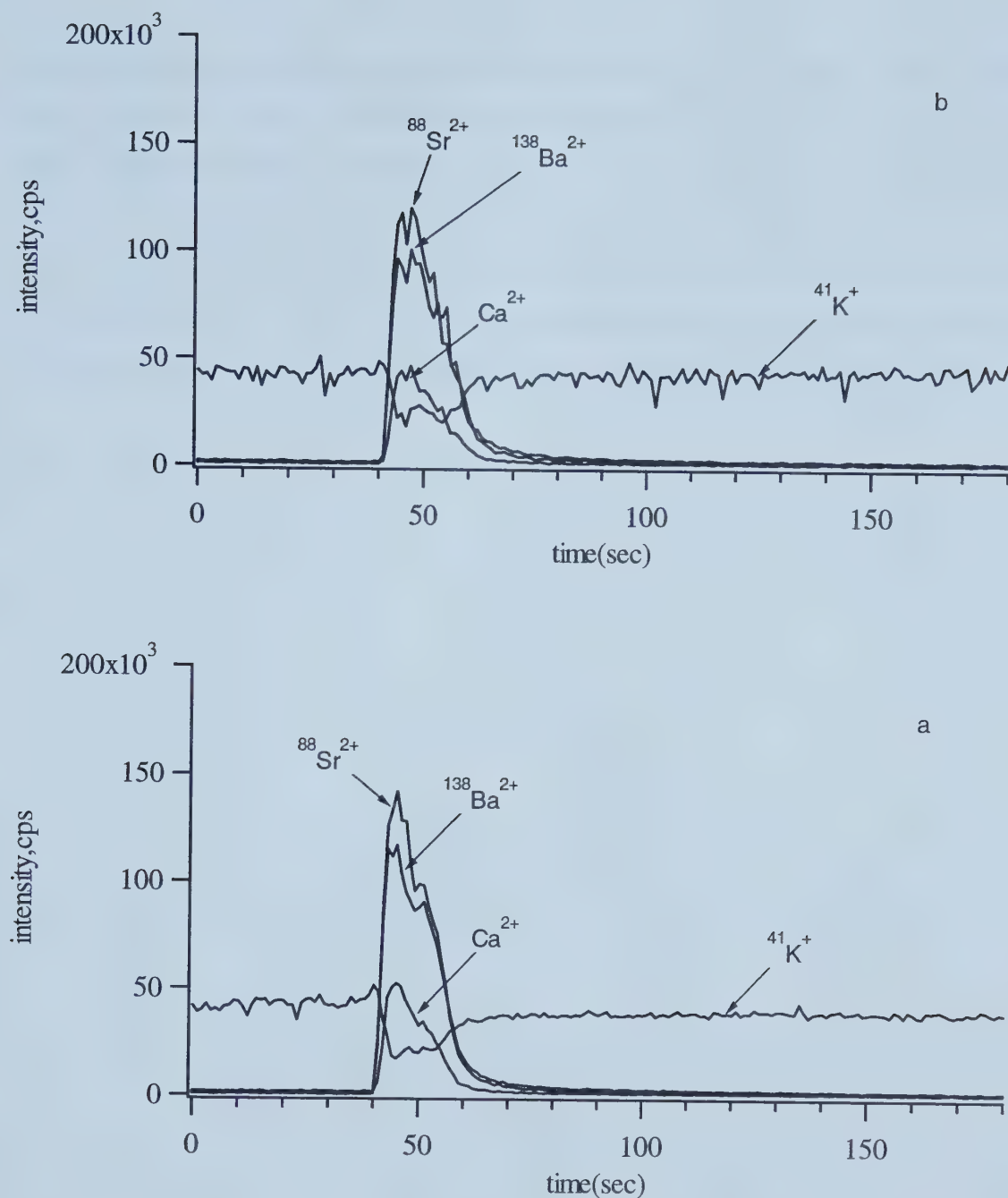


Fig. 3.10 Selective ion monitoring mass spectra of 0.5 mM methanolic solution of SrCl_2 , BaCl_2 , CaCl_2 , with 0.5 mM KCl as carrier ion, at varying length of ES tip, (a) 1 mm, (b) 4 mm, acquired under conditions: 2.0 $\mu\text{L}/\text{min}$ flow rate, 7.1 kV valve voltage, 3.3 kV tip voltage, 180 V sampling plate, 5 V skimmer voltage.

Flow rate of carrier solution is another parameter which can be used to control peak tailing. Similar to carrier ion concentration, flow rate of carrier solution affected the peak shape and analyte signal intensities contrarily. Higher flow rate and smaller sample volume will bring about less tailed peaks but lower signal intensity. The trend in the effect of flow rate tends to level out in the high flow rate value region. So the normal flow rate range is 1.0 ~ 6.0 $\mu\text{L}/\text{min}$. In general, parameters of flow rate and concentration of carrier solution should be adjusted based on the individual experimental purpose.

3.6 References

1. Agnes, G. R.; Horlick, G., *Appl. Spectrosc.*, **1995**, 49, 324-34.
2. Agnes, G. R.; Horlick, G., *Appl. Spec.*, **1994**, 48, 655-61.
3. Agnes, G. R., Ph. D. Thesis, University of Alberta, Edmonton, Alberta, 1994.
4. Stewart, I. I.; Horlick, G., *TRACTrends Anal. Chem.* **1996**, 15, 80-90.
5. Colton, R.; D'Agostino, A.; Traeger, J. C., *Mass Spectrom. Rev.* **1995**, 14, 79-106.
6. Hop, C. E. C. A.; Bakhtiar, R., *J. Chem. Ed.* **1996**, 73, A162-A169.
7. Gatlin, C. L.; Turecek, F., Electrospray ionization of inorganic and organometallic complexes, in: R. B. Cole (Ed.), *Electrospray Ionization Mass Spectrometry: Fundamentals, Instrumentation, and Applications*, Wiley, New York, 1997, pp. 527-570.
8. Stewart, I. I., *Spectrochim. Acta B*, **1999**, 54, 1649-1695.
9. Kebarle, P.; Tang, L., *Anal. Chem.*, **1993**, 65, 972A-986A.
10. Agnes, G. R.; Horlick, G., *Appl. Spectrosc.*, **1994**, 48, 649-54.
11. Thomson, B. A.; Iribarne, J. V., *J. Chem. Phys.*, **1979**, 71, 4451-4463.
12. Iribarne, J. V.; Thomson, B. A., *J. Chem. Phys.*, **1976**, 64, 2287-2294.

Chapter 4

Flow Injection Electrospray Mass Spectra of Inorganic Solution Ions

4.1 Introduction

The major impact of ESMS to date on the analytical community has been in the area of biological and organic applications, because the gentleness of the electrospray process has allowed the generation of intact gas-phase molecular ions from in-solution analytes of very large molecular weight, and such attainment is impossible with most other ionization methods. Systematic studies of ESMS in inorganic and elemental analysis have been relatively few in number, but already sufficient to show the impressive potential of this technique for determination of inorganic solution ions. For elemental analysis, the inductively coupled plasma (ICP) has been the predominant ion source for emission and mass spectrometry since 1980[1-5]. ICP related techniques actually provide the information of the total amount of an element existing in a sample, because in the high-temperature environment of the plasma essentially all analytes are converted into their elemental forms. Important chemical information about the nature of the element in the sample is not available with the ICP ion source. The combination of separation techniques and ICP-MS as a solution to the problem has been extensively investigated and so far still problematic due to ambiguous identification of separated peaks. In this approach the capability of mass spectrometry to provide charge state and molecular information is of no use. In contrast, such solution information as chemical form and oxidation state of target ions could be retained by an electrospray ion source and readily obtained by the direct detection of mass spectrometry. This has aroused the initial and still-increasing interest in the inorganic application of ESMS.

The major advantage of inorganic ESMS may lie in its versatility. It can perform elemental analysis through high energy CID which decomposes the analyte to its elemental form and results in a spectrum similar in appearance to, but lower sensitivities than, that observed by ICP-MS. ESMS can also provide molecular information for general inorganic compound identification, including thermally labile and nonvolatile compounds[6-8], and it can provide speciation of both positive and negative inorganic ions in solution [9]. Since the charges on most inorganic ions are small, and often only singly charged ions are observed in the ES mass spectrum, the characteristic isotopic

patterns of elements can be readily resolved in most cases to give unambiguous identification.

Horlick and colleagues [10-19] have investigated the effectiveness of ESMS as a technique for the elemental analysis and speciation of simple inorganic solution ions, both positive and negative. They illustrated the typical ion species observable and examined both the qualitative and quantitative aspects. The system they used for their studies employed the continuous sample introduction method. In this chapter the capabilities of flow injection electrospray mass spectrometry are examined with a focus on the method of ES condition adjustment for obtaining informative mass spectra of analyte ions. A variety of simple inorganic ions were tested, ranging from singly and multiply charged monoatomic ions to oxoanions.

4.2 Experimental

All the experiments were carried out on the flow injection electrospray source and the modified Sciex/Perkin-Elmer ELAN Model 250 ICP-MS mass spectrometer as described in Chapter 2. Two main modes of operation were undertaken: a 'bare metal ion' mode where the ions were essentially declustered to elemental or molecular (oxide ions) form; and ion-solvent cluster mode where relatively gentle conditions (small sampling plate voltage and CID energy) were used. Both positive- and negative- ion modes were operated.

4.2.1 Some Important Features

Mass spectra were collected when the sample portion of the stream took place at the ES tip and achieved its steady-state electrospray. In order to catch the mass spectrum of a sample solution which passed through the ES tip quickly, proper choice of several parameters must be undertaken. The largest available sample volume of 0.5 μL was used to obtain the longest duration time of sample zone. The flow rate of carrier solution was

1.0 $\mu\text{L}/\text{min}$. The scan speed of the mass spectrometer was set to the fastest which corresponded to measurements at 10 ms per point (10 points per amu). Trial and error was used to estimate the suitable mass range and the time span between injection and mass scan. If the mass range was set too large, then the scan time would be longer than the duration of time the sample zone was dominating the electrospray process, and the information on high-mass ions would be missed. After the injector was switched to the 'inject' position, a period of 30-120 seconds must pass before the mass scan is performed; otherwise, the mass scan would be started when the analyte ions have not arrived at the detector, and the information on low-mass ions would be missed. Optimum parameters such as valve voltage, tip voltage, sampling plate voltage and carrier solution flow rate were sometimes dependent on sample composition. They had to be adjusted in order to obtain stable electrospray condition for a specific sample by continuous delivery of sample solution. Other parameters were held constant: the ES tip was positioned along the central axis of the orifice in the front plate, at a separation distance of 5 mm; both the front plate and the skimmer were constantly biased at 600 V and 5 V; the flow rate of curtain gas was 1.0 L/min; the length of ES tip was 2 mm.

4.2.2 Reagents

The specific analyte solutions were prepared by dissolving the reagent (ACS-grade) in nanopure water and diluting to $1.0 \times 10^{-2} \text{M}$. An aliquot of the solution was then diluted with reagent-grade methanol to $5.0 \times 10^{-4} \text{M}$. Typical water content in these solutions was about 5% by volume.

4.3 Results and Discussion

The ES mass spectra of an equimolar mixture of Li^+ , Na^+ , K^+ , Rb^+ , and Cs^+ is shown in Fig. 4.1. The methanolic sample solution contained $5 \times 10^{-4} \text{M}$ alkali metals, and the composition of carrier solution was $5 \times 10^{-4} \text{M}$ KCl in methanol. In order to capture the ES mass spectrum of the sample zone, the elution profile was first inspected by selective ion monitoring, shown in Fig.4.1 (a). It can be seen that the time available for capturing

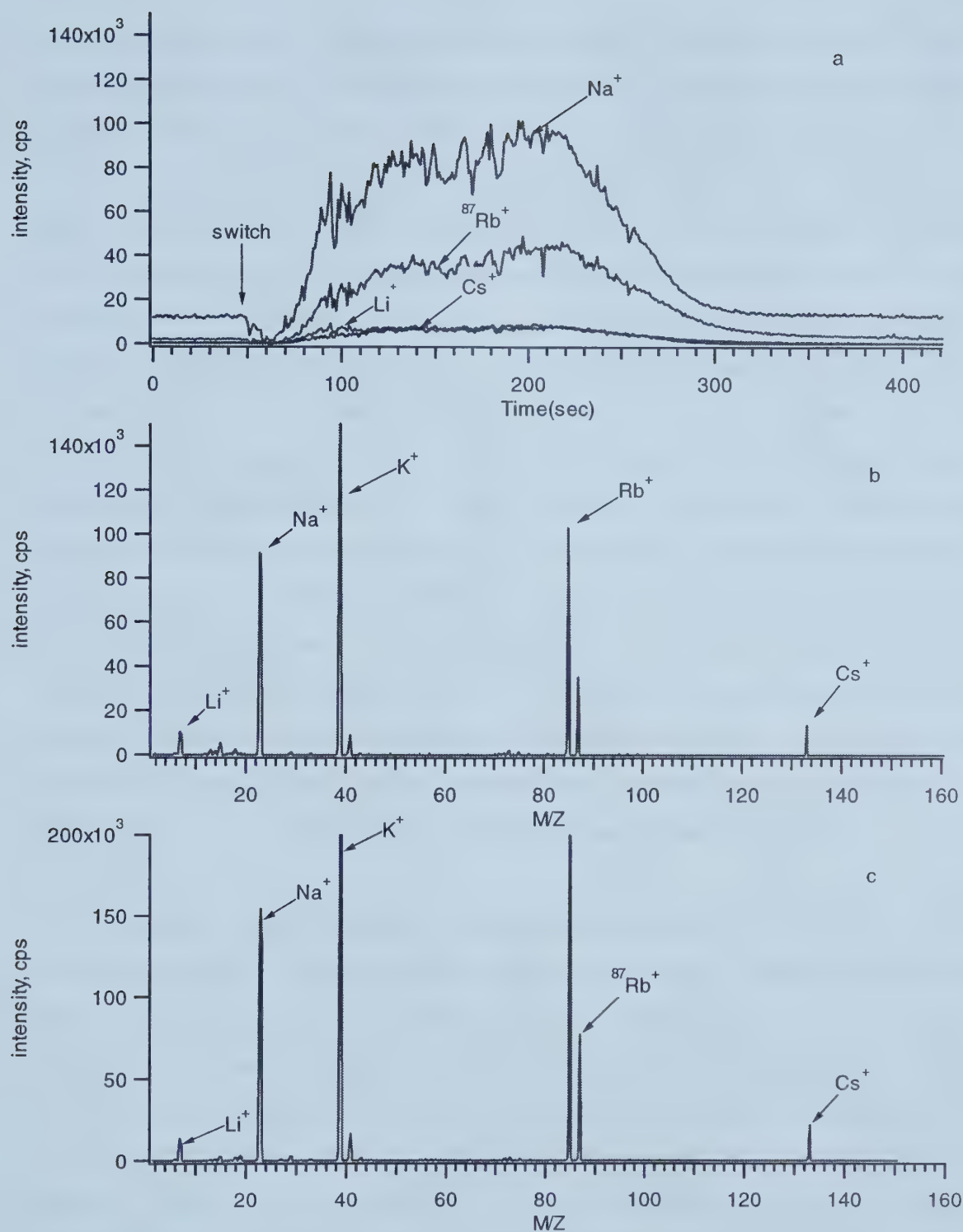


Figure 4.1 Mass spectra of 0.5 mM alkali metals in methanol, (a) SIM spectrum (b) flow injection ESMS spectrum (c) continuous ESMS spectrum

the sample portion's mass spectrum was about 2 minutes. The scan time for the whole mass range was about 45 seconds determined by making the same measurement under the same condition except using continuous sample delivery. There is a time span from the moment of switching the injector to injection position to the point at which analyte signals began their steady states. This time span must be taken into account to order to start the spectrum scan at the proper instant, and it was 80 seconds in this case. The time needed for instrument response and data acquisition was in the range of 10-15 seconds. Different sample solutions take different times to reach the steady state, so the way of 'trial and error' had to be used. This kind of difficulty could be overcome by up-dated software and instrument design. The mass spectrum obtained with flow injection sample introduction is presented in Fig.4.1(b), which is similar to that acquired with continuous sample introduction, shown in Fig.4.1(c), their experimental conditions being the same. The only significant difference between the spectra obtained with the two different sample introduction methods is that FI-ESMS yields lower signal intensities than steady-state ESMS. This may be rationalized by the dispersion of the sample zone in the stream of carrier solution. If a longer sample zone can be somehow realized, so that mass spectra could be taken with a less dispersed sample portion, then the spectra measured by FI-ESMS or continuous sample introduction ESMS would be essentially the same.

For alkaline earth metals, solutions of doubly charged ions (Mg^{2+} , Ca^{2+} , Sr^{2+} , Ba^{2+}) in methanol were tested. The concentrations for both carrier and M^{2+} sample solutions were 5×10^{-4} M. Fig.4.2(a) shows the profile of the Mg^{2+} -solvent complex ion in the sample solution using a small value of voltage difference, $\Delta V = 25.7$ V, between the sampling plate and skimmer. Fig 4.2(b) is the mass spectrum collected under the same conditions as in Fig. 4.2(a), illustrating that little charge reduction of Mg^{2+} occurred, and the dominant species was $\text{Mg}(\text{H}_2\text{O})_4^{2+}$, with other species such as $\text{Mg}(\text{H}_2\text{O})_5^{2+}$, $\text{Mg}(\text{MeOH})(\text{H}_2\text{O})_3^{2+}$ detected as well. Small CID energy had to be imposed in order to observe Mg^{2+} -containing ions as major ions since Mg^{2+} is prone to charge reduction due to the high ionization energy of Mg^+ . Blades and co-workers have reported their theoretical study of the formation, acidity and charge reduction of alkaline earth metal ions [20-22]. For an alkaline earth metal, which has a high second ionization energy, a

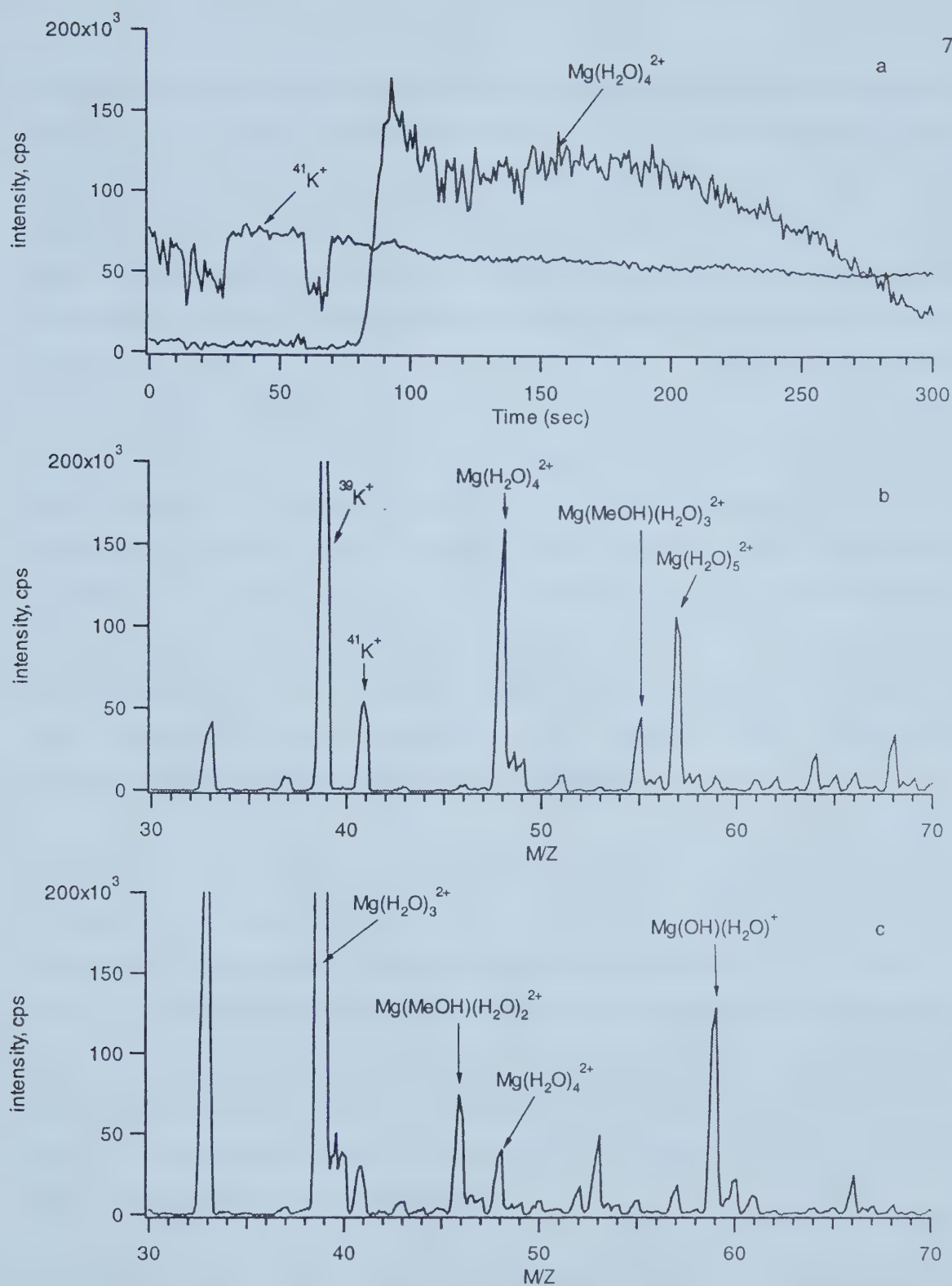


Figure 4.2 FI-ESMS spectra of 0.5 mM Mg^{2+} in methanol at ΔV settings of (a) 25.7 (SIM) (b) 25.7 (c) 35 volts.

minimum solvation number, n , exists where a charge reduction reaction competes with simple ligand loss. Their theoretical calculation of the transition state energies of the two competing processes for Mg^{2+} and Ca^{2+} shows that the transition state energy for charge reduction is much lower than that for ligand loss at a ligand number of 2[22], so that charge reduction dominates. However, as the solvating number increases, simple ligand loss becomes dominant. Experimental results shown in Fig. 4.2(c) are in agreement with their prediction. The ΔV value for Fig.4.2 (c) was 35 volts and the hydrate hydroxide, $\text{Mg}(\text{H}_2\text{O})\text{OH}^+$, a charge reduced species, was present in considerable amount. $\text{Mg}(\text{H}_2\text{O})_3^{2+}$ yielded the most intense peak under this condition, and others such as $\text{Mg}(\text{H}_2\text{O})_4^{2+}$, $\text{Mg}(\text{MeOH})(\text{H}_2\text{O})_2^{2+}$ also existed, although $\text{Mg}(\text{H}_2\text{O})_3^{2+}$ was overlapped by the major peak of potassium. The species $\text{Mg}(\text{H}_2\text{O})_2^{2+}$ was under no conditions observed, which indicates that at ligand number of 2 the solvent sheath is too small to stabilize the charge on the ion and charge reduction occurs. It is also observed that even though the water content in the sample solution was about 5%, water molecules were preferentially forming complex ions with magnesium ions over methanol molecules. This was also found to be true for other metals.

The experimental observation for calcium was not consistent with previous results from Peschke and co-workers [22]. Fully declustered Ca^{2+} ions were observed at a declustering voltage of 65 volts, as shown in Fig.4.3. The valve and tip voltages were 6.0 and 3.2 kV, respectively, and the flow rate of carrier solution was 0.85 $\mu\text{L}/\text{min}$. The mass spectrum scan was started after the injector had been switched for 60 seconds. Fig.4.3(b) clearly indicates the existence of Ca^{2+} as the major ion. The profile of Ca^{2+} ion, shown in Fig.4.3(a), gives evidence of stable electrospray for the sample zone. Some $\text{Ca}(\text{H}_2\text{O})^{2+}$, CaOH^+ were also present in a small amount.

With relatively low values of the second ionization energy, the desolvated doubly charged ions of strontium and barium were easily obtained under normal conditions, as shown in Figs. 4.4, 4.5, and 4.6. The experimental conditions in Fig. 4.4 and Fig. 4.5 differed only in the declustering voltage, ΔV , which was 65 volts in Fig. 4.4 where Sr^{2+} is the major ion, and 175 volts in Fig. 4.5 where the charge reduced species Sr^+ was

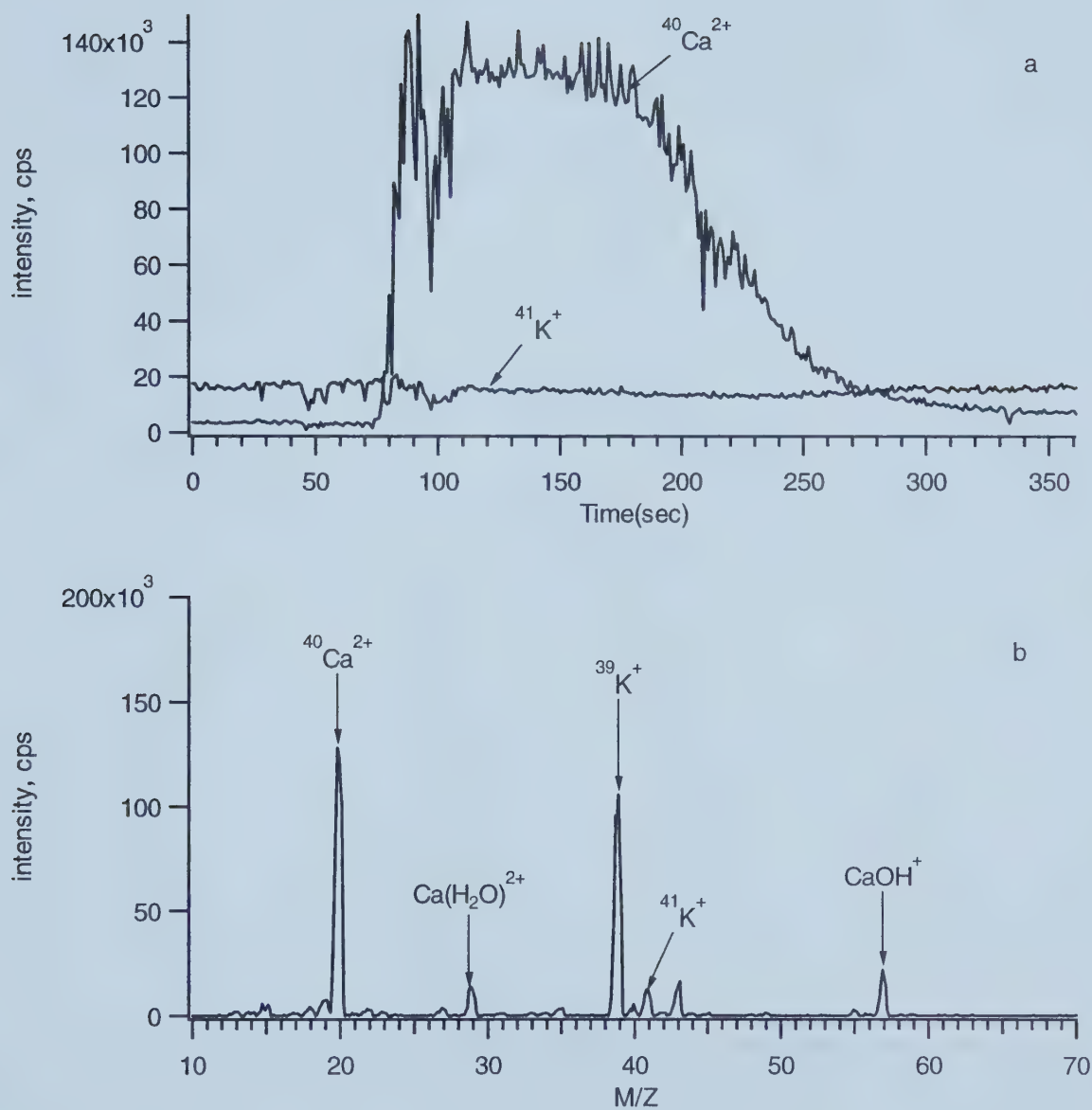


Figure 4.3 FI-ESMS spectra of 0.5 mM Ca^{2+} in methanol, $\Delta V = 65$ volts.

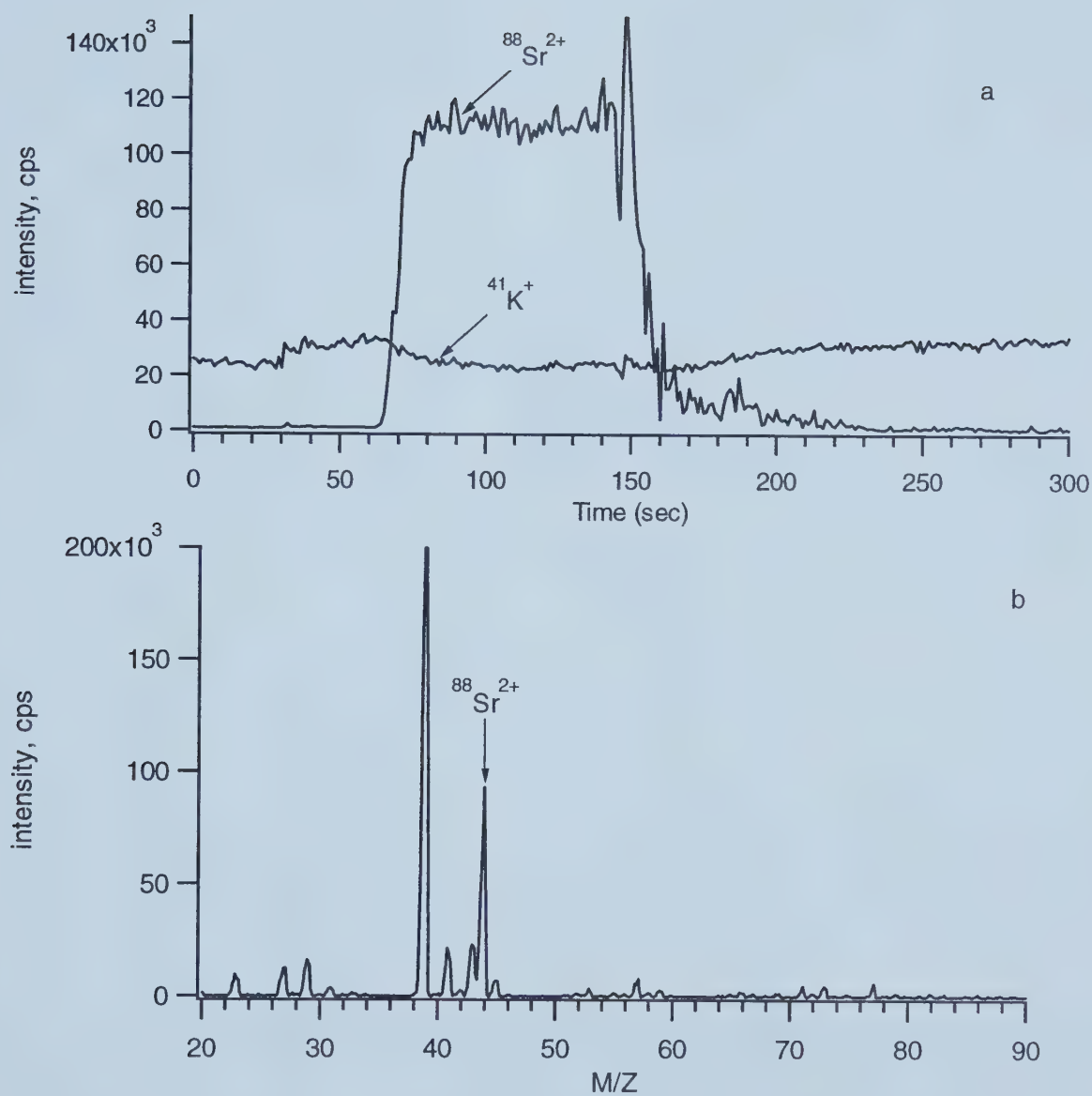


Figure 4.4 FI-ESMS spectra of 0.5 mM Sr^{2+} in methanol, $\Delta V = 65$ volts.

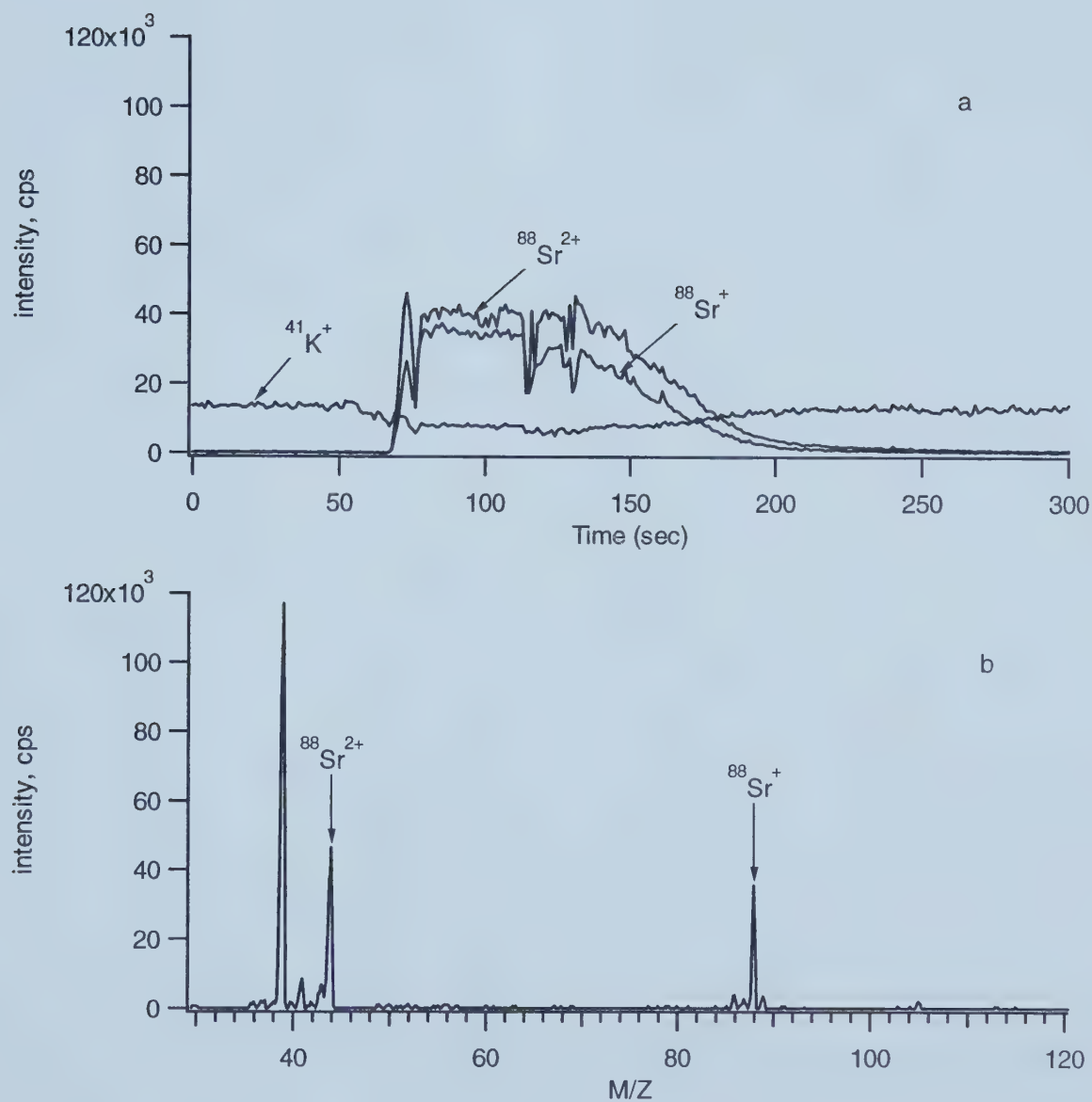


Figure 4.5 FI-ESMS spectra of 0.5 mM Sr^{2+} in methanol, $\Delta V = 175$ volts.

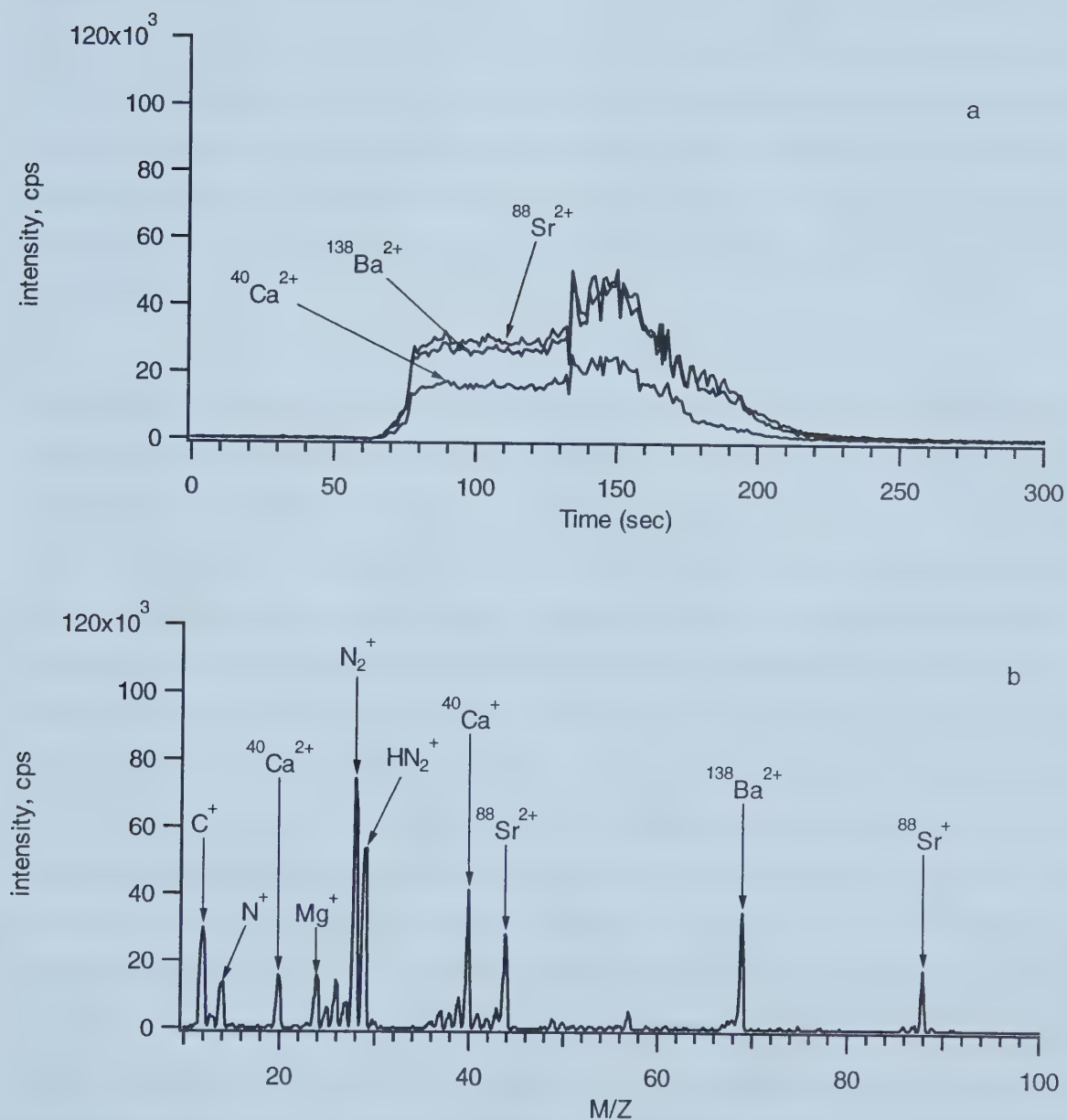


Figure 4.6 FI-ESMS spectra of an equimolar mixture of Mg^{2+} , Ca^{2+} , Sr^{2+} , Ba^{2+} , $\Delta V = 180$ volts.

present. Fig. 4.6 shows the results for an equimolar mixture of Mg^{2+} , Ca^{2+} , Sr^{2+} , Ba^{2+} using flow injection electrospray mass spectrometry. In order to avoid too complex a spectrum the declustering voltage, ΔV , was set high (180 V). The selective ion monitoring spectrum, Fig.4.6 (a), indicates the stable state of the electrospray of the sample solution under proper parameter settings. The resulting mass spectrum was collected after the injector had been switched for 40 seconds. Charge reduced ions were observed for all except barium. The second ionization energy of barium is so low that the ligand loss process is always favored over charge reduction. No reduced species for barium ion were observed. For calcium, even though high CID energy was imposed, bare Ca^{2+} still existed.

Most transition metals have relatively high second ionization potentials. Therefore, their charge reduced species in the gas phase were readily obtained through electrospray. On the other hand, transition elements with multiple charges were sometimes difficult to observe, depending on the nature of the individual element. Some examples are given below. Under a low declustering voltage, Cobalt and Nickel ions appeared as dipositive ion-solvent clusters. With an increase in ΔV , the solvation sphere was diminished and no longer able to stabilize the charge on the metal ion center, consequently charge reduced species occurred, shown in Fig. 4.7 and Fig. 4.8. The SIM spectrum of K^+ is presented in Fig. 4.7(a) to show that the stability of the on-going-electrospray process could be inspected by monitoring the carrier solution ion. The mass spectrum in Fig. 4.7(b) was recorded under the same experimental conditions as in Fig. 4.7(a). The major Co-contained species were Co^{2+} -water clusters with $\text{Co}(\text{H}_2\text{O})_5^{2+}$ yielding the most intense peak. We could see in many cases that although electrospray solutions were primarily methanolic with less than 5% of water present, ion-solvent clusters with methanol in the coordination sphere were rare. This may be attributed to the rapid evaporation of methanol from electrospray droplets and preferential solvating by water [23]. In Fig. 4.7(c) and (d), the voltage difference, ΔV , was set to a higher value of 75 V, and charge reduced species were produced. Among them Co^+ was present, and CoH^+ , $\text{Co}(\text{OH})^+$, $\text{Co}(\text{H}_2\text{O})^+$ were also observed.

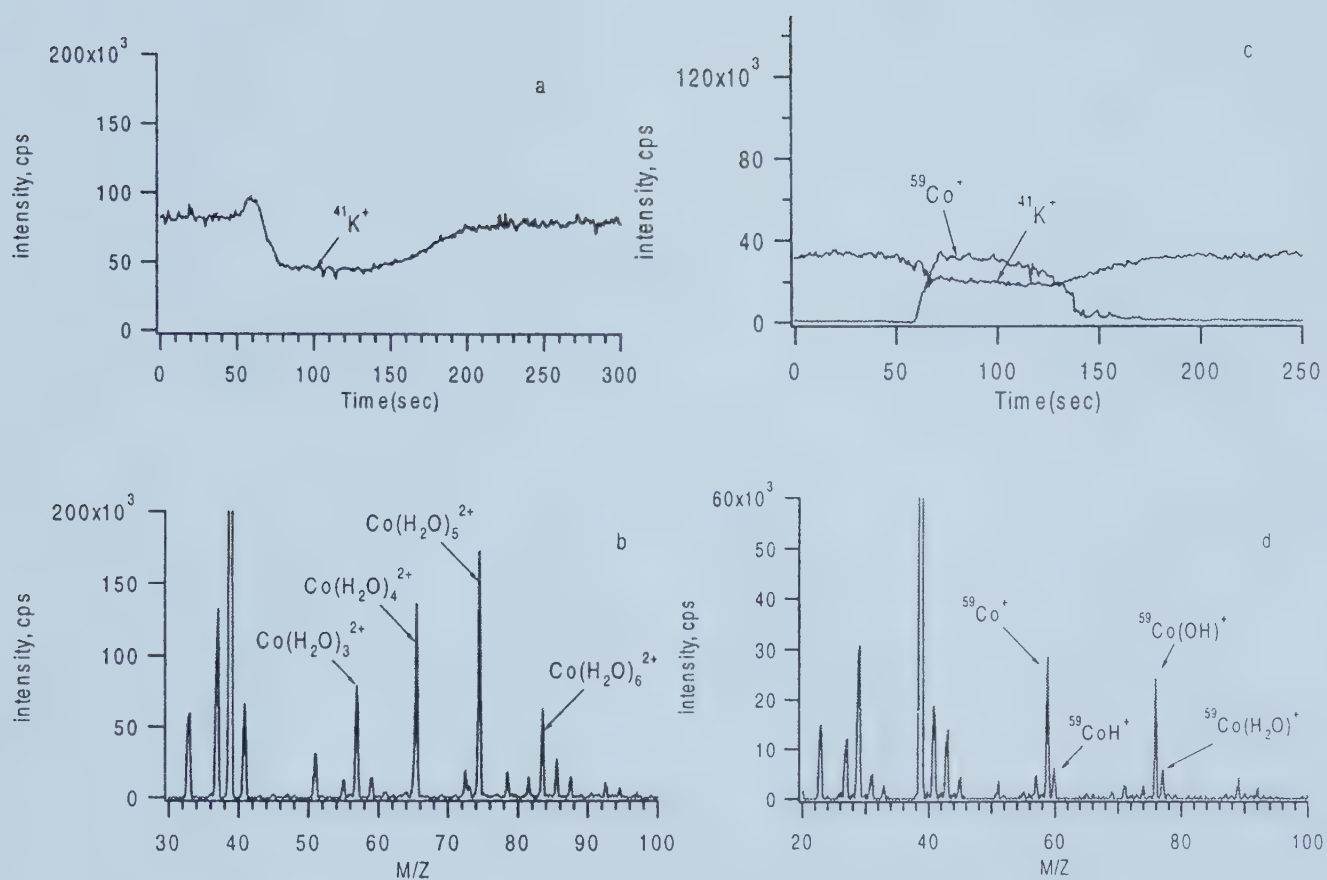


Figure 4.7 FI-ESMS spectra of 0.5 mM Co^{2+} in methanol at ΔV settings of (a) 25 (b) 25 (c) 75 (d) 75 volts.

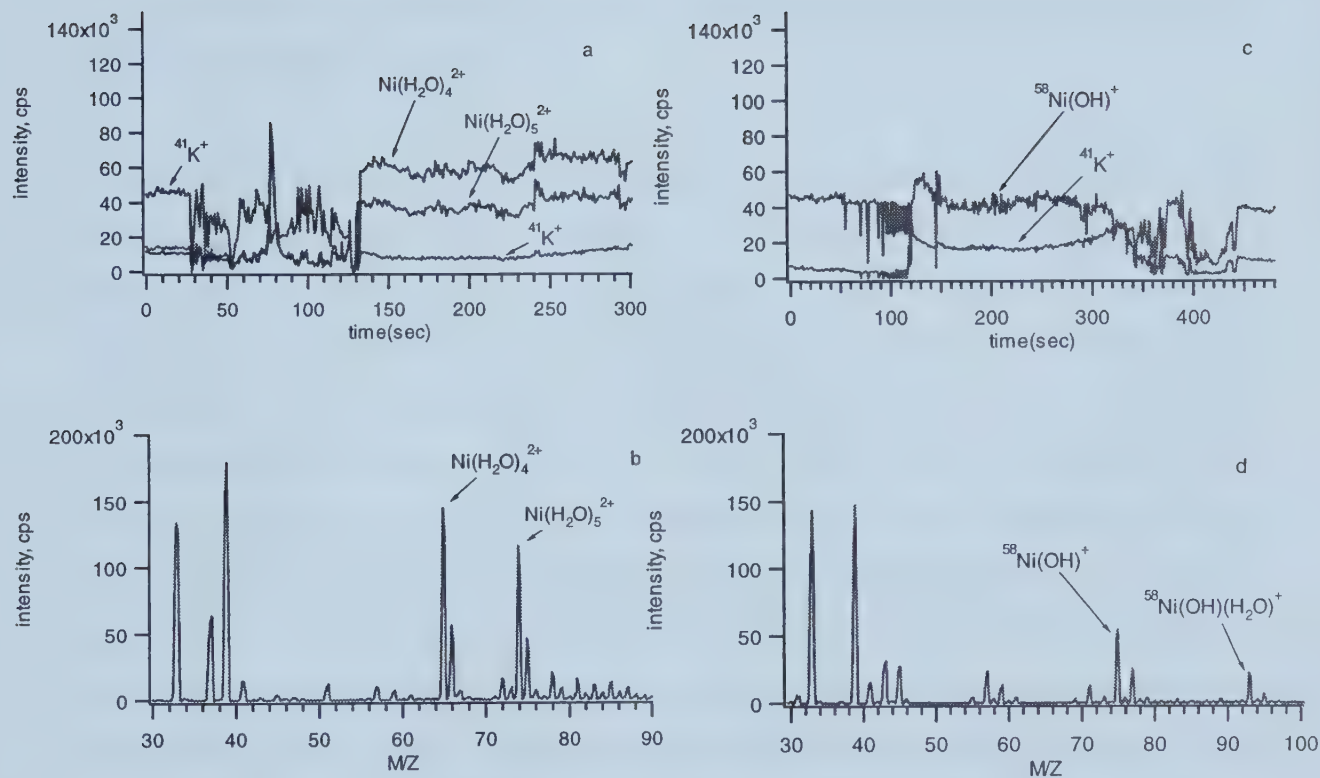


Figure 4.8 FI-ESMS spectra of 0.5 mM $\text{Ni}(\text{NO}_3)_2$ methanolic solution at ΔV settings of (a) 30 (b) 30 (c) 50 (d) 50 volts.

Fig. 4.8 contains a series of mass spectra of 0.5 mM $\text{Ni}(\text{NO}_3)_2$ solution. Somehow a longer time, 120 seconds, was needed to establish stable electrospray of the sample zone at a ΔV of 30 V, shown in Fig. 4.8(a). Erratic signals also occurred at a ΔV of 50 V, shown in Fig. 4.8(c). For this particular sample solution electrospray signals did not change smoothly when the composition of solutions in the process changed between carrier solution and sample zone. $\text{Ni}(\text{H}_2\text{O})_4^{2+}$, $\text{Ni}(\text{H}_2\text{O})_5^{2+}$ were observed at the lower ΔV , and $\text{Ni}(\text{OH})^+$, $\text{Ni}(\text{OH})(\text{H}_2\text{O})^+$ at the higher ΔV . The target species were recognized by their characteristic isotope patterns.

For Copper and Zinc, only charge reduced species were observed. No matter how low the declustering voltage was, there appeared to be no evidence for the multiply charged species of these elements. Fig. 4.9 shows the data for copper. When the declustering voltage, ΔV , was set to 75 v, shown in Fig. 4.9(a) and (b), copper ions were declustered and reduced to Cu^+ . At lower ΔV , 55 V, in Fig. 4.9(c) and (d), $\text{Cu}(\text{CH}_3\text{OH})^+$ occurred as a stable form with lower intensity. At ΔV of 35 V, in Fig. 4.9(e), intensities of Cu^+ -contained species were even lower. Cu^{2+} -contained species could not be observed under any ΔV setting. It is well known that $\text{Cu}^{2+}(\text{aq})$ is its only stable aqueous ion in solution because of the strong complex formation and high hydration energy compared with Cu^+ . Cu^+ is stable in solution only if suitable precipitating and complexing agents are present. This means hydration plays a critical role in the stability of Cu^{2+} . The desolvation in an electrospray process might be harsh enough, even under gentle conditions, to prevent efficient hydration occurring in gas phase. Considering the stable electronic configuration of $\text{Cu}^+(3d^{10}4s^0)$, Cu^+ is favored over Cu^{2+} under all conditions in the vapor state.

Similar observations were seen for Zinc as well, shown in Fig. 4.10. Spectra for Fig. 4.10(a) and Fig. 4.10(b) were collected at declustering voltage (ΔV) of 95 V. Zn^+ is recognized from its characteristic isotope pattern. When declustering voltage (ΔV) was decreased to 55 V, $\text{Zn}(\text{OH})^+$ was the major ion recorded, shown in Fig. 4.10(c) and Fig. 4.10(d). In Fig. 4.10(e) declustering voltage (ΔV) was at 45 V, and more Zn^+ -solvent clusters with low intensity were observed. When the declustering voltage was below 35

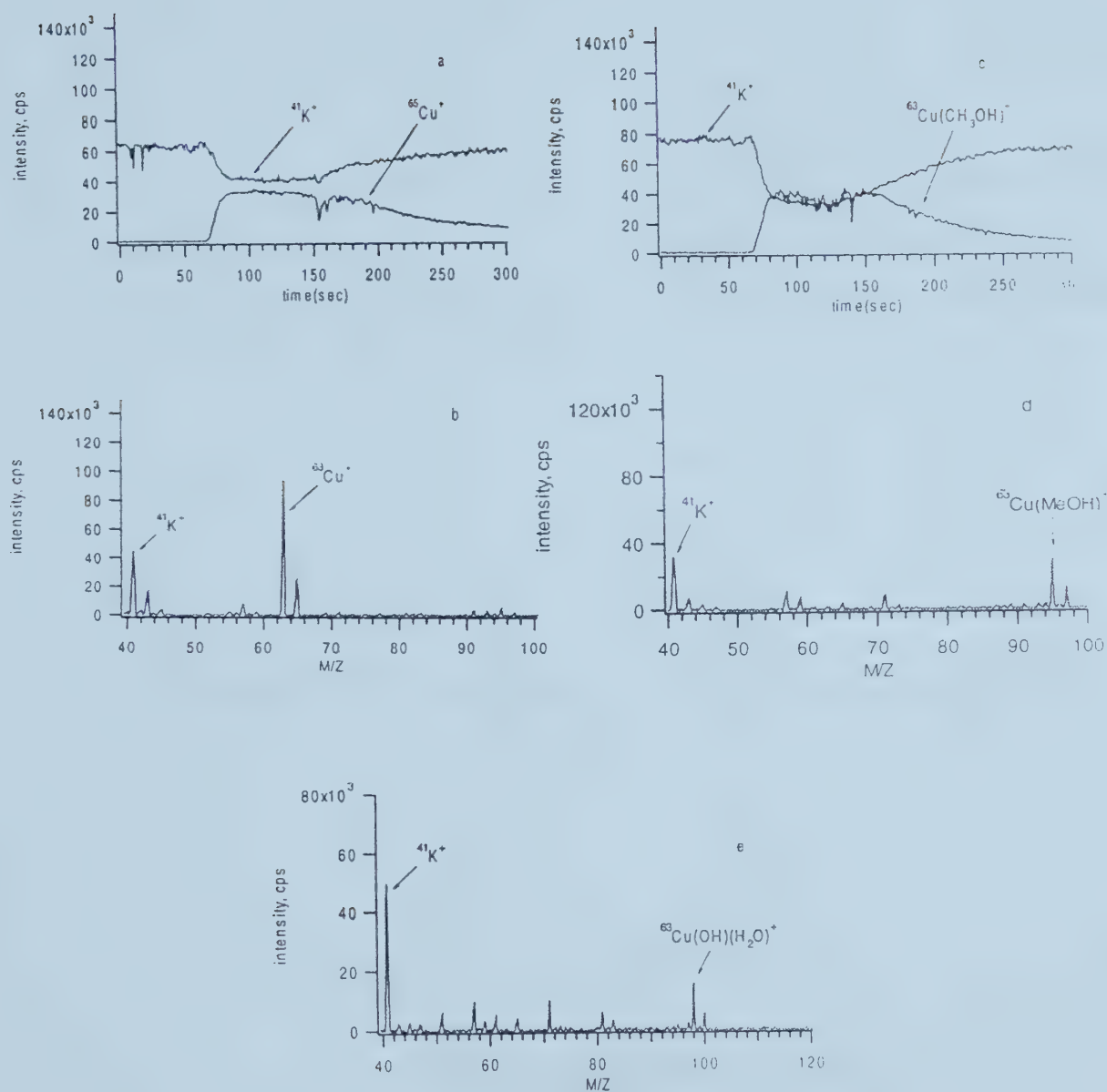


Figure 4.9 FI-ESMS spectra of 0.5 mM copper bromide methanolic solution at ΔV settings of (a) 75 (b) 75 (c) 55 (d) 55 (e) 35 volts.

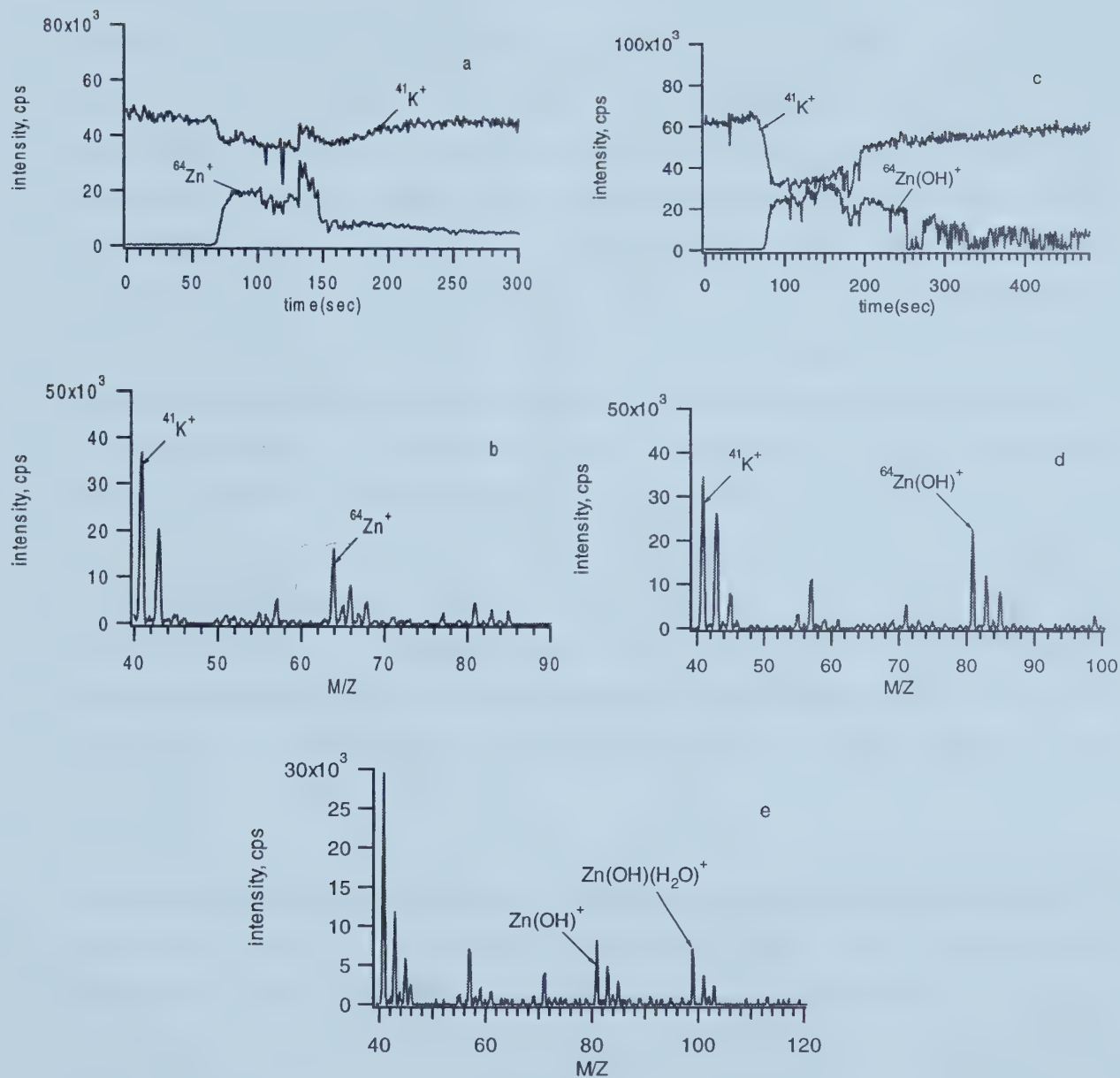


Figure 4.10 FI-ESMS spectra of 0.5 mM zinc nitrate in methanol at ΔV settings of (a) 95 (b) 95 (c) 55 (d) 55 (e) 45 volts.

volts, the background noise and interference from other species were so severe that unambiguous identification of Zinc was impossible.

The ability of the flow injection ESMS system to directly measure anionic species present in solution was also explored. In order to perform negative-ion mode analysis, the power supply boards for the detector and deflector of the mass spectrometer need to be switched from positive to negative. The operational parameters for negative-ion mode electrospray are listed in Table 2.1. A 0.5 mM methanolic solution of KCl was used as the carrier solution for all the negative mode experiments. There is a problem with the modified Perkin Elmer SCIEX Elan Model 250 ICP-MS. The original Elan software used to control data acquisition provides no function of selective ion monitoring for negative ion mode, therefore, the electrospray profile of target species, which provides the important information about the stability of on-going-electrospray-process and the time span needed for analyte signal to reach its steady state, could not be obtained. Consequently, trial and error had to be used to determine the adequate duration time between the moment of switching the injector to injection position and starting the mass spectrum scan. However, this inconvenience could be easily eliminated with advanced modern data acquisition system and software, yielding no real drawback to the application of this method.

It was found that there was no necessity of applying an electron-scavenging gas to reduce the tendency towards electric discharge, though only a few anionic solutions were analyzed. First, obtaining a mass spectrum of an equimolar ($5.0 \times 10^{-4} \text{ mol l}^{-1}$) mixture of F^- , Cl^- , Br^- and I^- was attempted. The results are presented in Figs. 4.11 (a) and (b), with a voltage difference between the sampling plate and skimmer of -65 volts. After the injector was switched to injection, a 70 second interval was needed before starting the mass scan. The mass range was from -10 to -130 amu. The results shown in Fig. 4.11 (a) indicate clearly that the whole scan time needed was longer than the duration time of the sample zone, and the information for high-mass ions was missed. With such a wide mass range and small sample volume capacity, it is impossible to obtain the whole information in one scan. In Fig.4.11 (b) the mass range was set from -60 to -130 unit in order to

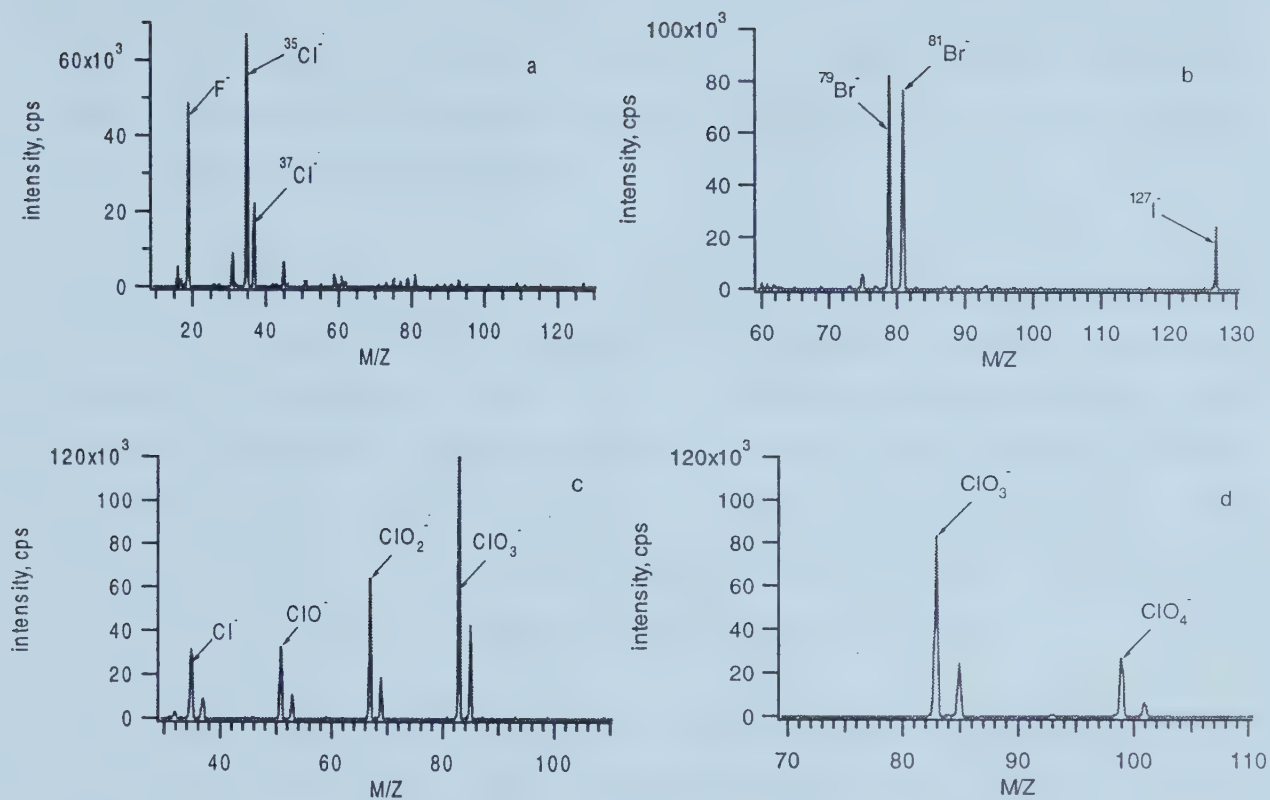


Figure 4.11 Flow injection electrospray mass spectra of (a), (b) a 0.5 mM methanolic solution of fluoride, chloride, bromide and iodide at ΔV of -65 volts and (c),(d) a 0.5 mM methanolic solution of chloride, chlorate and perchlorate at ΔV of -95 volts.

observe Bromide and Iodide. A similar situation happened in obtaining the mass spectra of an equimolar (0.5 mM) mixture of chloride, chlorate, and perchlorate ions. The mass range were from -20 to -110 amu in Fig. 4.11(c) and from -70 to -110 amu in Fig. 4.11(d) respectively. All other parameters were exactly the same in both. The voltage difference between sampling plate and skimmer was -95 volts under which the fragment ions ClO^- and ClO_2^- occurred.

Depicted in Fig.4.12 is a series of spectra of 0.5 mM HNO_3 . In the first spectrum the declustering voltage was -35 V, and only NO_3^- was observed. The second spectrum was acquired at a declustering voltage of -55 V and the increased collisional energy has resulted in the formation of the decomposition product NO_2^- . The declustering potential in the third spectrum was increased to -75 V resulting in a significant increase in the observed intensity for NO_2^- and a decrease in NO_3^- intensity. The time interval between the switching of the injector and starting of mass scan was 100 seconds.

A series of mass spectra of 0.5 mM Na_2SO_4 methanolic solution is given in Fig.4.13. It is noticed that under the normal range of declustering voltage settings, approximately from -25 V to -100 V, all the observed anions were stripped completely of their solvation spheres to their bare molecular form. Consequently, the mass spectra acquired in negative mode are less complex than in positive mode. In Fig.4.13 (a), the declustering voltage was -25 V and the dominant species signaled was HSO_4^- as the result of desolvation and charge reduction of $\text{SO}_4(\text{H}_2\text{O})_x^{2-}$. With an increase in ΔV , fragmentation of HSO_4^- took place and produced SO_3^- ion, as illustrated in Figs.4.14 (b) and (c).

4.4 Conclusions

One important strength of ESMS is that it provides a direct method of detection. So obtaining and investigating mass spectra by electrospray mass spectrometry with flow injection sample introduction became the second attempt of this research. Since the modified ELAN Model 250 ICP-MS possesses an instrumental and data acquisition design of 15 years old, the measurements of mass spectra were experimentally

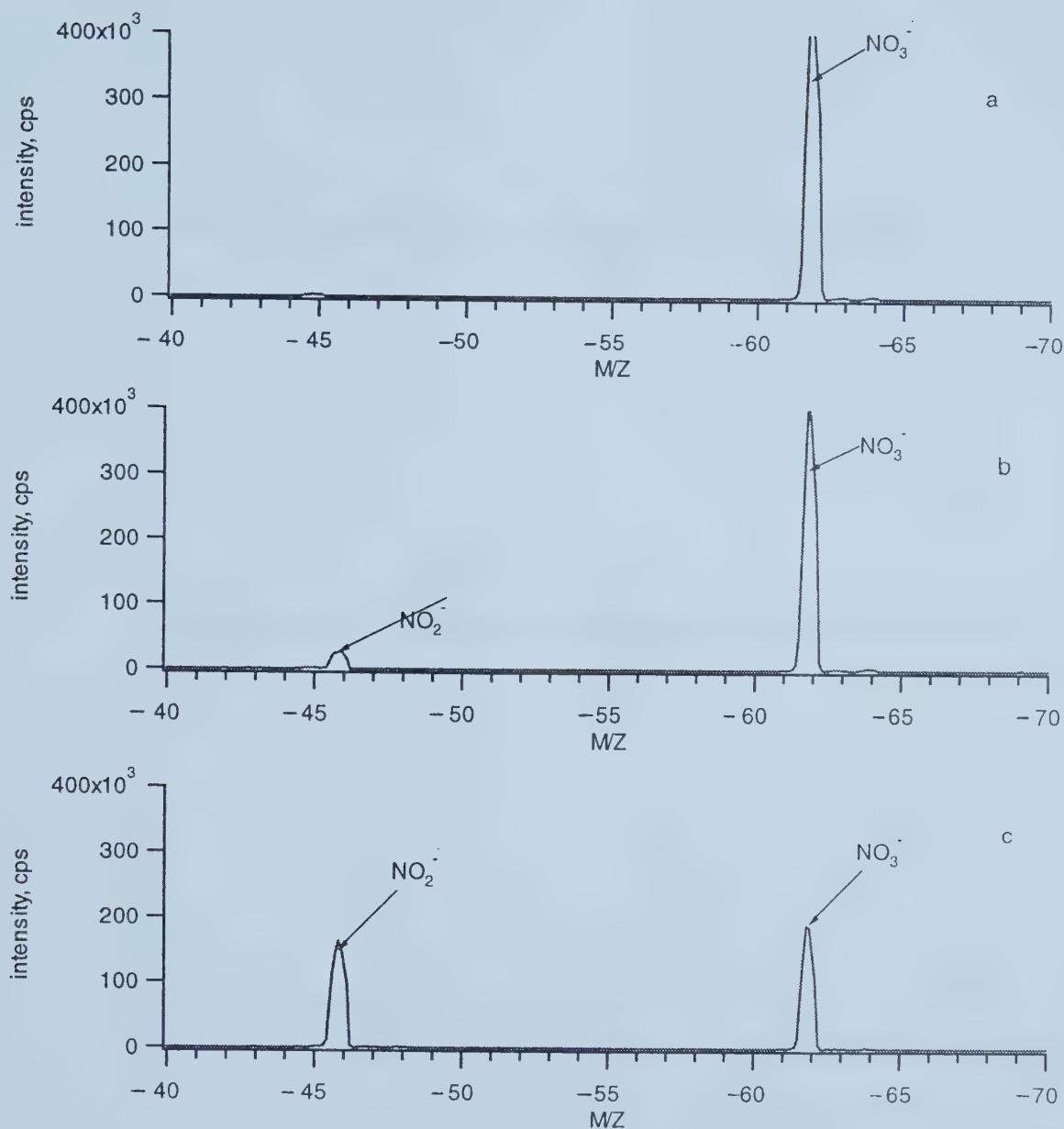


Figure 4.12 Flow injection electrospray mass spectra of a 0.5 mM HNO₃ methanolic solution acquired with varying ΔV settings: (a) -35 V, (b) -55 V, (c) -75 V.

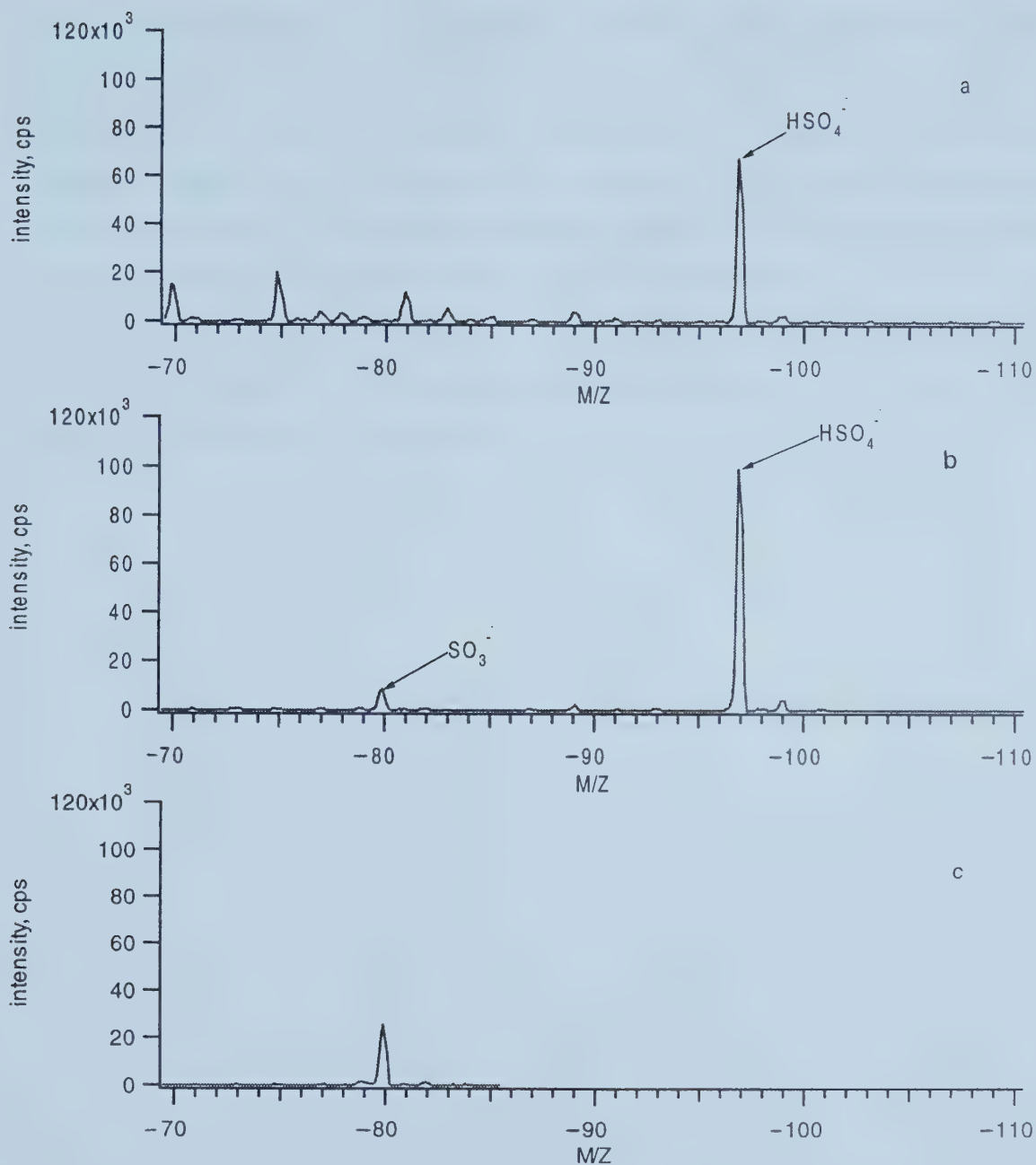


Figure 4.13 Flow injection electrospray mass spectra of a 0.5 mM Na_2SO_4 methanolic solution acquired with varying ΔV settings: (a) -25 V, (b) -55 V, (c) -75 V.

inconvenient and difficult to some degree. For instance, continuous sample introduction and “trial and error” were used to determine some experimental conditions and parameters. Nevertheless, the results presented show clearly that stable electrospray of a transient sample zone in a stream can be established, and the mass spectra captured provides information similar to those revealed in continuous electrospray mass spectra. It is expected that such difficulties in mass spectrum measurements as encountered in this work would be eliminated with the employment of more advanced instrumental and data acquisition design in which the elution profile and mass spectrum at each point of the elution may be monitored simultaneously.

4.5 References

1. Horlick, G., *Spectroscopy*, **1992**, 7, 22-9.
2. Horlick, G., *J. Anal. At. Spectrom.*, **1994**, 9, 593-7.
3. Hieftje, G. M., *J. Anal. At. Spectrom.*, **1992**, 7, 783-90.
4. Broekaert, J. A. C., *Mikrochim. Acta*, **1995**, 120, 21-38.
5. VanLoon, J. C.; Barefoot, R. R., *Analyst*, **1992**, 117, 563-70.
6. Colton, R.; D'Agostino, A.; Traeger, J. C., *Mass Spectrom. Rev.* **1995**, 14, 79-106.
7. Hop, C. E. C. A.; Bakhtiar, R., *J. Chem. Ed.* **1996**, 73, A162-A169.
8. Gatlin, C. L.; Turecek, F., Electrospray ionization of inorganic and organometallic complexes, in: R. B. Cole (Ed.), *Electrospray Ionization Mass Spectrometry: Fundamentals, Instrumentation, and Applications*, Wiley, New York, 1997, pp. 527-570.
9. Stewart, I. I., *Spectrochim. Acta B*, **1999**, 54, 1649-1695.
10. Agnes, G. R.; Horlick, G., *Appl. Spectrosc.*, **1992**, 46, 401-6.
11. Agnes, G. R.; Stewart, I. I.; Horlick, G., *Appl. Spectrosc.*, **1994**, 48, 1347-1359.
12. Agnes, G. R.; Horlick, G., *Appl. Spectrosc.*, **1994**, 48, 655-661.

13. Agnes, G. R., Ph. D. Thesis, University of Alberta, Edmonton, Alberta, 1994.
14. Agnes, G. R.; Horlick, G., *Appl. Spectrosc.*, **1994**, 48, 649-54.
15. Agnes, G. R.; Horlick, G., *Appl. Spectrosc.*, **1995**, 49, 324-334.
16. Stewart, I. I.; Horlick, G., *J. Anal. Chem.*, **1994**, 66, 3983-3993.
17. Stewart, I. I.; Horlick, G., *J. Anal. At. Spectrom.*, **1996**, 11, 1203-1214.
18. Stewart, I. I.; Barnett, D. A.; Horlick, G., *J. Anal. At. Spectrom.*, **1996**, 11, 877-886.
19. Barnett, D. A.; Horlick, G., *J. Anal. At. Spectrom.*, **1997**, 12, 497-501.
20. Blades, A. T.; Jayaweera, P.; Ikonou, M. G.; Kekarle, P., *J. Chem. Phys.* **1990**, 92, 5900-5906.
21. Blades, A. T.; Jayaweera, P.; Ikonou, M. G.; Kekarle, P., *Int. J. Mass Spectrom., Ion Processes*, **1990**, 102, 251-267.
22. Peschke, M.; Blades, A. T.; Kekarle, P., *Int. J. Mass Spectrom.*, 185/186/187 **1998**, 685-699.
23. Barnett, D. A., Ph. D. Thesis, University of Alberta, Edmonton, Alberta, 1999.

Chapter 5

Quantitative Performance of FI-ES-MS

5.1 Introduction

To date, the major interest in electrospray mass spectrometry has been in its qualitative aspects. Quantitative studies, although fewer, have been undertaken by some research groups and revealed significant results. Kebarle et al. [1,2] have investigated the inherent non-linearity of ESMS signal response as a function of concentration and discussed the important features that must be considered for quantitation. Agnes and Horlick [3] have reported this problem could be overcome in part and obtained linear calibration curves for a variety of metal cations with a linear dynamic range over four orders of magnitude by employing an appropriate internal standard. The added internal standard also supplemented the electrolyte present in a sample providing an overall conductivity that is amenable to the generation of a stable electrospray. Because of the fact that stable electrospray is dependent of the composition of the sprayed solution, the addition of a certain amount of internal standard helps to diminish the perturbation of a stable electrospray by changes in composition from sample to sample or standard to standard. Agnes and Horlick also suggested that the selected internal standard should be similar in chemical character and charge to the analyte, so that optimum conditions for detection will be similar for both ions (e.g. K^+ and Cs^+ , and Co^{2+} and Zn^{2+}). If an internal standard electrolyte is chosen that is too surface active (i.e. has greater transfer efficiency to the gas phase), it will suppress the trace analyte excessively, making detection difficult.

Barnett and Horlick [4] reported the analytical utility of negative ion ESMS for quantitation and speciation of halides and halogenic anions and determined fluoride in mouth wash samples using the standard addition method. Stewart, Barnett, and Horlick [5] determined sulfate in a wastewater sample by using standard addition to overcome matrix effects present in real sample cases. Signal suppression and matrix effects due to the competition between component ions present in the droplets will inevitably come to affect the linearity of concentration response. The complex and competitive nature of ion production in the electrospray process has made quantitation in ESMS a significant challenge.

In this chapter, the quantitative performance of the electrospray mass spectrometer employing an injector to introduce sample to the electrospray tip was presented.

5.2 Experimental

All experiments were carried out on the flow injection electrospray source and the modified Sciex / Perkin-Elmer Elan Model 250 ICP-MS as described in Chapter 2. Selective ion monitoring of metal cations was used to measure transient signals of sprayed solution. Data used for quantitation were acquired in the sequential measurement mode with an integration time of 100 ms per point. In order to obtain a wide linear dynamic range and a low detection limit, the injector sample plates of relatively large volume (i.e. 0.2 or 0.5 μL) and low flow rate (about 1 $\mu\text{L}/\text{min}$) were used. The most abundant isotopes of target ions were typically chosen for measurement. Carrier solution for all experiments consists of 0.5 mM KCl in methanol. Operation conditions were optimized before measurements for calibration curve data. The voltages applied to the injector and the electrospray tip were composition dependent and varied from solution to solution. Other parameters were held constant. Among them, the voltages applied to front plate, sampling plate, and skimmer were 600 V, 70 V, 5 V respectively. The ES tip, of 2 mm long, was positioned along the central axis of the orifice in the front plate at a separation distance of 5 mm.

5.2.1 Reagents

Stock solution of metal ions were prepared by dissolving the ACS-grade halogen salts in distilled, deionized water to a concentration of 0.01 M or 0.1 M. The stock solution was then diluted to volume with reagent-grade methanol, to prepare lower concentration solutions used for calibration curve measurements.

5.3 Results and Discussion

All the experiments resulting in the following results employed 0.5 mM methanolic KCl solution as the flow injection carrier. Calibration curves of alkali metal ions were first attempted. Fig. 5.1(a) presents a calibration curve for rubidium. Cesium chloride (0.1 mM) was added to standard solutions of rubidium as internal standard. Experiments were carried out under conditions of 8.0 kV valve voltage and 3.2 kV tip voltage. Because operation parameters were set to favor the largest instrumental response obtainable rather than the best peak shape, the peak area instead of peak intensity of target ions was used for the signal. The slope of log-log plot of the ratio of rubidium (mass 85) and cesium peak area vs rubidium concentration is 0.98.

Calibration curves for cesium and sodium, acquired in a similar manner to that for rubidium, are shown in Fig. 5.1(b) and Fig. 5.2 (a) respectively. In both cases, rubidium (mass 85) was chosen as internal standard. The slope of the log-log calibration plot was 0.98 for sodium and 1.00 for cesium. For all examples given in this chapter the linear dynamic range obtainable was around 3 orders of magnitude, corresponding to a concentration range of 1×10^{-6} to 1×10^{-3} M. However, linear calibration curves over a dynamic range of four orders of magnitude for a variety of positive and negative inorganic ions have been achieved by the system employing continuous sample introduction method [5]. Trace analyte as low as 10^{-7} M has also been determined [6]. The major reason for this may be related to the diminished sensitivity associated with the flow injection method. Some evidence and discussion about the sensitivity in FI-ES-MS was presented in Chapters 3 and 4.

Calibration curves of alkaline earth metal ions were obtained as well. Ions of dipositive form were chosen as analytes of interest. In comparison to the case of alkali metal ions, more care had to be taken with respect to operation conditions, especially for calcium which has a relatively high second ionization potential. Because more than one form exists, there is more variability. Moderate changes in electrospray operating parameters could cause considerable error in the quantity of the actual ion monitored. The experiments for calcium were carried out under conditions of 7.0 kV valve voltage and 3.1 kV tip voltage. SrCl_2 (0.1 mM) was used as the internal standard. The ratio of $^{40}\text{Ca}^{2+}$

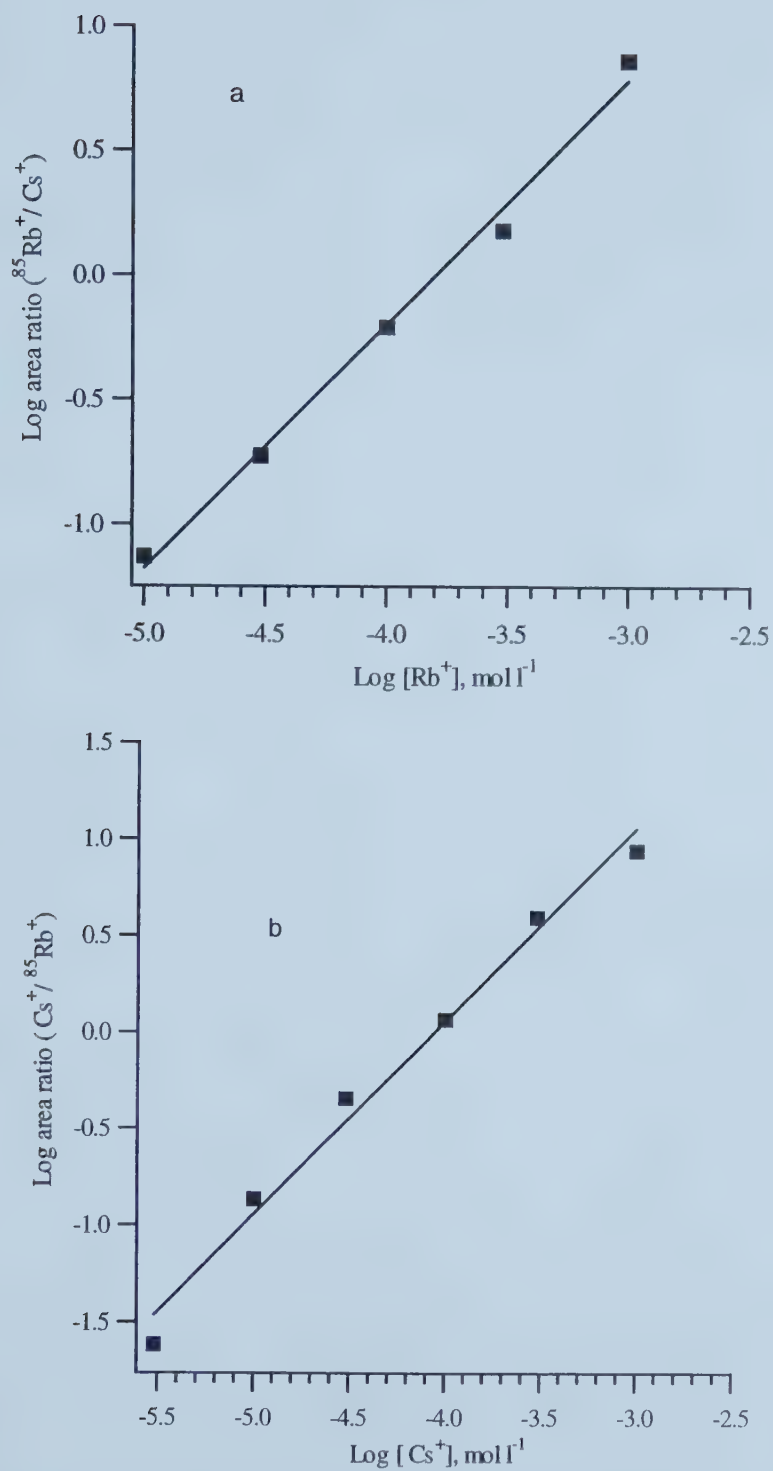


Figure 5.1 Analytical curves for (a) Rb and (b) Cs, employing 0.1 mM Cs and Rb, respectively, as an electrospray stabilizer and internal standard.

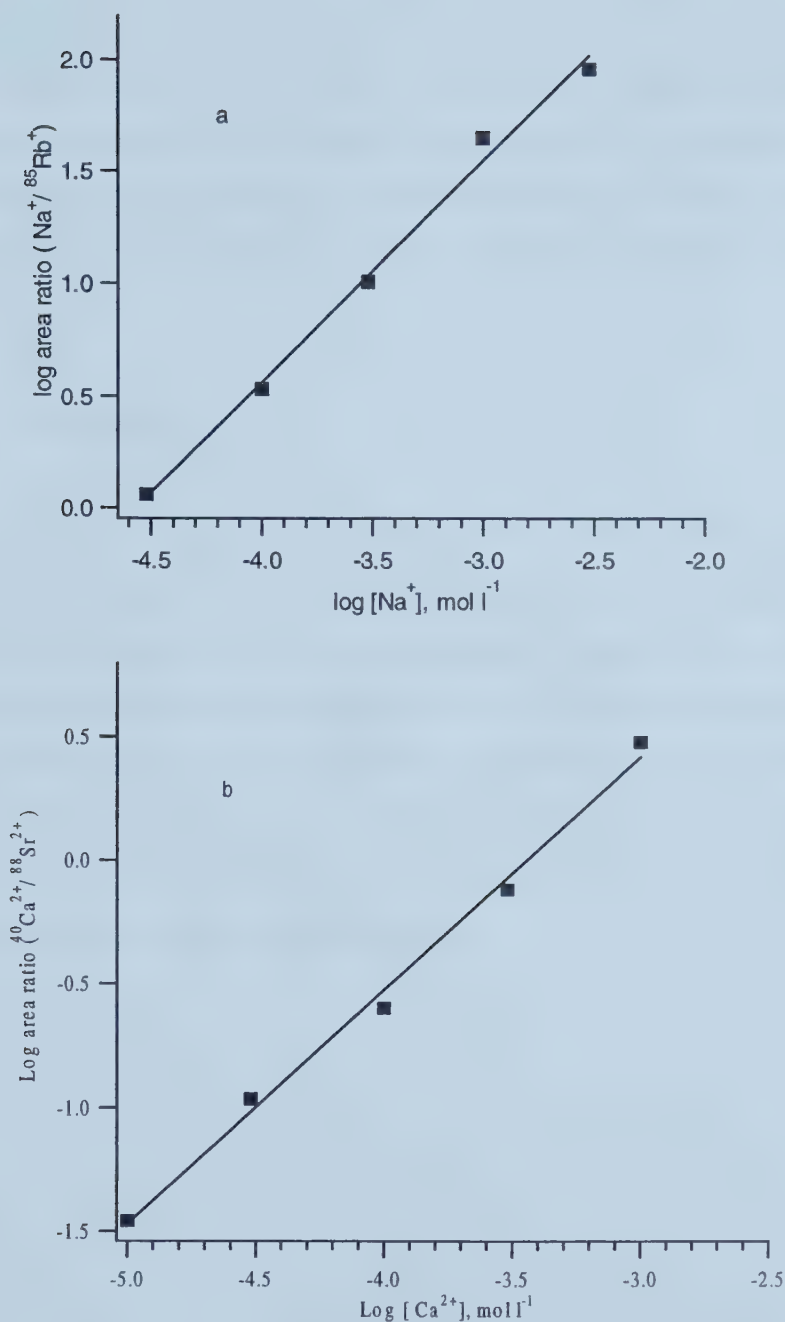


Figure 5.2 Analytical curves for (a) Na and (b) Ca, employing 0.1 mM Rb and Sr, respectively, as an electrospray stabilizer and internal standard.

(20 amu) and $^{88}\text{Sr}^{2+}$ (44 amu) peak area is plotted against concentration. The log-log slope of the plot is 0.95. The calibration curve of strontium using barium (0.1mM) as the internal standard is presented in Fig. 5.3(a), and the plot has a slope of 1.00. Strontium at mass 44 and barium at mass 69 were monitored. For barium, its low second ionization potential permits use of its doubly charged ion which is always present as the major species under normal electrospray operating conditions. When 0.1 mM $^{88}\text{Sr}^{2+}$ was used as internal standard, the acquired log-log calibration plot exhibits a slope of 0.98, shown in Fig. 5.3 (b).

5.4 Conclusions

In the quantitative aspect of electrospray mass spectrometry with flow injection sample introduction, because of the capability of the injector delivering a certain volume of sample solution in a accurate and reproducible manner, linear calibration curves over three orders of magnitude for simple metal ions can be readily achieved with employment of an internal standard. This obtainable linear dynamic range, however, is narrower in comparison to continuous sample introduction method. Reasons for this shortcoming may be related to the set-up of the system and nature of flow injection where the analyte peak is dispersed in the stream of carrier solution.

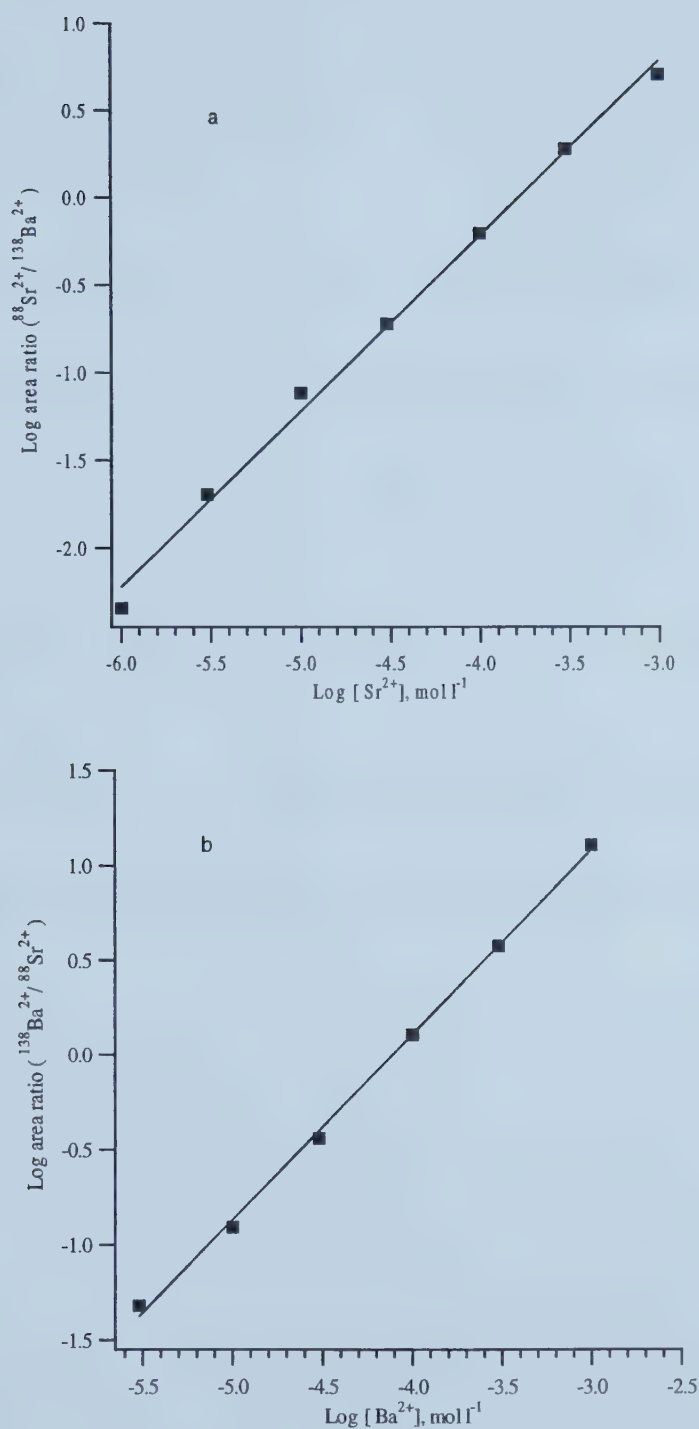


Figure 5.3 Analytical curves for (a) Sr and (b) Ba, employing 0.1 mM Ba and Sr, respectively, as an electrospray stabilizer and internal standard.

5.5 References

1. Kebarle, P.; Ho, Y., In *Electrospray ionization mass spectrometry: Fundamentals, Instrumentation, and Applications*, Cole, R. B. (Ed.), John Wiley & Sons: New York, 1997, pp 3-63.
2. Kebarle, P.; Tang, L., *Anal. Chem.*, **1993**, 65, 972A-986A.
3. Agnes, G. R.; Horlick, G., *Appl. Spectrosc.*, **1994**, 48, 649-54.
4. Barnett, D. A.; Horlick, G., *J. Anal. At. Spectrom.*, **1997**, 12, 497-501.
5. Stewart, I. I.; Barnett, D. A.; Horlick, G., *J. Anal. At. Spectrom.*, **1996**, 11, 877-886.
6. Agnes, G. R., Ph. D. Thesis, University of Alberta, Edmonton, Alberta, 1994.
7. Barnett, D. A., Ph. D. Thesis, University of Alberta, Edmonton, Alberta, 1999.

Chapter 6

Conclusions

6.1 Summary

Electrospray ionization for mass spectrometry possesses several important advantages over other major ionization methods. It offers a relatively simple means to transfer non-volatile solution phase ions and polar molecules to the gas phase. It can generate negative gaseous ions. In particular, its unique nature of mildness allows few fragmentation of analyte ions. Consequently, important solution information such as chemical forms and oxidation states tends to be preserved. Molecular ions of fragile molecules and thermally-sensitive compounds could be kept intact. Combining the sensitive and direct detection of mass spectrometry, ESMS has quickly captured the great interest of analytical community.

The majority of research on electrospray mass spectrometry as a analytical tool of extraordinary potential has been related to the development, application or fundamentals of ESMS. The number of analysis has been an insignificant issue. Therefore, sample introduction in ESMS has been taking an minor role in the development of electrospray mass spectrometry. In the event that ESMS is to be employed in the routine analysis and a large quantity of sample measurements is to be performed, small consumption of samples and a simple and fast way of changing sample would certainly be desired. The introduction of samples by flow injection method, which has been well investigated in flow injection analysis, seemed well suited to the goal. Although electrospray process is dependent of the composition of spraying liquid, evidences show that the switch of spraying liquid between carrier solution and sample portion of the eluent exerts no significant perturbation on the continuance of the steady state of established electrospray. The two processes are compatible to some degree as to allow the sample zone of the stream reaching the ES tip and yielding stable electrospray signals.

Peak tailing has been a major concern for the system constructed for this study. The adsorption of analyte ions onto the inside wall of the ES capillary may be one of the origins of the tailed peaks, which can be reduced significantly by increase of carrier ion concentration. On the other hand, the increase of carrier ion concentration has the

unwanted effect of suppressing the intensities of analyte signals. At compromise, the optimal carrier solution concentration used for most work of this thesis is 0.5 mM. It is noticeable that the carrier solution has many functions in the FI-ESMS system. Basically it carries sample solutions to the ES tip. With respect to the electrospray process, carrier ions are the major contributor to required conductivity of the sprayed liquid, and may also function as electrospray stabilizer. The ES signal of carrier ion can be monitored continuously as a indicator of the status of on-going electrospray. Furthermore, carrier ions can block the active sites of the capillary wall and attenuate the degree of peak tailing due to the adsorption of analyte ions.

Flow rate of carrier solution and the sample volume are parameters which can be used to control peak tailing from the constructional origin of the system. Similar to carrier ion concentration, these parameters affect the peak shape and analyte signal intensities contrarily. Higher flow rate and smaller sample volume will bring about less tailed peaks but lower signal intensity. The trend in the effect of flow rate tends to level out in high flow rate value region. So normal flow rate range is 1.0 ~ 6.0 $\mu\text{L}/\text{min}$. In general, parameters of flow rate and concentration of carrier solution and the sample volume should be adjusted based on the individual experimental purpose.

The flow injection electrospray mass spectra of some inorganic solution ions provides similar information to those obtained by ESMS employing continuous sample introduction method. Some inconvenience was associated with the measurement of mass spectra due mostly to the outdated instrumentation of the mass spectrometer used for this study. This hardship can be overcome by modern generation of electrospray mass spectrometer. In the quantitative aspect of electrospray mass spectrometry with flow injection sample introduction, linear calibration curves over three orders of magnitude for simple metal ions can be readily achieved with employment of internal standard. This obtainable linear range is narrower in comparison to continuous sample introduction method. Reasons for this shortcoming may be related to some constructional origins and natures of the way of flow injection where the analyte peak is dispersed in the stream of carrier solution.

6.2 Future Work

The internal injector used in this study employs sample plates which are sized to contain exact, specified volumes of a sample solution. Only 5 types of sample plates are available, and their volume sizes are 0.02 μl , 0.05 μl , 0.1 μl , 0.2 μl , 0.5 μl . Sometimes we need a long analysis time to determine stable electrospray conditions or to perform detailed mass spectral analysis for a specific sample. Therefore, an injector of large sample capacity is needed. An external injector may be suitable for this purpose. The sample loop of an external injector consists of a capillary of specified length. By adjusting the length of the capillary sample loop, we can inject whatever sample volume we want.

Matrix effect studies should be done in the future. In this study, the carrier solution and sample solution had similar matrix. Therefore, the change of spraying solution from carrier to sample did not cause significant perturbation of the electrospray. For real samples with a complicated matrix, the drastic change in composition between carrier and sample could affect the established electrospray and should be investigated.

A on-going goal associated with the flow injection method is to reduce mixing effects and peak tailing. Improving the connection between the ES capillary and the injector could be another aspect of future work.

Finally, other projects could involve utilizing a coated capillary and varying the pH of the carrier in order to alter and perhaps eliminate solute wall interactions.

University of Alberta Library



0 1620 1493 8144

B45435